

Using a 148km long cross-section of Holocene deposits, to study natural subsidence along the Dutch coastal plain

MSc graduation research

Author: M.F. Andeweg
Student number: 5623960
MSc Earth Surface & Water

Supervisor: Dr. K. M. Cohen
Faculty of Geosciences
Department of Physical Geography

Utrecht University

03-08-2022



**Utrecht
University**

Abstract

This two-part research into subsidence over the Dutch coastal plain uses a 147.7 km long cross-section to study differences in subsidence between the south and the north of the Netherlands. The focus lies on splitting the total natural subsidence into three components: Glacio-isostatic adjustment due to the collapse of the peripheral forebulge when the Scandinavian-British ice sheet started to melt; Tectonic subsidence, caused by the lowering of the North Sea depocentre; And, compaction of Middle-Holocene peat layers, due to peat compression and oxidation.

In the first part, a vertical profile is created that describes lithogenetic units along the full cross-section, with a focus on Noord-Holland where lithological descriptions are scarce. The lithological relations from the cross-section, in combination with ¹⁴C samples, are used to create isochrones that span the whole study area. The depths of the isochrones are measured at 5km intervals. These values are used to calculate spatial isochrone depth differences, which provides a quantification of differential subsidence. The results from this exercise were compared to interpolated subsidence values from parallel research by De Wit et al., (in prep.) and used to quantify differences in reconstructed and interpolated isochrones characteristics.

Comparing differential subsidence along the cross-section shows that in the north isochrones lie up to two meters deeper compared to the south. This difference is largely described by subsidence due to glacio-isostatic adjustment and tectonic subsidence. However, subsidence due to peat compaction also causes large differences in isochrone depths. Peat compaction is a likely cause to why the reconstructed isochrones are found deeper compared to the interpolated isochrones from De Wit et al., (in prep.), which excludes this effect of compaction.

Table of contents

Contents

Abstract.....	1
Table of contents.....	2
1. Introduction.....	4
1.1 Setting.....	4
1.2 Aim and research question.....	4
1.3 Hypotheses.....	5
2. Background.....	6
2.1 Area description.....	6
2.2 Theoretical framework.....	8
2.2.1 Sea Level Rise and the response of the Dutch coast.....	8
2.3 Middle- to Late-Holocene tidal inlet systems.....	10
2.3.1 Northerly systems.....	10
2.3.2. Southerly systems.....	13
2.4 Land subsidence.....	13
2.4.1 Glacio-isostatic adjustment component.....	14
2.4.2 Basin subsidence component: depocenter tectonics and deep layer compaction.....	14
2.4.3 Peat compaction component.....	15
2.4.4 Relation to accommodation space.....	16
3. Materials.....	17
3.1 Cores and 14C samples.....	17
3.1.1 Sediment cores descriptions.....	17
3.1.2 14C dated peat samples.....	17
3.2 Existing cross-sections.....	18
3.3 Maps and GIS datasets.....	19
3.4 Interpolated groundwater isochrones.....	19
4. Methods.....	19
4.1 Literature study and data availability review.....	19
4.2 The location of the cross-section.....	19
4.3 Creating the cross-section.....	20
4.4 Lithogenetic interpretations.....	21
4.4.1 Tidal: Naaldwijk Formation Wormer Member (NAWO).....	21
4.4.2 Fluvial.....	23
4.4.3 Organic - Nieuwkoop Formation peats and gyttja.....	23
4.5 14C samples and creating isochrones.....	24

4.6 Approach for comparing land subsidence.....	24
4.6.1 Extra 14C samples for subsections 1 and 6	25
5. Results.....	27
5.1 Cross-section descriptions.....	27
5.1.1 Subsection 1: Dordrecht.....	29
5.1.2 Subsection 2: Rhine-Meuse Paleovalley.....	30
5.1.3 Subsection 3: Transition from fluvial to tidally dominated environments.....	32
5.1.4 Subsection 4: Amsterdam	34
5.1.5 Subsection 5: Beemster polders.....	36
5.1.6 Subsection 6: Wieringen.....	38
5.1.7 Peat layer thickness.....	40
5.2 Isochrones from the cross-section	41
5.2.1 Reconstructed isochrones	41
5.2.2 Interpolated isochrones	42
5.2.3 Comparison measured and interpolated isochrones	43
6. Discussion.....	46
6.1 Interpreting the shape of the isochrones.....	46
6.1.1 Isochrone variations in the south.....	46
6.1.2 Isochrone trend in the north	46
6.1.3 Depth variations in the center	46
6.2 Differences between South and North.....	48
6.2.1 Average depth comparison	48
6.2.2 Selective averages comparison.....	50
6.2.3 Comparing depth differences with values from literature	52
6.3 Interpreting differences between measured and interpolated	53
6.4 Differentiating between different sources of land subsidence	54
6.5 How suitable is this cross-section for researching differences in subsidence	55
7. Conclusions.....	56
Acknowledgements.....	56
References.....	57

1. Introduction

1.1 Setting

The Dutch coastal plain is heavily affected by land subsidence stemming from different causes, resulting in significant societal impacts today. The total land subsidence consists two major components. One anthropological component which has been active in the last millennial and natural components which have been affecting the Dutch landscape for much longer. The components that make up the natural subsidence are: Glacio-isostatic adjustment due to the collapse of the peripheral forebulge, which started when Scandinavian-British ice sheet began to melt shortly after the Last Glacial Maximum (Vink et al., 2007); Tectonic subsidence, caused by the lowering of the North Sea depocentre (Arfai et al., 2018; Cohen et al., 2022); And, compaction of Middle-Holocene peat layers (Van Asselen et al., 2009). From the last glacial maximum (LGM) to the present day these subsidence components all contributed to the lowering of the Dutch coastal plain throughout the Late-Pleistocene and Holocene.

Much effort has already been put into researching natural subsidence during the Holocene period in the Netherlands (Kooi et al., 1998; Kiden et al., 2002; Vink et al., 2007; Van Asselen et al., 2009; Koster et al., 2018), motivated by the importance of understanding subsidence for proper delta management. Previous research has shown spatial and temporal variations between the different subsidence components. The north of the Netherlands generally shows higher rates of subsidence compared to the south (Kooi et al., 1998; Vink et al., 2007), an effect that is mainly controlled by the GIA and background components of subsidence.

Studying Holocene subsidence throughout the Netherlands is commonly done with the help of isochrones (time lines through deposits of synchronous age). In a cross-section, drawing such lines bounds the time frame in which certain successions of sediment are formed (Gouw & Erkens, 2007; Hijma et al. 2009). One way to create isochrones, is with the help of cross-sections. Studies covering lithological Formations in the Dutch subsurface often contain isochrones that are made using a combination of ¹⁴C-samples and lithological relations (Gouw & Erkens., 2007, Hijma et al., 2009). These cross-sections come in many different lengths, from several kilometres up to ~70 kilometres. But, as of now, none of these cross-sections has been long enough to cover the entirety of the Dutch coastal plain. Other methods of creating isochrones are proposed in a large study into paleo-groundwater levels is conducted by De Wit et al., (in prep.). This study uses interpolation and trend fitting to create different time intervals for paleo groundwater levels in a 3D-model covering the Holocene period.

1.2 Aim and research question

Creating such a large scale cross-section that covers Early- and Middle-Holocene deposits, opens up the possibility to study natural subsidence along a significant length of the Dutch coastal plain. Using the combination of ¹⁴C data and lithological information, it further allows the comparison between isochrones that were created with the lithological approach (this research) and with the interpolation approach from De Wit et al. (in prep.).

In addition, a cross-section of this scale further highlights subsurface composition in the area north of Amsterdam, where lithological detail at the depths of Early- to Middle Holocene deposition is relatively limited (Westerhoff et al., 1987; Vos 2015; Vos et al., 2015).

The aim of this MSc-Thesis is to create a cross-section of the Dutch coastal plain from a location in the South of the Netherlands (around Dordrecht, South-Holland) to a point in the North of the Netherlands (around Wieringen, North-Holland). Hereby, favouring covering a larger area over capturing smaller lithological details. ¹⁴C samples in combination with lithological relationships within the cross-section will be used to create isochrones. These isochrones can then be used to analyse differences in subsidence throughout the

whole cross-section, including a comparison with the data from De Wit et al., (in prep.).

The main question of this research is: How large are the differences in natural land subsidence during the Holocene between the North and the South of the Netherlands?

In a cross-section with isochrones the difference in subsidence can be expressed in the difference in isochrones depths (in meters) along the cross-section. These differences may then be used to determine subsidence differences on local and regional scales.

Some sub-questions that I will try to answer in this research are:

- What are the causes of land subsidence along the cross-section? The three natural subsidence components are expected to behave differently these difference might be expressed in the isochrones characteristics. It might be possible to connect isochrone characteristics to the different subsidence components.
- How well does this method work for researching land subsidence differences along a coastal plain? The results can be evaluated with literature and discussed in terms of how well they represent reality. The quality of data gathering and data processing can also be discussed and how it may have affected the results.
- What are the differences between the reconstructed isochrones from this research and the interpolated isochrones from De Wit et al., (in prep.)? The isochrones depths from the cross-section can be compared to interpolated isochrones by extracting interpolated values at the same locations as the reconstructed isochrones and determining the differences in depth at these locations. These differences can then be interpreted.

1.3 Hypotheses

Based on Vink et al. (2007) and unpublished research by De Wit et al., (in prep.) it is expected that the North of the Netherlands has experienced more subsidence than the south between 10,000BP and 4000 BP (Kooi et al. 1998; Vink et al., 2007). This difference is mainly caused by subsidence from GIA and tectonics, whereas subsidence due to peat compaction is expected to be much more local.

The differences between subsidence rates should increase with the distance between the southern and northern data point, i.e. the subsidence difference between Zeeland and Groningen (de Wit et al. 2002) should be larger than the subsidence differences between Zeeland and Noord-Holland (Vink et al. 2007 and Kooi et al. 1998). Figure 1.1 shows a strongly simplified representation of the expected isochrone positions and how they have displaced over time.

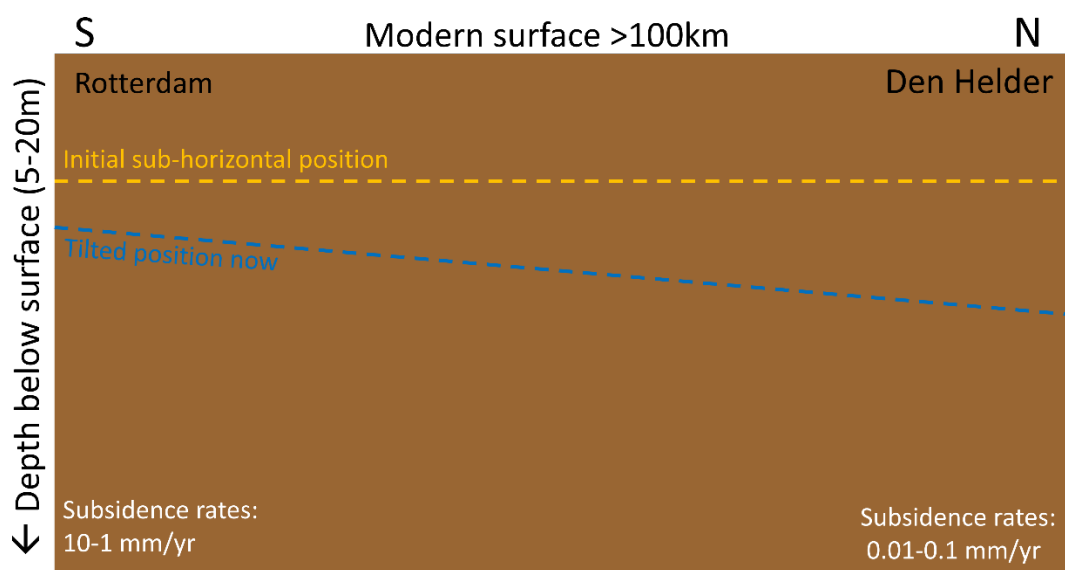


Figure 1.1: Simple representation showing expectations of how isochrones were displaced over time.

2. Background

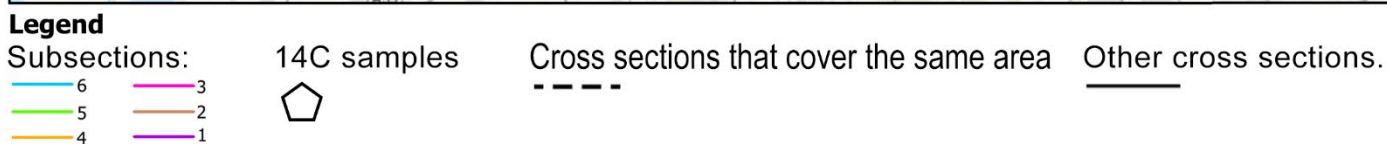
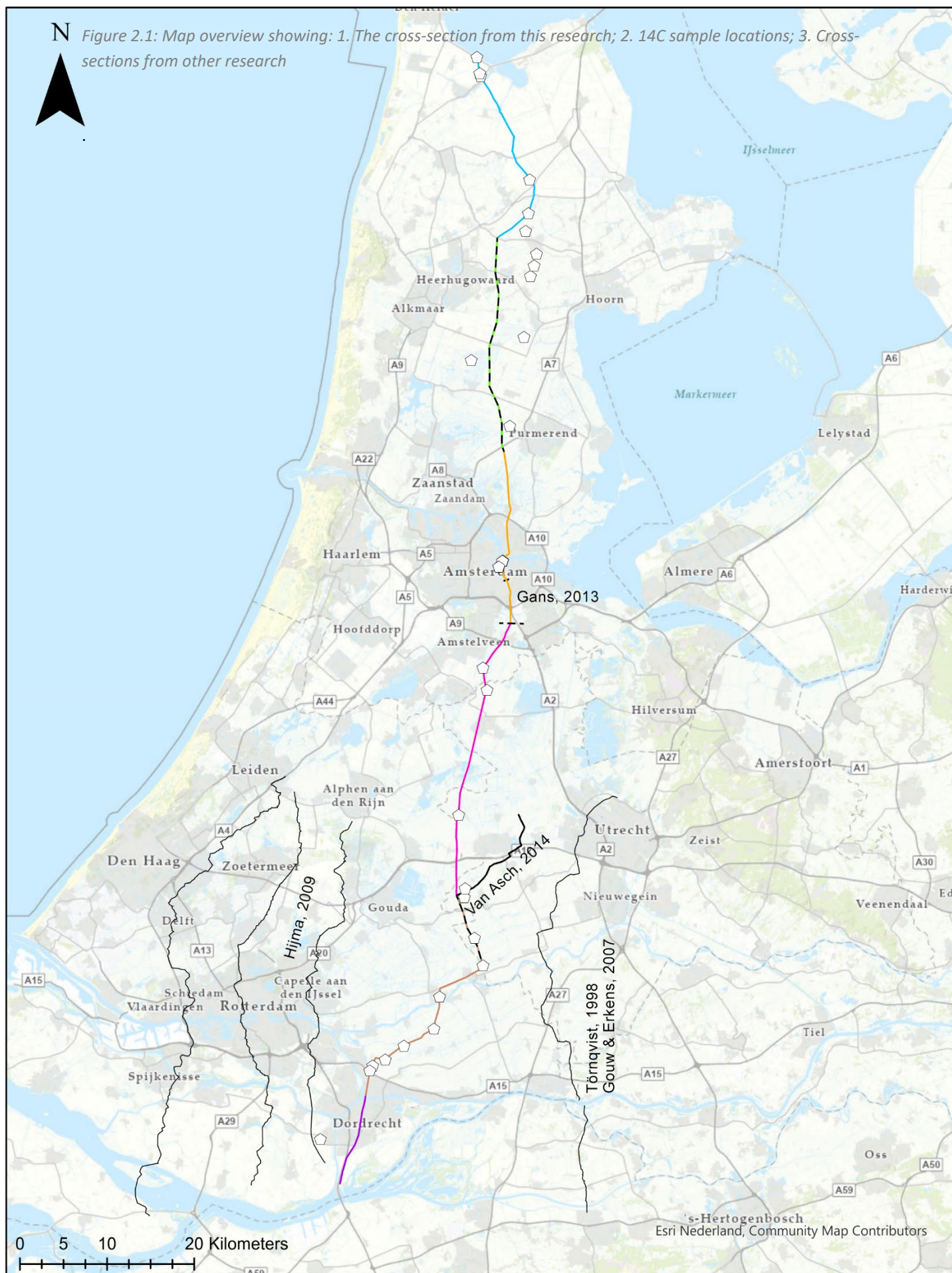
2.1 Area description

The study area of this thesis encompasses the Provinces of Noord-Holland and Zuid-Holland (Figure 2.1). It also covers a small, western part of the Province of Utrecht. The cross-section covers a substantial part of the Dutch coastal plain. At the southern end, the cross-section approaches the southern rim of the Holocene coastal plain. In the North, the cross-section borders the Waddenzee in the vicinity of the Wierden-Texel Pleistocene subcrop. In other words: here it can be considered to stretch to Northern the rim of the Holland coastal plain as it was up to ca. 2000 years ago (Vos, 2015; Pierik et al. 2017; De Haas et al. 2018). The cross-section runs over two large paleo valleys that were created during the Pleistocene. One is an old valley created by the Rhine river in the northern part of the cross-section and the other is the Rhine-Meuse paleo valley in the south (fig 2.2). Between both valleys there is a shallower part of the Pleistocene surface, consisting of cover sands.

For the sake of convenience, the entire cross-section is split into six sub-sections (Figure 2.1). This made drawing, interpreting and presenting the cross-section easier. The location where the cross-section is split was sometimes based on existing cross-sections (Subsection 5), sometimes on the length (2,3,4), and sometimes on the location (subsection 1 over the Island of Dordrecht).

Figure 2.1 shows a map with the location of the cross-section, where each colour represents a different subsection. The 14C sample locations are represented by a white pentagon. The maps show the location of the profiles by Hijma et al., (2009); Gouw & Erkens, (2007); Van Asch (2014), and De Gans, (2015).

Figure 2.1: Map overview showing: 1. The cross-section from this research; 2. 14C sample locations; 3. Cross-sections from other research



2.2 Theoretical framework

2.2.1 Sea Level Rise and the response of the Dutch coast

At the start of the Holocene (11,700BP), the mean sea level was still at minus ~35m below the present MSL (Vos, 2015). During this time no areas of the Netherlands were yet inundated, and the surface was still covered by the Pleistocene river sediments (Kreftenheye Formation) and cover sands (Boxtel Formation). During the end of the Early-Holocene the relative sea level rose by roughly 10 mm/yr (Hijma & Cohen, 2010). The map in figure 2.2 shows the land surface elevation at the start of the Holocene.

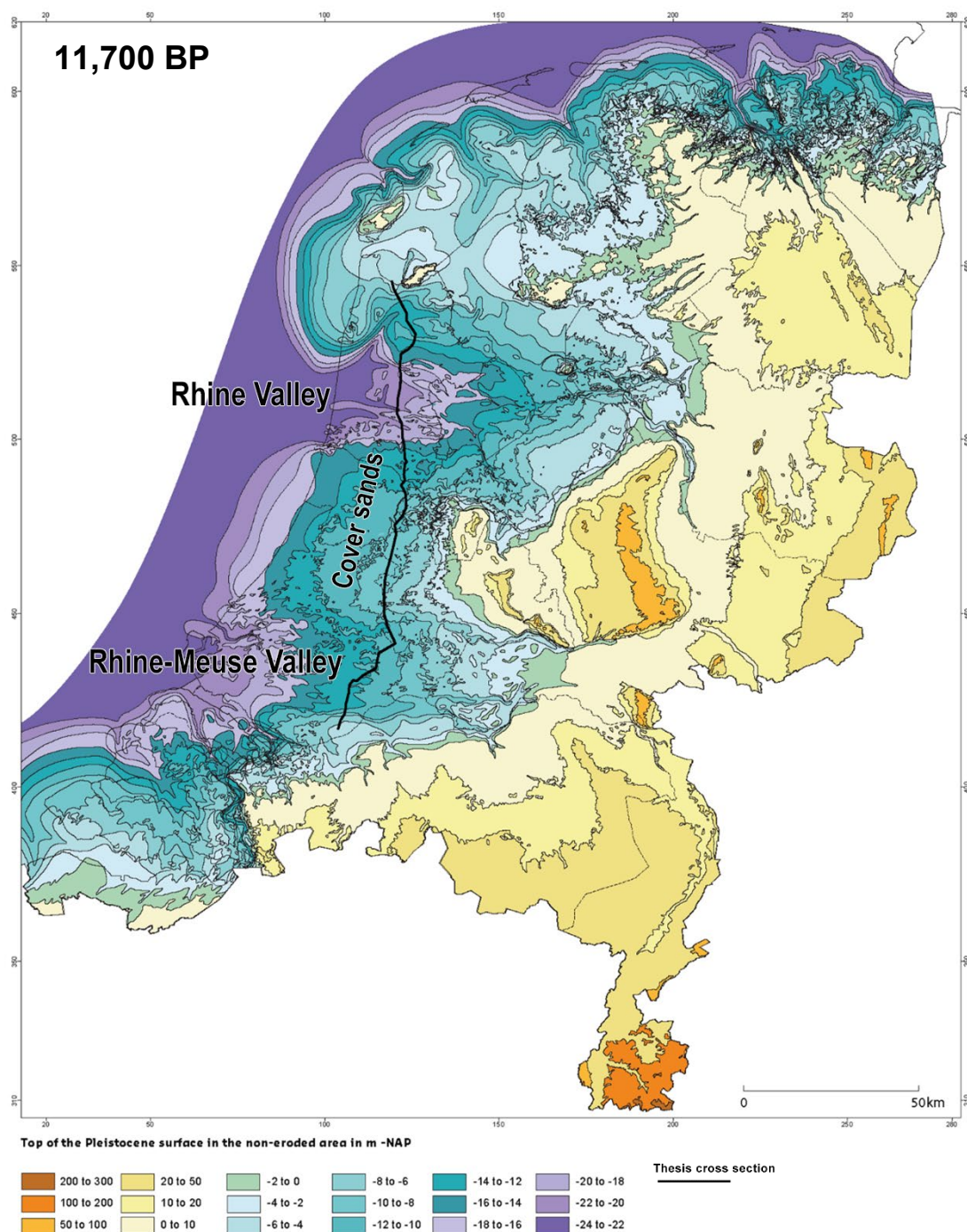


Figure 2.2: Map from Vos (2015) showing the elevation of the landscape at the start of the Holocene at 11,700BP

During a short period between ~8500 to 8000BP (Early Atlantic) the rate of eustatic-SLR doubled due to the massive influx of water from two Canadian glacier lakes that drained into the Atlantic Ocean (Hijma & Cohen, 2010; Törnqvist & Hijma, 2012). During this period, in the Netherlands the coastline reached roughly its current position. The landward shift of the coastline continued after this period moving the coastline further inland, past its current position.

Forward to 7500 BP (Middle-Atlantic), the sea level has risen to completely flood the Pleistocene valleys (Vos, 2015, Pierik et al, 2017; Haas et al. 2018). Along a large portion of the Dutch coastal plain a back barrier basin formed (Figure 2.3). With the exception of the very south of the Netherlands and the area of the current Wadden Sea. The increased accommodation space trapped a large succession of tidal sediments (Naaldwijk Formation) along the coastal plain.

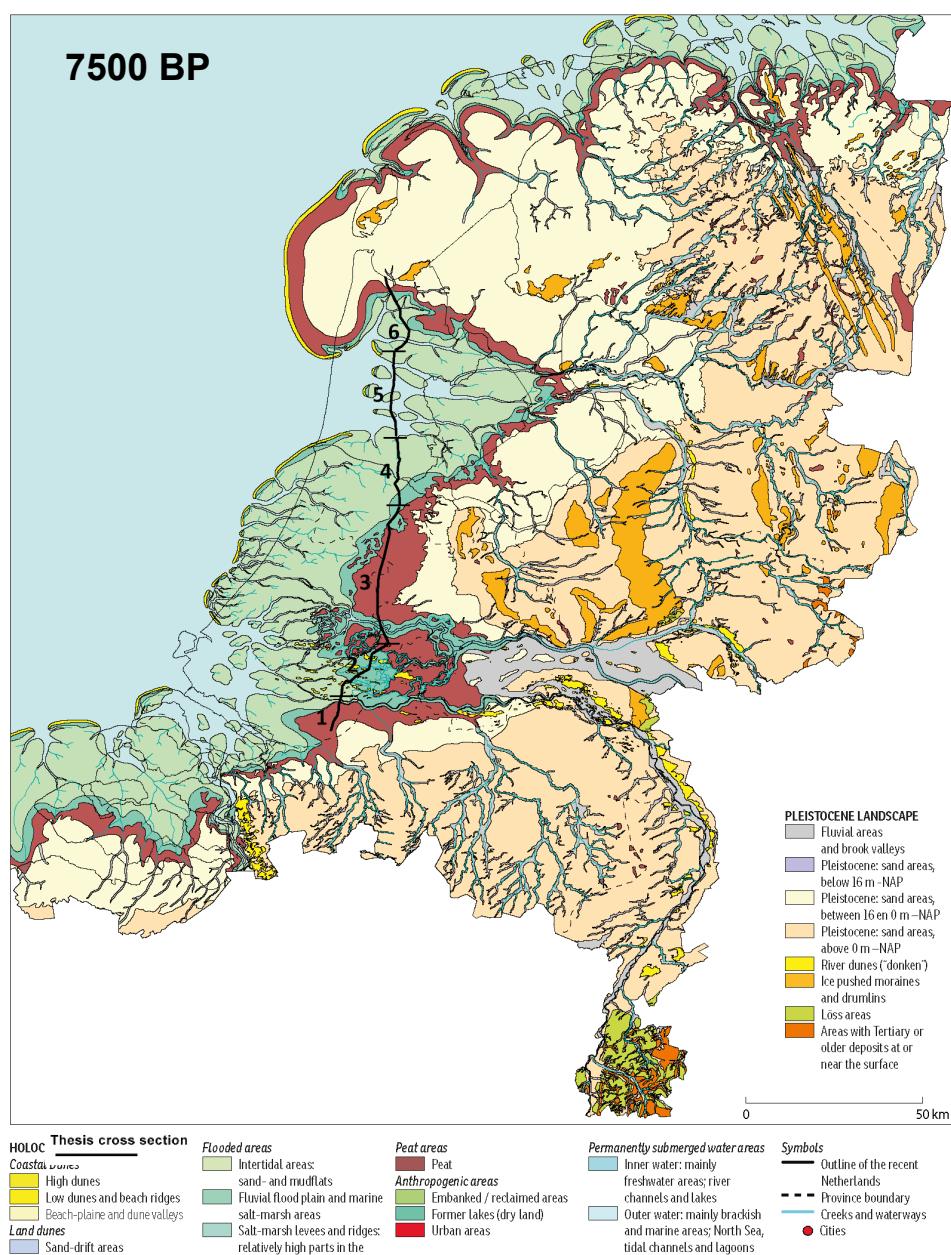


Figure 2.3: Map from Vos (2015) showing the Dutch landscape at 7500BP.

After the Middle-Atlantic, until about 4500BP, the rate of sea level decreased and the balance between the creation of accommodation space and sediment supply shifted in favour of the latter (Hijma et al., 2009, Pierik et al., 2017; Haas et al., 2018). As a result, the coastline prograded back to roughly its current position. By 4750

BP (Figure 2.4) beach ridges had formed along large parts of the coastline with large peat beds forming in the areas behind these ridges.

2.2.2 Basal peat Formation

Rising groundwater levels, due to relative SLR, triggered the Formation of large peat beds on top of the Pleistocene surface and Early-Holocene river sediments. This basal peat formed between 9000 and 6000 BP with the oldest peats in the west and the youngest peats in the east, following the transgression of the coastline and inundation of the land throughout this period (Pierik et al., 2017; Haas et al., 2018). In many areas, this basal peat layer is still present on top of the incompressible Pleistocene surface, making it an excellent layer for dating purposes. Because this layer is still presents in many areas along the Dutch coastal plain, has not been greatly affected by compaction and serves as a marker of inundation of the coastal plain.

In some areas, the peat is missing due to different causes: (i) The peat is eroded by fluvial or tidal processes, (ii) No peat could form due to the presence of Early-Holocene rivers of the Rhine and Meuse river systems. In the latter case, the basal peat layer is intersected with coarser-grained channel beds that are incised into the Pleistocene surface (Gouw & Erkens, 2007).

2. 3 Middle- to Late-Holocene tidal inlet systems

2.3.1 Northerly systems

At the start of the Holocene (11.700 years cal BP), the Pleistocene incised Rhine-valley carried the water of the Vecht to the sea, which was located further west compared to the present (coastline not visible in figure 2.4)

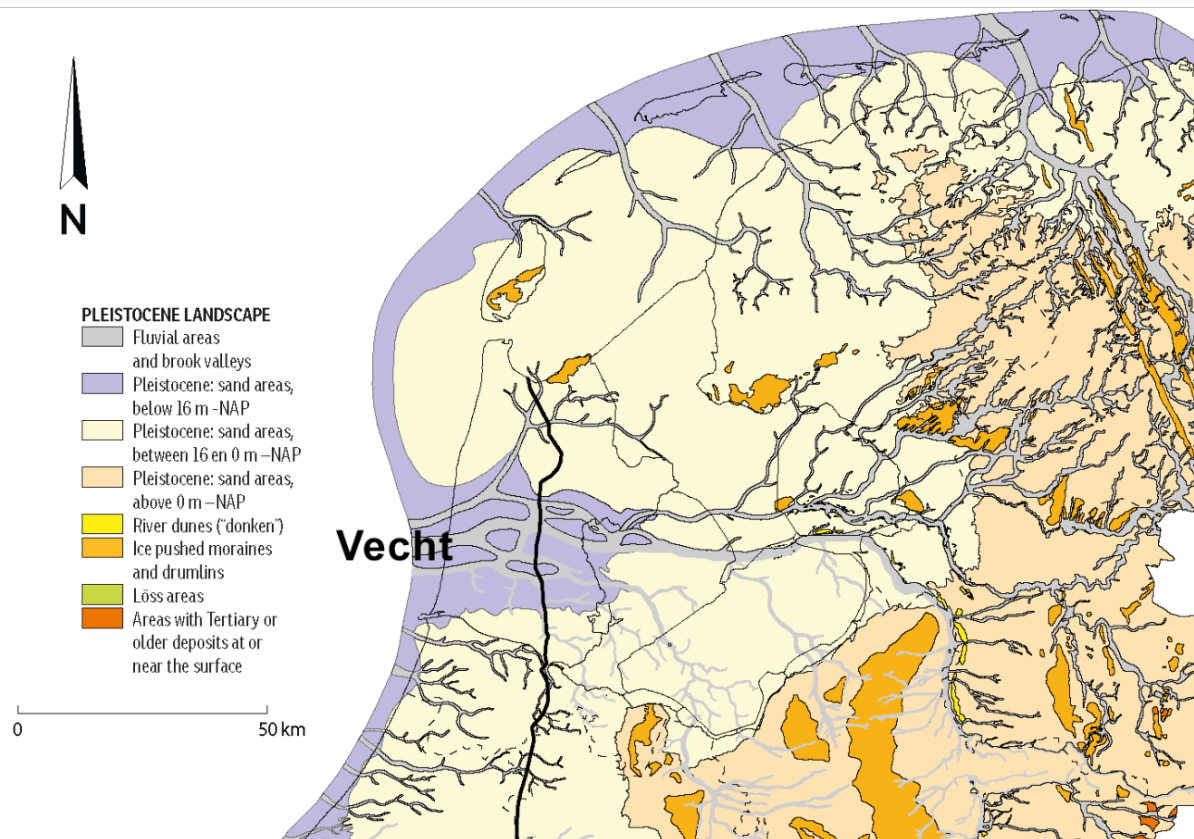


Figure 2.4: Zoomed in and adjusted map from Vos 2015 showing the northern paleo valley from where the Vecht debouches.

During the Atlantic (figure 2.5) the inundation of the Rhine valley started. By 7500 cal BP the sea had inundated large areas of the area above Amsterdam, creating a large tidal system (fig 2.3). This tidal system was characterized by several large tidal channels and extensive intertidal flats, basins, and supratidal salt marshes (Vos, 2015, Haas et al., 2018).

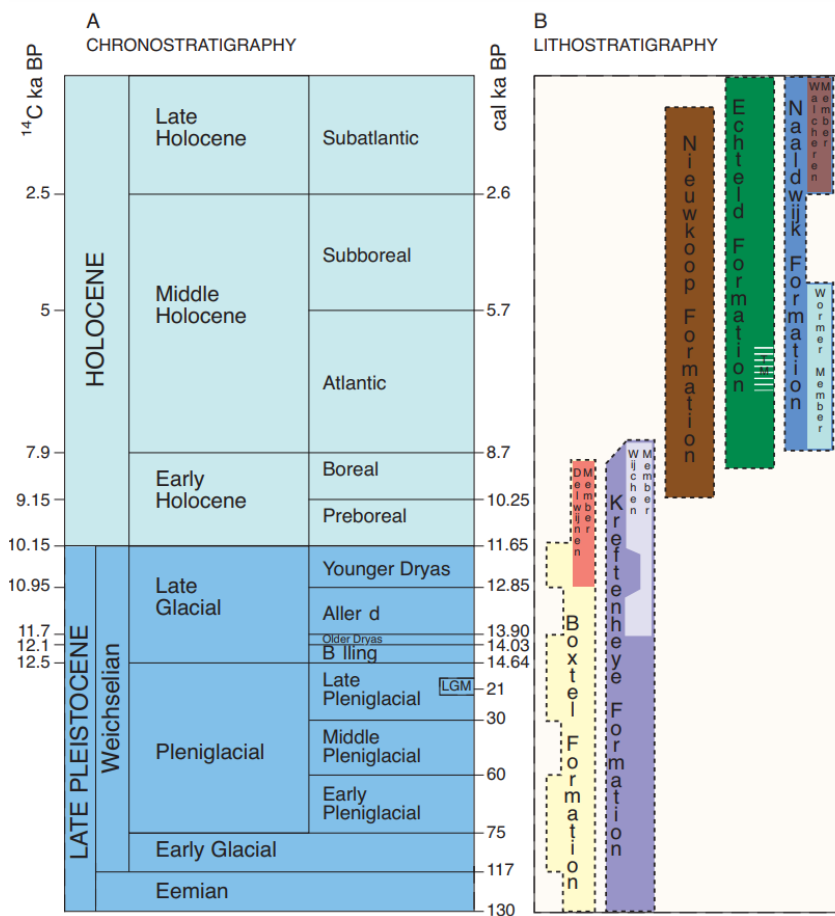


Figure 2.5: Chronostratigraphic and lithostratigraphic timelines from Hijma et al., (2009) showing both the ^{14}C ages and corresponding calibrated ages of different periods in the Late-Pleistocene and Holocene, including the ages of different lithostratigraphic units mentioned in this research.

After 7500 BP the tidal system extended eastwards, with its margins reaching towards the Province of Overijssel near the city of Zwolle. During this time vast areas of Noord-Holland are either covered by (brackish) intertidal areas or open water (Vos, 2015). Below Amsterdam, large peat bogs started to expand seawards.

When the relative sea level rise slowed down, the system was slowly abandoned and filled with marine sediment and large peat bogs, as demonstrated by figure 2.6 showing the landscape at 4750 BP. Two tidal inlets remained active, with the Bergen inlet being significantly larger than the Oer-IJ inlet. The Bergen inlet covered a large area, stretching from the coast towards the current city of Hoorn. The coastline moved further westwards closer to its current position together with large peat bogs.

By 4750BP most of the tidal inlets that dented the Noord-Holland coastline had closed off, with the exception of the Oer-IJ inlet and the remaining channels of the Bergen inlet (fig 2.6) (Haas et al. 2018). These channels now functioned as drainage channels for the peatlands rather than being tidal channels (Vos et al., 2015). A lot of these peat bogs have been excavated in the last two millennia creating large lower lying areas in the province of Noord-Holland.

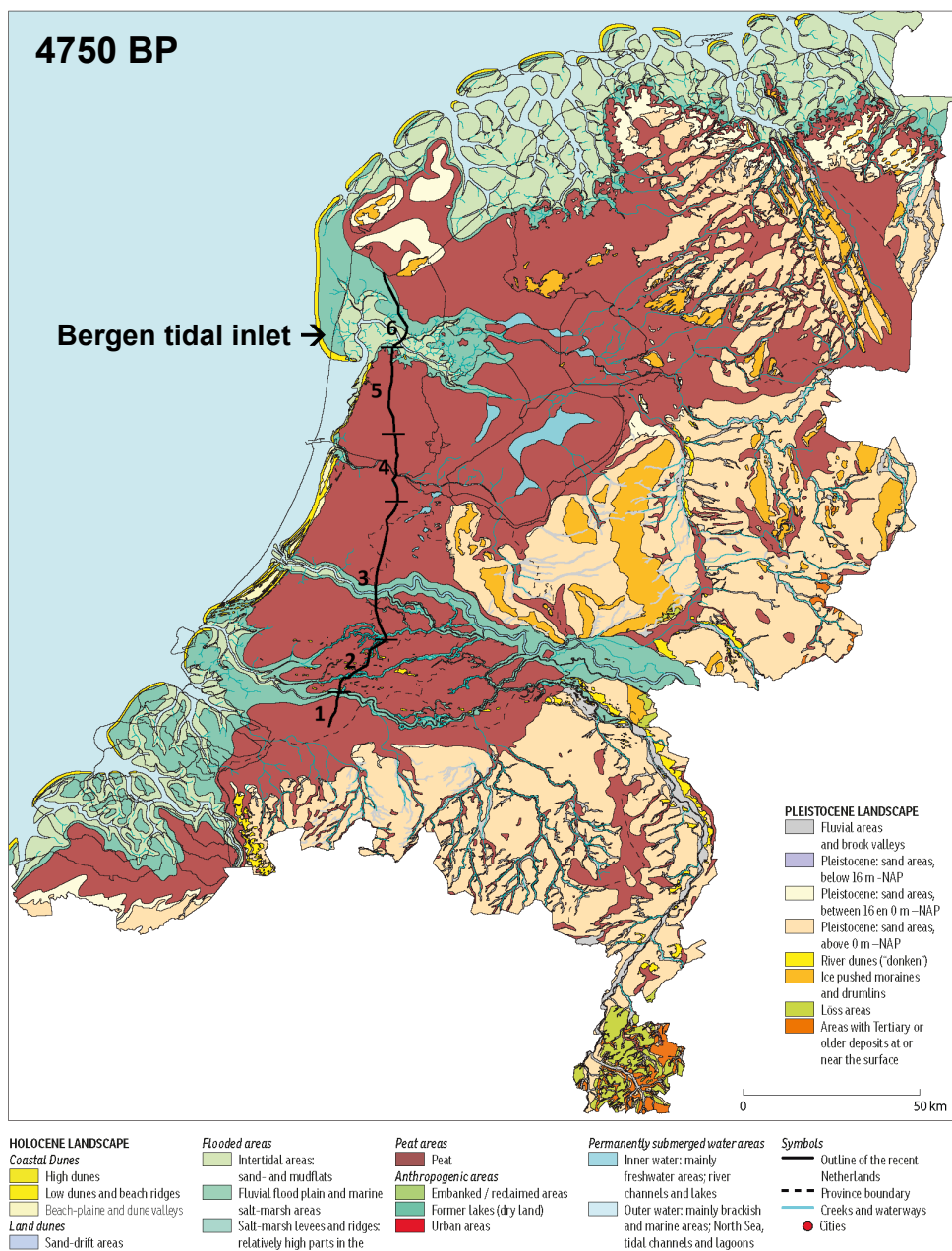


Figure 2.6: image adjusted from Vos (2015) showing the Dutch landscape at 4750BP

2.3.2. Southerly systems

In the south (subsections 4,5 & 6) the sea transgressed the southern paleo valley in the Early-Atlantic (9-8ka Cal BP) transforming it into a major estuary (Hijma et al., 2009; Hijma & Cohen, 2011). Before inundation, the influence of sea level rise was already felt by the rivers in the form of an increase in flood deposits around the channel belts due to the reduction in river gradient.

Around 8000 BP the flood plains in this area were permanently flooded. Later, after 8000 cal BP a bay-head area delta formed near Delft, seaward of the cross-section in this research. Many avulsions shifted the Rhine river mouth from around Rotterdam to the north until the river mouth reached its most northern point near Leiden at around 6.5ka. The Meuse river kept its river mouth near Rotterdam throughout the Holocene (Hijma et al., 2007).

The transgression of the North Sea continued to about the Late-Atlantic (6000 cal BP). By this time a large portion of the current Dutch Coastline was covered by a Tidal Basin and Estuary. The eastern border of this tidal basin is slightly west of my cross-section. The most eastern cross-section from Hijma et al., (2009) shows no tidal sediments, so it is unlikely to find tidal sediments in subsection 2 of this research.

The period after the Mid-Atlantic marked the moment that the balance between sediment supply and the creation of accommodation space changed. As a result, the landward shift of the coastal depositional environments halted. Around 6000 BP the tidal inlets started to close, eventually leaving only the Rhine estuary near Leiden and the Meuse estuary near Rotterdam as the only openings in the barrier ridge system.

Later in the sub-boreal, extensive peat beds formed in the low energy environments of the flood plains. These peat beds get progressively thicker in the landwards direction. The different kinds of peats that formed during this time are characterized in the Holland Veen member of the Nieuwkoop Formation.

2.4 Land subsidence

The total land subsidence during the Middle-Holocene is made up of three different components: (i) Glacio-isostatic adjustment (GIA) due to the collapse of the forebulge from the Weichselien ice age (Vink et al., 2007); (ii) The compaction of weak sediment and peat layers (Van Asselen et al., 2009) (iii) And, a variety of other background subsidence such as the tectonic motion of the North Sea depocenter (Arfai et al., 2018; Cohen et al., 2022) and the compaction of Tertiary and younger sediments (Kooi et al., 1998). In figure 2.7 an estimation is given for subsidence rates over the Netherlands for each component. In this figure it is clear that the Northern areas of the Netherlands experience higher subsidence rates compared to the south, for each component. This section continues shortly describing each subsidence component in the context of this research.

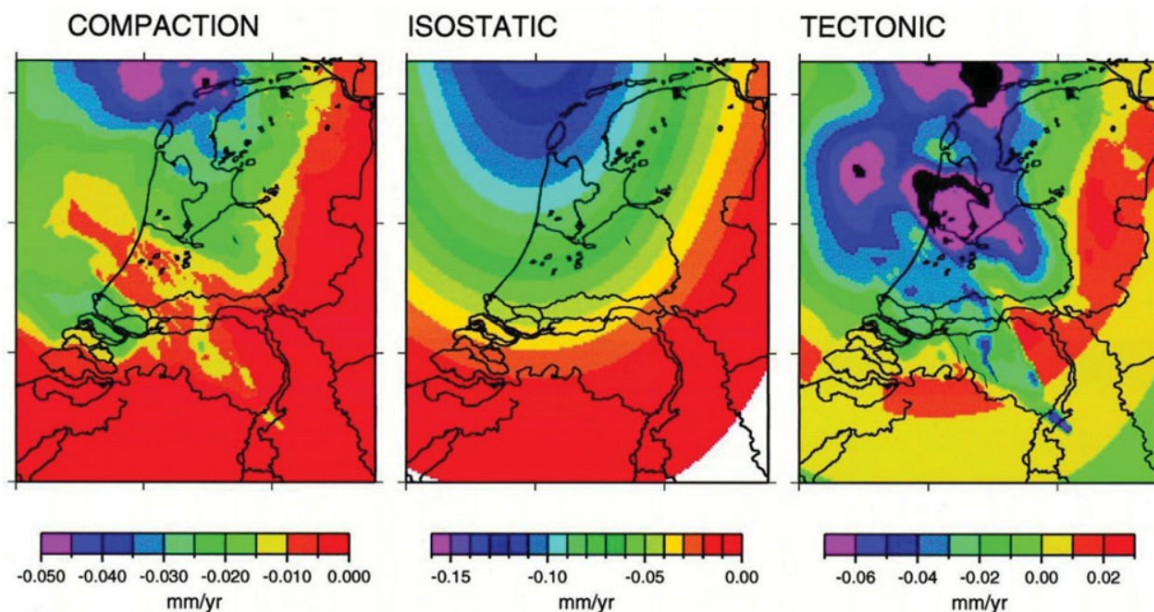


Figure 2.7: vertical land movement for each component for the last 2.5M years. constructed by three-dimensional backstripping of Cenozoic stratigraphy of the Netherlands and the southern North Sea basin. (figure from Kooi et al., 1998).

2.4.1 Glacio-isostatic adjustment component

During the last Ice-age, the Netherlands was located relatively close to the crest of the forebulge, with an average height difference of +100m to the Earth's geoid. This forebulge formed as a response to the loading of the lithosphere by the LGM ice sheet. Since 27.000 years BP this forebulge crest is receding back at an average rate of 0.1-1mm/yr (Vink et al., 2007; Vermeersen et al., 2018). This process of isostatic relaxation is not linear but started off relatively fast when the Earth's crust bounced back from the reducing weight of the ice masses (Vink et al., 2007). This means that by the start of the Holocene a significant part of the forebulge had already sunk. The bounce-back of the mantle is however much slower, due to its viscous nature. Again, this subsidence rate has not been linear through time, it is estimated that the subsidence rates were higher in the Early to Middle-Holocene compared to now. The area of the most significant forebulge subsidence is modelled to be a narrow band between Lower saxony and the Dogger bank area in the Southern North Sea (Vink et al., 2007). This is to the north of the study area in this paper. Data analysis studies and geophysical modelling by Kiden et al., 2002 found an increase in glacio-isostatic lowering from the Southwest to the Northeast along the Belgian and Dutch coastline, which is also hypothesized in this research.

2.4.2 Basin subsidence component: depocenter tectonics and deep layer compaction

The North Sea Depocenter is an active area of subsidence from continental rifts, sediment loading as well as GIA. Averages subsidence rates for this area were determined over the last 2.6Myr and are presented in figure 2.8 (Cohen et al., 2022). Another source for background subsidence is deep layer compaction (Kooi et al., 1998). This research found variation in subsidence with higher rates in the north of Noord-Holland compared to Zeeland (Table 2.5)

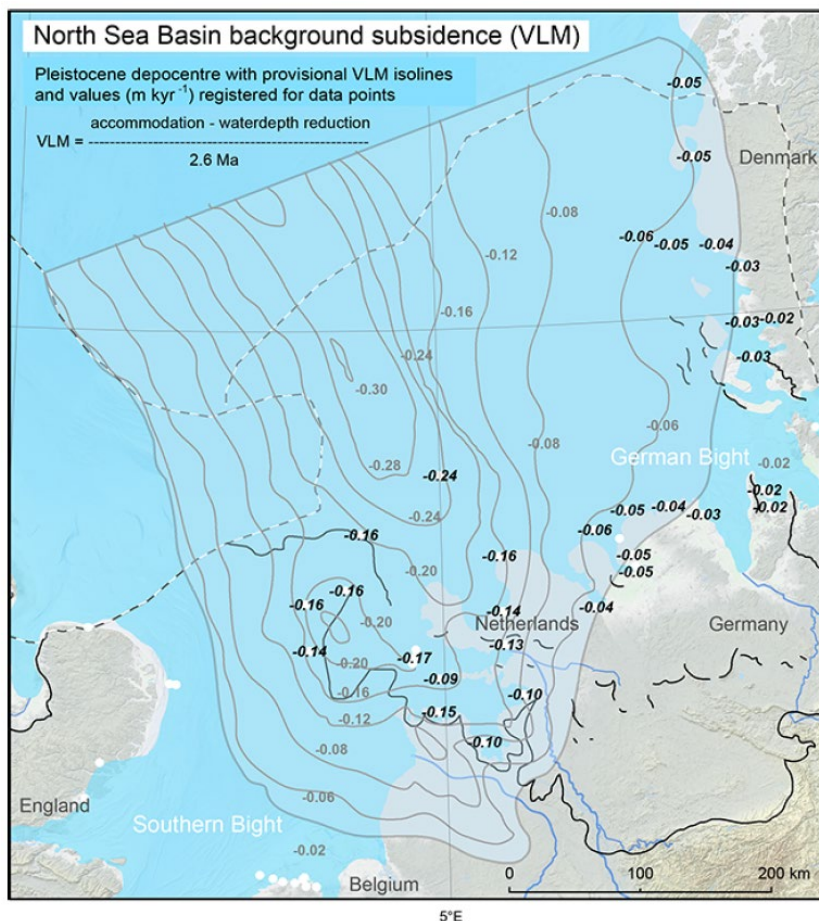


Figure 2.8: Map (fig.3) from Cohen et al., showing rates of vertical land motion (subsidence) over the North Sea basin using last interglacial data points. Grey lines represent contours of equal subsidence. Black italic values are WALIS VLM entries for late interglacial data points. Notice the area of the Netherlands with the paleogeography of the Eemian highstand. Dark black lines show ice extent before and after the last interglacial.

2.4.3 Peat compaction component

Being the most compressible natural sediment, peat is easily deformed by weight from overlying sediments (loading). Its volume furthermore decreases due to biological (microbial decomposition) and chemical processes (oxidation) as explained by Van Asselen et al. (2009). Koster et al. (2018) studied compaction along the Dutch coastal plain and found compaction up to 3m in rural areas and as high as 5m in urban areas, by comparing ^{14}C dated peat depths with reference groundwater levels.

Similar to peat, clay can also induce subsidence due to a variety of processes, such as consolidation by compaction (Changxing et al., 2007; Vonhögen et al., 2010, Kooi & Erkens, 2020) and dehydration (Liu et al., 2001; Kooi & Erkens, 2020).

The subsequent subsidence has an influence on delta Formation and river characteristics (Van Asselen et al., 2009). Subsidence of peat layers plays a significant role throughout the Holocene and is still a relevant topic today. Due to its irregular occurrence in the sediment record and the different causes of peat volume loss, the influence of peat-related subsidence can differ on local scales. Due to the resolution of the transect of this research (any structures smaller than one kilometre are not well defined), local differences at scales smaller than one kilometre will not be visible. Differences at larger scales will likely be visible and recognizable in the transect.

Subsidence rates from these different components that make up the total subsidence in the Netherlands have been collected in Table 2.1. All rates have been changed to mm/yr. These values will later be used to estimate the different causes for subsidence along the cross-section for validating the results from this research.

2.4.4 Relation to accommodation space

Both eustatic sea level, as well as subsidence, create accommodation space for sediments. Gouw & Erkens (2007) estimated that before 5000 BP eustatic sea level rise is the dominant driver that is reflected in the sedimentary architecture of the Rhine-Meuse delta. Between 5000 and 3000BP the dominant driver became land subsidence.

Table 2.1: Table with collected subsidence rates for different subsidence components. Values for specific values were not found for each component so the average values were used.

Type	Specific area	Rate in mm/yr	Constant through time?	Local (<20km or regional (>20km)	Source
Glacio-isostasy	-	0.1-1	No	Regional	Vink et al. (2007); Vermeersen et al. (2018)
Tectonic subsidence	Zeeland	Ca 0.05	Yes	Regional	Kooi et al. (1998); Vink et al. (2007); Cohen et al., 2022
	Western-Netherlands	Ca 0.1			
	Noord-Holland	0.12-0.17			
Holocene-averaged subsidence rates GW-rise interpolations	Zeeland	0.1	Assumed yes		De Wit et al., 2022
	Groningen & Wadden Sea	0.4	Assumed yes		De Wit et al., 2022, Vermeersen et al., 2018
Peat oxidation and compression	Noord-Holland	1-12			Koster et al. 2017
Differential subsidence along fault-zones (interpolated)	Zuid-Holland / Rhine-Meuse Delta	0.03–0.07			Cohen, 2005
Peat oxidation and compression		1-140			Van Asselen et al., 2018

3. Materials

For this research a variety of sediment cores, 14C samples and GIS-datasets were used. In this chapter I will list the materials and describe how they were used.

3.1 Cores and 14C samples

3.1.1 Sediment cores descriptions

To create the lithogenetic cross-section, that describes the Dutch subsurface structures, sediment core descriptions were used. These descriptions were obtained from TNO, and are part of the GeoTOP v1.4.1 datasets. GeoTOP is a model which uses digitalized sediment cores to create a three-dimensional voxel map of the Dutch subsurface (available through DINOloket.nl). For this research, only the cores that contained sediments from the Naaldwijk Formation, Wormer Member (including the Velsen Member), and the Nieuwkoop Formation, Basal Peat Member were downloaded from the GeoTOP website and plotted into ArcGIS Pro.

When deciding on the definitive cross-section location, the cross-section was first adjusted to the nearest, suitable 14C location. Then the GeoTOP v1.4.1 cores were used to finalize the location of the cross-section. Since most areas had an abundance of GeoTOP v1.4.1 cores, this was relatively easy. However, in some areas the amount of available cores was limited, such as the urban areas of Amsterdam and Dordrecht. In the better areas, with plenty of options, cores were chosen based on their depths and location. Cores already close to the cross-section were preferred over cores further away and deeper cores were preferred over shallower cores, to ensure all of the Holocene deposits were present in the core.

After the core selection was completed, the original, detailed core descriptions (in PDF format) were requested for each core from TNO. In total 241 TNO cores were used. The core descriptions were of varying quality, from very detailed descriptions of every decimetre to very simple descriptions of meters of sediment at a time. A full list of cores, with the core numbers, can be found in appendix A.

3.1.2 14C dated peat samples

To create the isochrones 14C dated peat samples were used as a basis for age-depth relationships within the cross-section. All of the 14C dated peat samples were made available through WikiWFS (wikiwfs.geo.uu.nl) with all the core datasets from the University over the last couple of decades. Appendix B gives a full list of all 91 14C samples used in this research.

The two main criteria in selecting which 14C samples to use were location and age. Samples that were within 5km of the initial cross-section line were prioritized and samples of ages younger than 3500yr cal BP were discarded during the initial selecting phase.

Many of the 14C samples are located on or very near the cross-section. However, in several cases the samples are located further from the line, with the most extreme cases the extra cores in the north of the cross-section, with distances of 16km to the cross-section. There is a risk that the ages from these C14 samples do not correspond to the ages of the sediments in the vertical profile. However, since the amount of 14C samples is limited, the decision was made to use them. To fit them to the line, they were projected on the cross-section using a straight East to West line.

14C calibration in OxCal

The obtained 14C dates were not yet calibrated. In order to get dates in yrs cal BP, the 14C samples were calibrated with the online tool OxCal (c14.arch.ox.ac.uk). For the calibration output the following settings were

used:

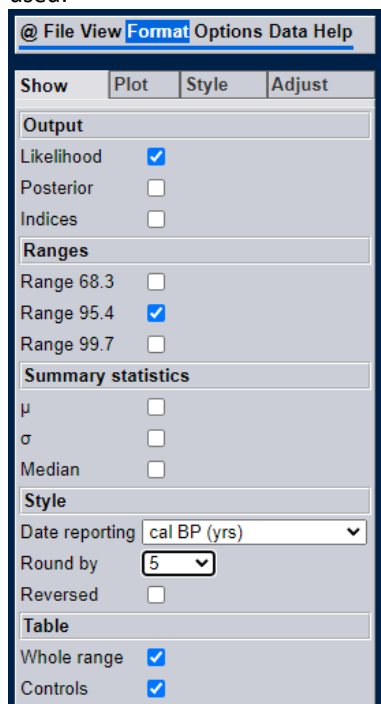


Figure 3.1: Settings in used in exporting calibrated 14C samples

3.2 Existing cross-sections

The cross-section in this thesis was purposely linked to cross-sections from other researchers (Figure 2.1). This way this thesis is nestled into the already established knowledge, extending the existing cross-sections and linking different cross-sections together. Furthermore, these existing cross-sections also aided in interpreting sediments from core descriptions, by being an example of how others interpreted certain deposits.

Starting from the Northern edge of the cross-section, the first cross-section that I fitted into my own cross-section is created by Westerhoff et al., (1987). This older cross-section uses the stratigraphic descriptions from Zagwijn & Van Staaldunin, 1975 (Replaced by a new system from (Weerts, 2003) and does not offer much detail for the focus period of this thesis (Early and Middle-Holocene). It does however show the structure of the Pleistocene surface and it is linked to geological maps of the area.

The second cross-section, included in my cross-section, is a smaller cross-section (D-D') from De Gans, (2015). This cross-section is a small part of a larger study, done during the construction of the North-South metro line in Amsterdam. It covers the streets of Rokin and Damrak in the city centre of Amsterdam. This includes the channel of the Amstel river.

The third cross-section that was included is from Van Asch, (2007). Only part of their cross-section is used. Starting in the North near the provincial border between Zuid-Holland and Utrecht and ending at the Southern end of the cross-section by Van Asch, (2007) at the Zevender river dune. This cross-section shows the locations of river dunes and the structure of peat and clay layers. All cross-sections mentioned above can be found in appendix C.

3.3 Maps and GIS datasets

Digital and physical maps of lithology and subsurface structures were used to determine the location of my cross-section. With the maps areas of interest could be identified and I could adjust my cross-section to this area of interest. For example, in the north, I adjusted the line to include tidal channels in the area. Secondly, the maps were used to avoid running my cross-section parallel to a channel belt. This would create a large body of sandy deposits in my cross-section, while it also means that the cross-section loses detail. Since this is undesirable, I made sure the cross-section line ran perpendicular to the direction of the channel belts, using these maps.

3.4 Interpolated groundwater isochrones

In the past Cohen (2005) and Koster et al. (2017) have used reconstructions of Holocene groundwater level rise to study subsidence during the Holocene in the Netherlands. The most updated version of this is being made by De Wit et al. (in prep.). This method uses trend fitting and interpolation by kriging to create a 3D-interpolation of groundwater level index points, using the age and depth of radiocarbon dated, coastal basal peat samples. The isochrones produced using this method show the relative GW-level rise over the Holocene, containing both the sea level rise and the post-depositional subsidence affecting the current depth of the groundwater index points. Some of the radiocarbon dated peat samples used for the interpolation, were also used in this study.

With the help from the author, I was able to obtain interpolated age-depth values for the exact location along the cross-section made during this thesis from the unpublished results from De Wit et al. (in prep.). The data I received for this research, is represented in figure 5.2.2 of the results.

4. Methods

4.1 Literature study and data availability review

At the start of this thesis, a literature study was conducted. The goals of this literature study were to: (i) Create the theoretical framework for this thesis in chapter 2; (ii) Find existing cross-sections that could fit into my cross-section or are located in the vicinity of my cross-section; (iii) Learn more about research using cross-sections.

Another goal of the data availability study was to find which data was available for creating the cross-section. I was greatly helped by my supervisor who could obtain original core descriptions through TNO. All the data sources and their use are described in chapter 3 of this thesis.

All the data that seemed useful, including the locations of cross-sections from the literature, were loaded into ArcGIS Pro to create a clear overview of the available data. The next step was to use this data to decide on a location for my cross-section.

4.2 The location of the cross-section

The location of the cross-section is decided based on a variety of conditions:

- First, the cross-section should span a large part of the Dutch coastal plain,
- while also running roughly parallel to the coastline.
- Existing cross-sections in literature offer extra detail for certain areas;
- Availability of sediment core descriptions is an important

The parallel nature is important for subsidence research, since it is preferable that the sediments in the north and the south were deposited around the same time at the same depth. Otherwise, there is a risk that the difference between where the sediments were deposited is caused by other factors than subsidence.

First, both of the most northerly and southerly ends of the cross-sections were decided. The northerly end was chosen to be 2.5km Northeast of the town of Breezand. Located on the Balgzanddijk which borders the Wadden Sea. The southerly end was chosen to be near the city of Dordrecht, at the embankments of the Hollandsch Diep waterways. In a straight line, the distance between these points is roughly 130 km. Following the shape of the cross-section the length is 147,7 km. With these locations, I ensured the cross-sections would cover a significant part of the coastal plain, from the shallower marine deposits of the Wadden Sea to the edge of the Holocene deposits in the South. Whereby the cross-section would cross the Pleistocene valleys in the provinces of Noord- and Zuid-Holland.

Another important factor in deciding where to place the cross-section, were other existing cross-sections in literature. This was mainly the case in the southern half of the cross-section, where a lot of studies have been conducted on the Rhine-Meuse Delta. A large number of cross-sections have been created in this area, both in the North-South direction (Hijma et al., 2009; Gouw & Erkens, 2007) as well as in the East-West direction. However, between the cross-sections of Hijma et al., (2009) and Gouw & Erkens, (2007) there is still a significant gap (figure 2.1). I chose to fill this gap with my cross-section. By laying my cross-section roughly in the middle of the gap between the other cross-sections I hope to help create a better image of the Rhine-Meuse Delta Deposits.

Some of the areas of interest that I wanted to include are: (i) The City of Amsterdam, where research surrounding the North-South metro line provided extra information (de Gans, 2015); (ii) The Island of Dordrecht, an area which has not been studied extensively due to the built-up areas. My aim is to improve on the knowledge of this area, by including it in my research.

Together, all these steps created a cross-section with a length of 147.7 km that contains 241 cores from GeoTOP v1.4.1 and 91 14C samples. The average distance between cores and 14C samples throughout the whole cross-section is ~520m. Compared to other cross-sections, the number of cores per unit of distance is lower. This is done in favour of covering a much larger area within the time constraints of this research. Besides, some areas did not have a core density high enough to achieve more cores per unit of distance.

4.3 Creating the cross-section

The next step is to turn the 2D line from ArcGIS Pro into a 2D vertical profile of the subsurface structures. For this, the cores (core information and coordinates) were exported from ArcGIS Pro into an Excel spreadsheet. The cores were separated into their subsections to make creating the 2D depth profiles more manageable.

The next step is to create graphs where the x-axis describes the length of the subsection and the y-axis the depth below the Dutch ordnance datum ($y=0$). The decision was made to have the Southernmost core at $x=0$ and the Northernmost core at $x=n$. This means that you are looking at the subsurface structures facing the North Sea and with your back to the hinterland.

First distances between cores were calculated with Pythagoras theorem, which is possible since the RD-new coordinate system works with meters:

$$\text{Distance between 2 cores} = \sqrt{(x_1 - x_2)^2 + (y_1 - y_2)^2}$$

X1= x-coordinate core 1

X2= x-coordinate core 2

Y1= y-coordinate core 1

Y2= y-coordinate core 2

Equation 1: Used for calculating distances between cores for 2D depth plot.

For the graph, the x-coordinate is calculated by adding up all the distances between the cores that are located before the core in question. The y-coordinate is the elevation of the land surface compared to the Dutch O.D. which is described in the core description. When this was done, more data was added, such as: (i) The core depths for each core. (ii) 14C sample depths and (iii) a line for the Pleistocene surface, which was plotted with

data from the Utrecht University. Initially, a line was added that described the surface elevation, extracted from AHN3 data (AHN, 2022) and based on the location of the cross-section line. However, the cores, and thus the surface elevations for the cores do not always correspond to the location of the cross-section, because some cores were projected on the cross-section line. As a result, too many mismatches between this surface elevation and the core elevations existed. This created a confusing situation in the drawing phase. Therefore, I decided to exclude this surface elevation line from the graphs, replacing it with a much simpler surface based on the surface elevation of the cores and details such as dikes. When the graphs were finished, they were printed on large-scale paper and cut to shape. These paper versions were used to create draft versions of the vertical profiles.

On the paper drafts the original core descriptions were plotted the corresponding depths, with which interpretation could be made on the shape and the extend of lithogenetic units.

4.4 Lithogenetic interpretations

The units in the cross-section are described based on their lithogenetic origin (e.g. Tidal channel, Natural levee, etc.). The deposits will then be further divided based on the commonly used system of Formations, members and layers.

Example: Tidal channel → Naaldwijk Formation → Wormer Member.

Below, I divided the deposits found in my study area into three categories: Tidal, Fluvial and Organic with their corresponding Formations (Naaldwijk, Echteld and Nieuwkoop). For each category I will describe the different lithogenetic units I considered for this research and the basis on which sediment was classed under a certain lithogenetic unit.

4.4.1 Tidal: Naaldwijk Formation Wormer Member (NAWO)

The Wormer Member of the Naaldwijk Formation contains the tidal deposits of the Early- and Middle-Holocene that are found in the western and northern Netherlands (Weerts, 2003). These tidal deposits include: Dune sands, beach ridges, tidal channels, mud and sand flats, lagoonal deposits and salt marsh deposits. Based on my initial research the presence of beach and dune sands in my study area was ruled out, since these deposits are only present in the western part of the Netherlands near the current coastline.

In my research I have chosen to differentiate the tidal deposits into the following lithogenetic units: (i) sand dominated tidal channel, (ii) mud dominated tidal channel, (iii) tidal channel fill, (iv) distal tidal clays, (v) Intertidal flats.

Sand/mud dominated (Sub)tidal channel

Sand dominated channels consist of sandy deposits, sometimes containing shells of different species. Where marine shells were found, it is presumed that the tidal channel was permanently submerged and thus lay below mean low water (Vos et al 2015). Tidal channels can contain clayey tidal laminations. Depending on the location these layers will either be classified as tidal flat or tidal channel.

During the drawing phase clayey deposits were found that had very similar characteristics as sand-dominated tidal channels. I later chose to describe these deposits as mud dominated tidal channels, indicating a lower energy environment. These channels contained clear tidal laminations, have similar shapes to tidal channels and in some areas have eroded the substrate. It is possible that some mud dominated tidal channels should be classified as tidal flats or vice versa. Figure 4.1 number 1 shows an example of a tidal channel in its geological setting.

Tidal channel fill

Sediments were classified as tidal channel fill deposits if they consisted of sandy clays overlying the sands of tidal channels. They are interpreted as the abandonment of the channel at this location and the decrease of the channel's ability to transport large, clastic sediments as sand. This is indicated by the switch to mainly sandy clays. The channel could have been abandoned either because the channel moved or because the channel was abandoned altogether.

Distal tidal clays

Within tidal basins, large areas of grey, organic clays containing shells and possible detritus can be found (Vos et al., 2015). Based on suggestions from my supervisor I classified these deposits under the lithogenetic unit called distal tidal clays, indicating clay that is deposited in relatively low energy environments. Mainly found along the edges of the tidal basin, further away from channels. Figure 4.1 number 2 shows an example of where distal clays in a tidal basin are located in relation to the other geomorphological units.

Intertidal flats

Intertidal flats were interpreted based on their composition and location. These tidal units are commonly found between tidal channel deposits and distal clays (fig. 4.1). Especially if the sediments were not above tidal channel deposits, I identified them as intertidal flats. Tidal lamination is common in these areas and this property is also used to identify flats. Figure 4.1 number 3 shows an example of where tidal flats in a tidal basin are located in relation to the other geomorphological units.

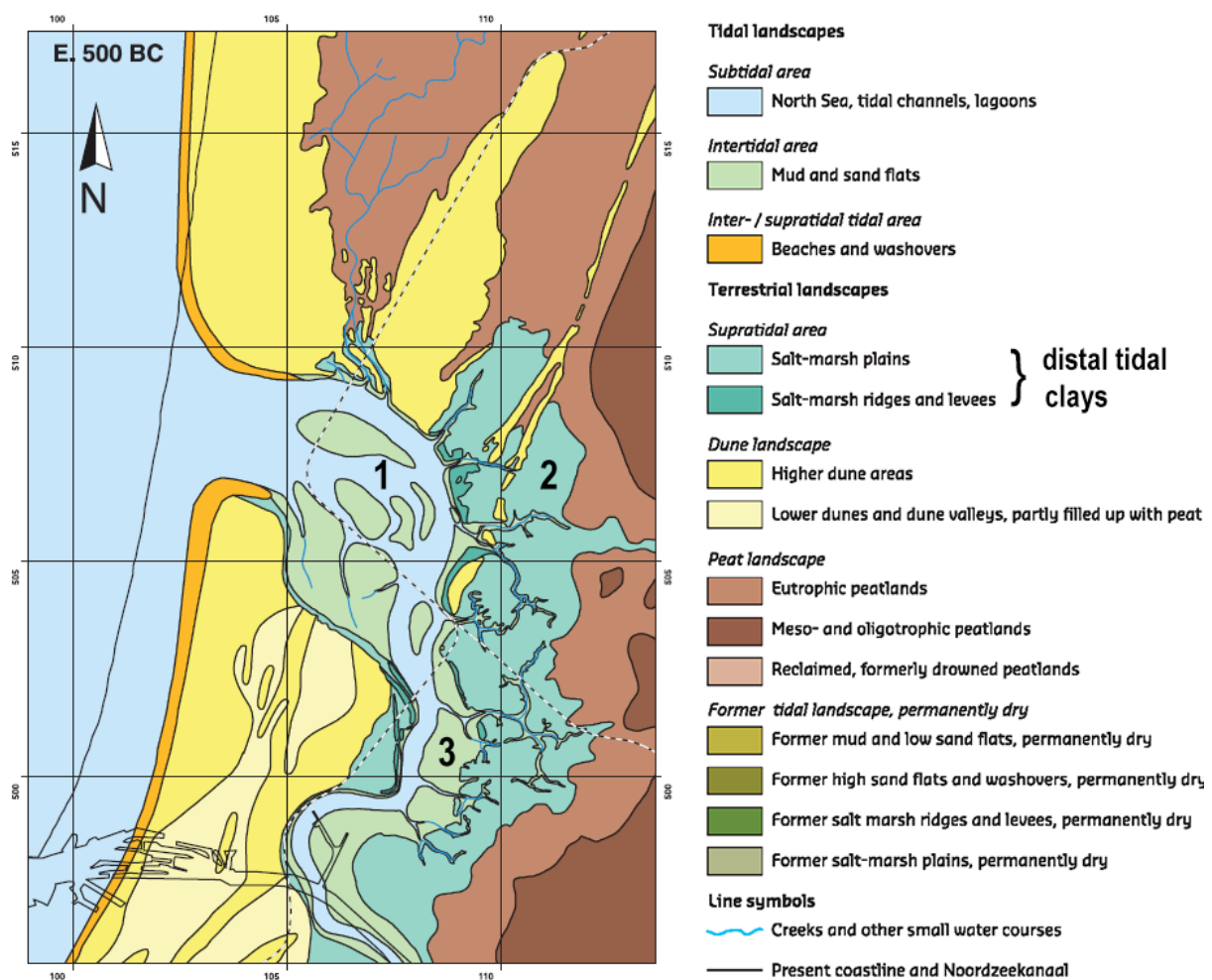


Figure 4.1: Altered figure from Vos et al., (2015) showing the Oer-IJ tidal inlet as an example of a tidal basin. This left over from the major tidal basin is many times smaller than what was once present. Numbers indicate certain areas, which are described in the text: 1: Tidal channel, 2 An area where distal clay deposits form; 3. Sand/mud dominated intertidal flats.

4.4.2 Fluvial

The Holocene fluvial and deltaic deposits of the Rhine and Meuse rivers, from the time that the delta formed, are categorized under the Echteld Formation (Weerts & Busschers 2003). Within this Formation, a classification exists based on lithogenetic origins. In my research I am making a distinction between the following lithogenetic units (i) Channel belt, (ii) Channel fill, (iii) Natural levee and crevasse splay, (iv) Proximal and (v) distal flood plain. Below is a more detailed description of each unit.

Channel belt

Channel belts are bodies of sand enclosed by natural levees and floodplain deposits. Within the Rhine-Meuse Delta, the sands are relatively fine grained due to their distance from deeper, coarser Pleistocene river deposits and the limited carrying capacity of the rivers in the deltaic plains. In some cases, the channel belts contain gravel at the bottom of the channel belt. The sand is part of the sediments that is deposited in the water carrying parts of the river. In the vertical profile the channel belts are drawn as U-shaped sand bodies, with natural levees on both sides. It is assumed that each channel belt has levees even when they are not found in the cores.

Due to the large horizontal scale of my profile, not all channel belts were present in my cross-sections. With the use of other vertical profiles (Hijma et al. 2009, Gouw & Erkens 2007) and GIS-datasets I tried insert all the major channel belts that I missed in the cores. Their depths are estimated by comparing the channel belt ages that are given in 14C years to the isochrones (in 14C years) I created. Where the top of the channel belt deposits marks the end of the channel belt's life and thus the youngest deposits from the channel. The depth of the channel belt was harder to determine and is often roughly estimated based on the shape and depths of other confirmed channel belts.

Channel fill

Sediments were interpreted as channel fill if they lie directly above channel belt deposits and show a clear upward trend from sand to clay and possibly to peat. Indicating the slow abandonment and filling of an old fluvial channel.

Natural levee and crevasse splays

Sandy clays with occasional sand layers are interpreted as natural levee and crevasse splays. Both lithogenetic units were combined into one, because the scale of the cross-section is too large to correctly identify between both deposits.

Proximal and distal floodplain deposits

Within the clays of the floodplains I made a distinction between proximal floodplain deposits and distal floodplain deposits. Proximal floodplain deposits consist of mild to very silty clays often found in the proximity of a channel belt. The high silt content indicates that the clays were close enough to an active river to receive relatively coarse sediments.

The distal floodplain deposits consist of mostly humic clays, with little to no silt mixed in. Indicating they were deposited further from the active channel belts than the proximal floodplain deposits. The presence of peat layers is not uncommon in these clays.

4.4.3 Organic - Nieuwkoop Formation peats and gyttja

All the peat that can be found along the Dutch coastal plain is classed under the Nieuwkoop Formation (Weerts & Busschers 2003). Several members further differentiate between different peat layers. The basal peat layer is categorized as the Bassiveenlaag Member (NIBA). The peats that formed on top of tidal or fluvial clays, are categorized as Hollandveen (NIHO). There are also thin peat layers that lay between the floodplain deposits of the Echteld Formation. These peat layers are often not labelled under a specific member of the Nieuwkoop Formation. In my research I stray away from this distinction in favour of differentiating between different kinds of peats (Gyttja, Reed, Sedge, Woody and Mossy peat).

In many cases the type of peat is identified in the core description. In cases where the type of peat is unknown, it is classified according to contextual information. For example, if the unknown peat on both sides is surrounded by reed peat, then the unknown peat is classified as reed peat. In cases where larger peat areas were not categorized in a specific peat, the peat layers are described as peat: unknown.

4.5 14C samples and creating isochrones

As mentioned, the calibrated 14C dates will be used to create isochrones, which are lines that bound the time frame in which a given part of lithological succession is formed. Step one is adding all the calibrated 14C dates to the correct sample depths to the vertical profiles. I then decided to create lines for the following ages (in years cal BP): 4000, 4500, 5000, 5500, 6000, 6500, 7000, 7500. Some calibrated 14C dates were close to these rounded numbers so I placed the lines close to these calibrated 14C dates.

For the 14C samples that differed more than 100 years from the ages described by the lines, I estimated the depth of the line. For this I calculated the average ages over the depth between two 14C samples. For example, between sample 1 and 2 there is an age difference of 1000 years and the thickness of the sediments between these two samples is 2 meters. Then each decimetre of sediment covers roughly 50 years. Using this measurement and the 14C sample that was closest to the line's ages should give a decent estimate for the line's depth.

Where possible I tried to connect the age lines to lithogenetic units in the vertical profile. For example, if the 14C sample was taken on the edge of a clay layer and the clay layer was relatively horizontal, I assumed that the edge was formed around the same time and the line follows this clay layer edge.

Normally when making isochrones, the isochrones follow the shapes of channel belts outer edge, since the channels often are situated in older sediments. In this research the choice was made not to do this, because the emphasis was put on the shape of the isochrones and not on the <100m scale details. So, the isochrones ignore channel belts and are represented as a dashed line when they go through channel belts of the Echteld Formation. Something similar is done for when isochrones cross into the Pleistocene surface. The isochrones continue into the Pleistocene surface as dashed lines. This is done so there are no gaps in the data and the overall shape of the isochrone is retained and they cover the whole coastal plain.

4.6 Approach for comparing land subsidence

The isochrones are used to compare the land subsidence between the southern end and the northern end of the Dutch coastal plain, by comparing at which depths the different isochrones of the equal age are currently found. By using a variety of isochrones (4000-7500 14C age) I hope to describe the difference in subsidence rates throughout the Middle-Holocene.

To compare the isochrones between the north and the south I make the following assumptions: (i) The materials that were dated were deposited at roughly the same level at the time of depositions. (ii) Land subsidence is caused by one of the processes as described in chapter 2.2.3.

The isochrones were extracted from the original lithogenetic cross-sections by measuring the isochrone depths at 5km intervals, starting at the most southern end. These sampled isochrone depths were then plotted in a graph (fig. 5.2.1). With these values calculations could be done for comparing depths between different regions of the cross-section.

To have an indication of the amount of possible subsidence due to compaction along the cross-section, the thickness of peat layers was measured at the same intervals as the isochrones. From this data bar plots are created for four depth categories (0-5m, 5-10m, 10-15m below Dutch O.D. and the total) that display the thickness of peat layers at each interval for the different depth regions.

4.6.1 Extra 14C samples for subsections 1 and 6

After obtaining the first results, it was clear that the most northern subsection had very limited 14C data availability. So, several more 14C-samples were taken from the 14C-dataset, indicated in red in the cross-section and graphs. Their locations are plotted in figure 4.2. Note that these 14C samples are located further away from the cross-section.

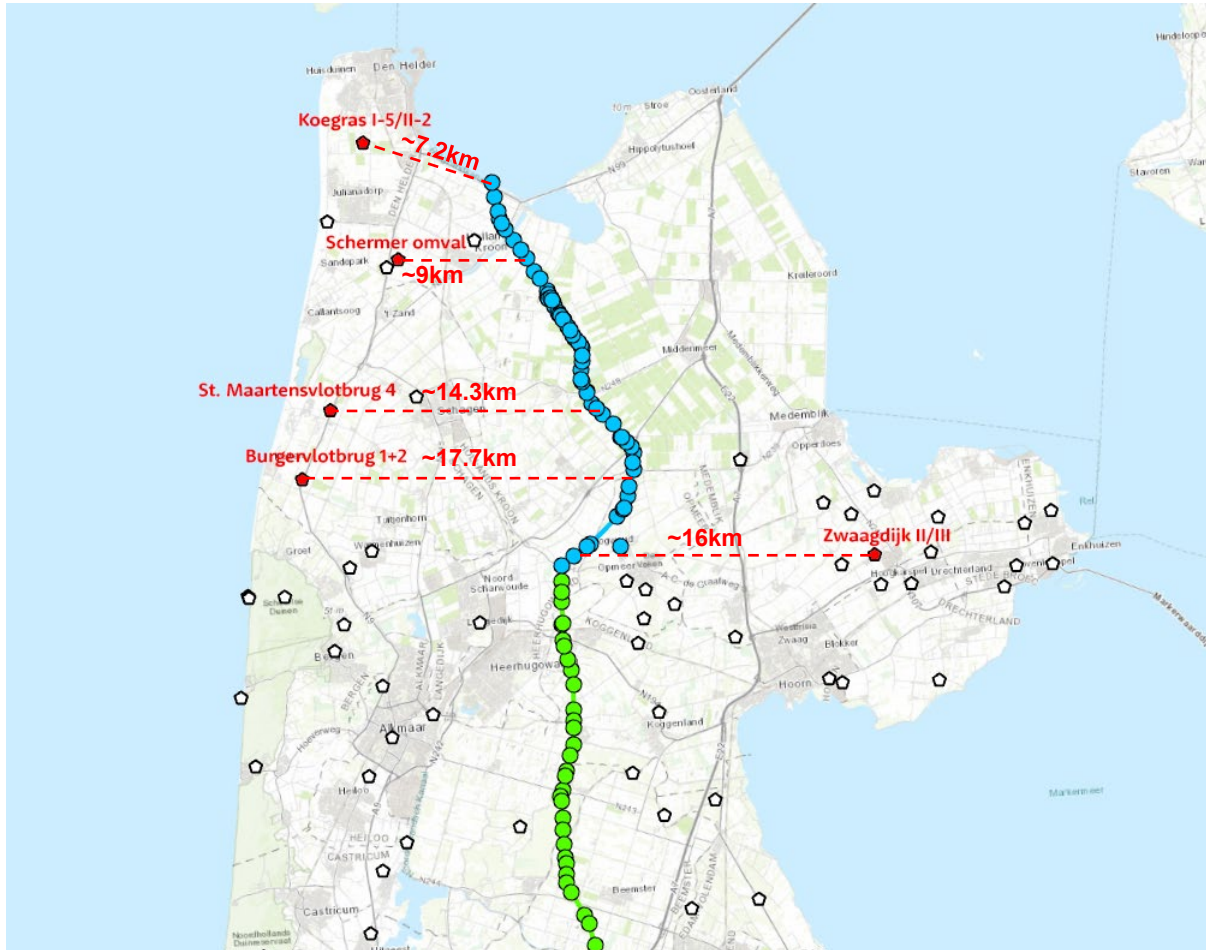


Figure 4.2: locations of extra 14C samples (red) in the north with their respective distances from the cross-section. Note that the other 14C samples shown did not have recorded ages that were old enough.

In the very south of the cross-sections (figure 5.2.1) the isochrones show a significant dip around the final 14C sample. Some extra 14C samples were taken between 5 and 6.5 km further south, to see if this dip would continue. The locations of these extra samples are shown in figure 4.3 below. These samples do not feature in the lithological cross-section.

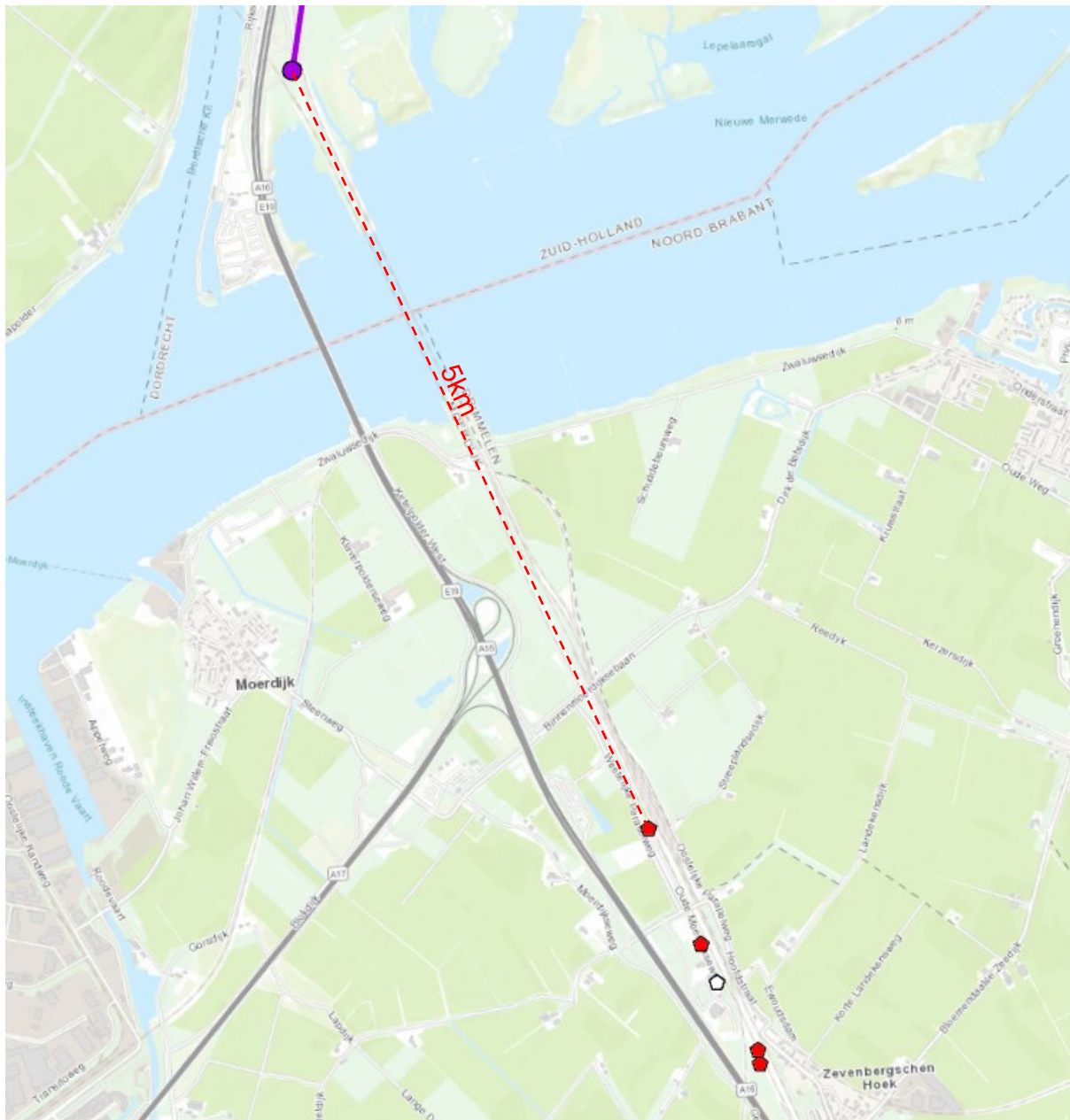


Figure 4.3: Extra cores in the south that were chosen to see how the trend in the isochrones continued to the south.

5. Results

5.1 Cross-section descriptions






The results start with descriptions for every subsection. The most detailed descriptions are reserved for the northernmost subsections, since the north of the Netherlands lacks sizable cross-sections that cover Holocene sediments.

Appendix D shows the entire cross-section as one image. The paleo valleys are clearly visible as thicker successions of Holocene deposits. The transition from left to right, from fluvial to tidal is also clearly visible. The legend (fig 5.1) below contains the units for the subsections and the overview maps.






Cross-section legend

Middle-Holocene

Naaldwijk Formation -Wormer member

-  Sand dominated channel
(Sand with shells and possible lamination)
-  Tidal channel fill
(Sandy clays)
-  Mud dominated tidal channel
(Sandy clays laminated with sandy layers)
-  Mud and sand flats
(Sandy clays with possible lamination)
-  Distal tidal clays
(Clays with possible shells and organic fragments)

Echteld Formation

-  Fluvial channel belt deposits
(Sand and gravel)
-  Levee and crevasse splay
(Sandy clays with possible lamination)
-  Fluvial channel fill
(upward fining of sediments above channel belt)
-  Proximal flood basin
(Silty clays)
-  Distal flood basin
(Humic clays)

Nieuwkoop Formation

-  Mossy peat
-  Sedge peat
-  Reed peat
-  Woody peat
-  Gyttja - lacustrine deposits
-  Undifferentiated peat





Pleistocene undifferentiated











Late-Holocene undifferentiated



Symboles

-  Core location
-  Core end
-  Core continues deeper
-  14C sample

Timelines yr cal BP

-  4000
-  4500
-  5000
-  5500
-  6000
-  6500
-  7000
-  7500

Channel ages in 14C yr 6745-6000

Figure 5.1: Legend for the cross-section descriptions and corresponding overview maps.

5.1.1 Subsection 1: Dordrecht

The most southern subsection (fig. 5.2a,b) is ~10.5 km long and is based on 15 cores, which means an average distance of ~700m between cores. One 14C sample location was present relatively close to this cross-section. Of this dated core, 5 different samples were used.

The early to middle Holocene deposits at the southern end of the cross-section only consist of basal peat layers, topped by Late-Holocene (NAWA) deposits. The core description did not mention what type of peat formed here, but based on the layers to the north it is likely to be woody peat.

At ~6km the Pleistocene surface lowers steeply, indicating the southern edge of the Rhine-Meuse paleo valley. At the lower end, this valley edge is bordered by an old channel that has carved into the Pleistocene surface. A much younger channel belt later covered the same area. A major channel belt is present at km 8.5 which was still active after the Middle-Holocene and thus the sediments that filled the channel belt are categorized as younger deposits.

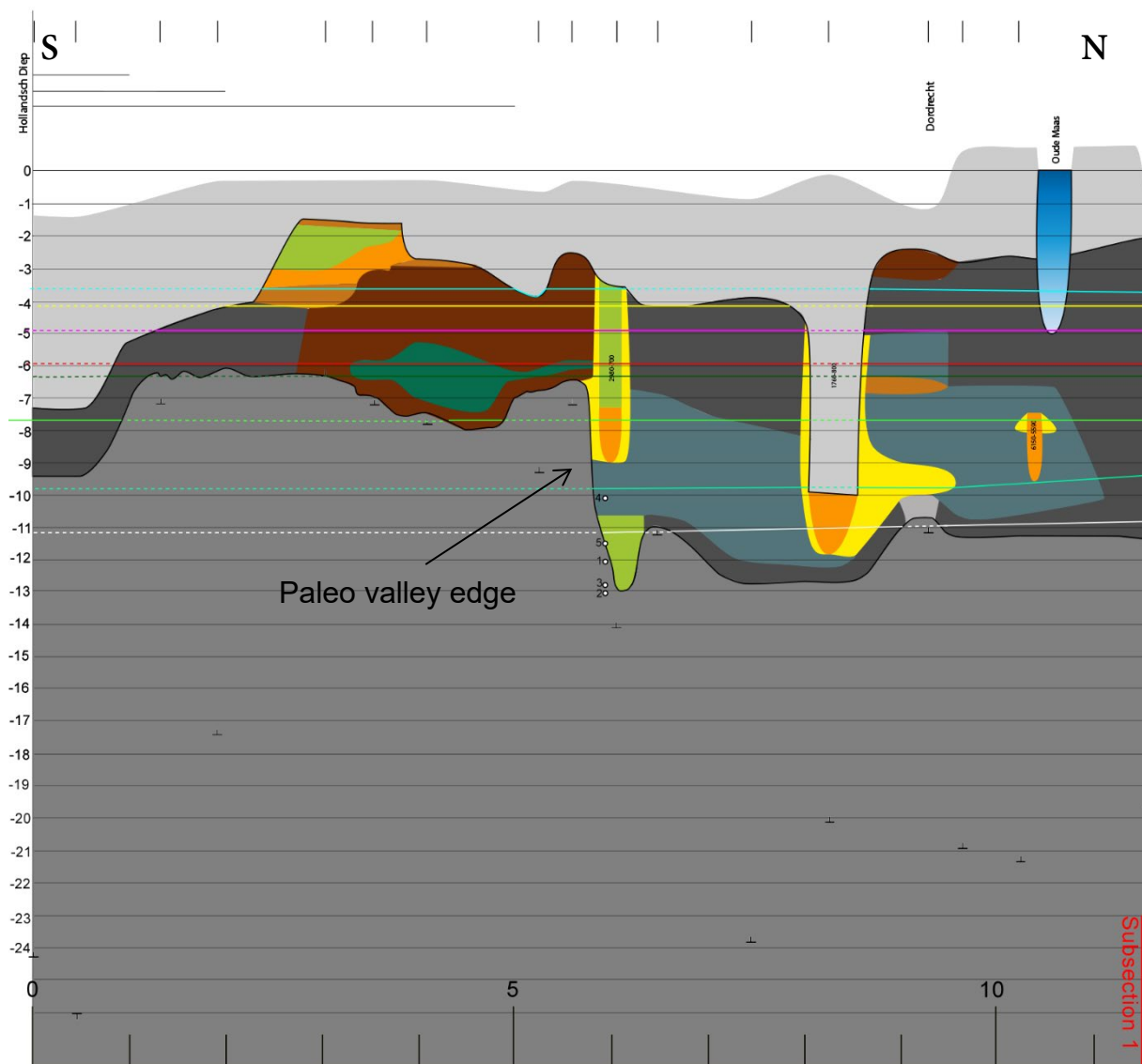


Figure 5.2a: Lithogenetic profile of subsection 1.

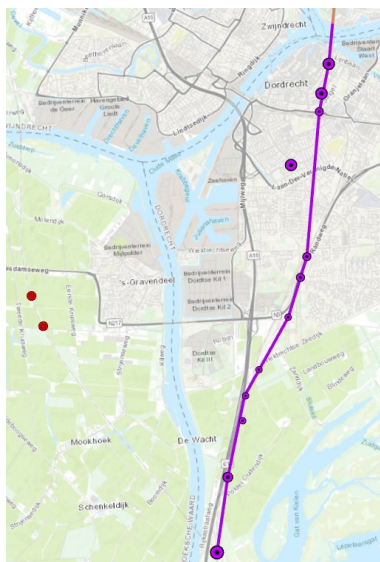


Figure 5.2b: Subsection 1 overview map.

5.1.2 Subsection 2: Rhine-Meuse Paleovalley

Subsection 2 (fig. 5.3a, b) is 31.5km long and contains 37 cores. Giving an average distance between cores of 851 meters. This cross-section includes a good number 14C-samples (38), many taken on one of the several river dunes in this area, which can be seen in figure 5.2a.

The cross-section is similar to those of Hijma et al. (2009) (cross-section A-A') and Gouw & Erkens (2007) (cross-section E-E'). With clastic sediments on top or in between the basal peat layer and a transition to more organic deposits towards the surface. At lower levels lake deposits (gyttja) can be found.

At ~33.5km the Zevender river dune can be found which is the tallest river dune in this area. The dune is enclosed by old channel belts on both sides. Other river dunes can be recognized as irregular heights in the cross-section.

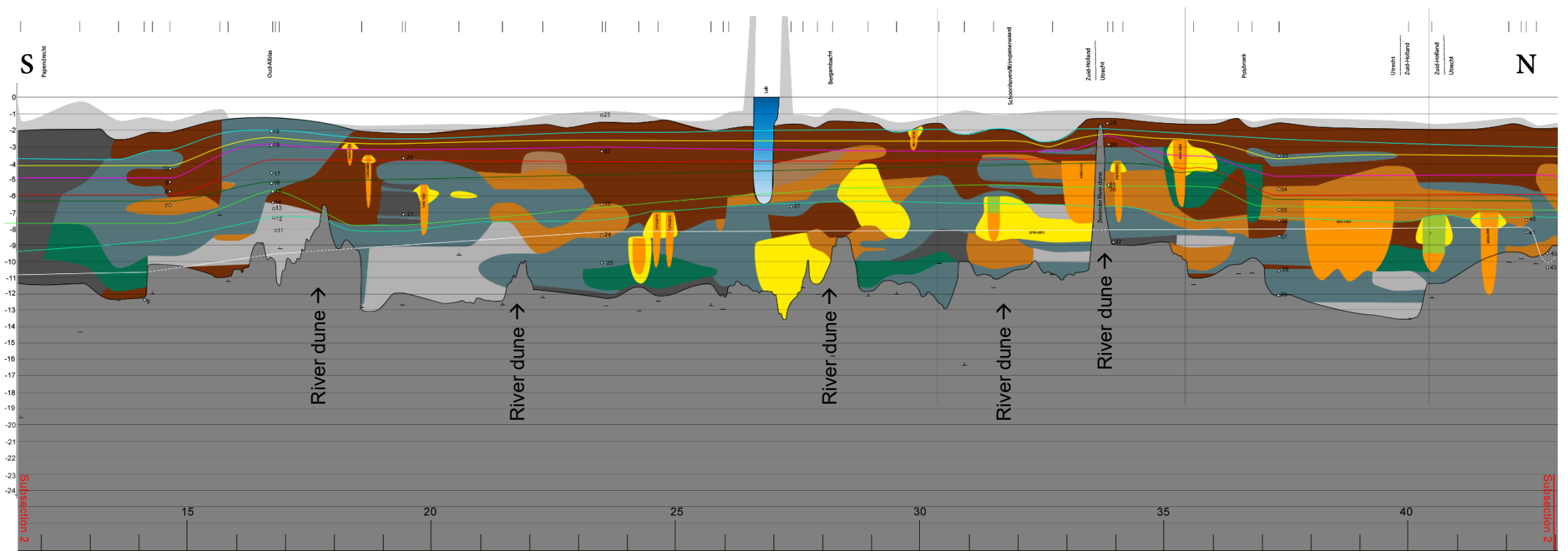


Figure 5.3a: Lithogenetic profile of subsection 2.



Figure 5.3b: Subsection 2 overview map.

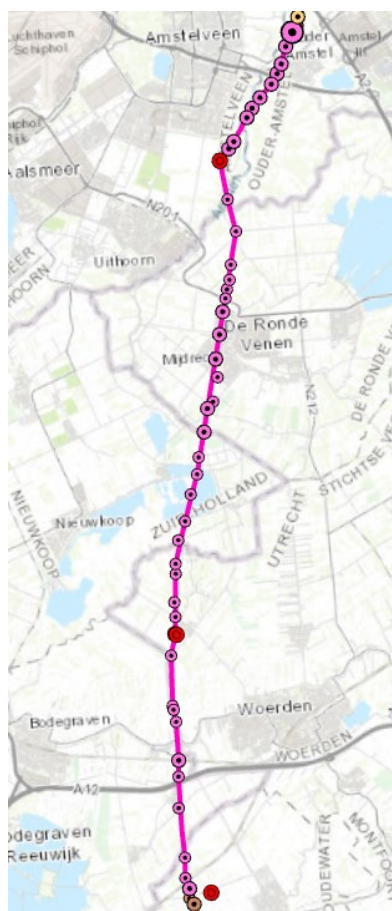
5.1.3 Subsection 3: Transition from fluvial to tidally dominated environments

The third subsection (Figure 5.4a,b) is 32.6 km long and consists of 48 cores and 9 14C samples, resulting in an average distance between cores of 679 m. The Early- to Middle-Holocene deposits, above the basal peat layer, are relatively thin in this area. The thicknesses range from 9 meters at the thickest area to 4 meters in the excavated areas.

What makes this cross-section interesting is the lateral transition from fluvial deposits of the Echteld Formation, to peats from the Nieuwkoop Formation to tidal deposits of the Naaldwijk Formation. At roughly km 54,5 the edge of the tidal basin can be found. Here, reed peat transitions into distal tidal clays. The clays contain reed debris indicating the reed was bordering open water of the tidal system. While at the same time, tidal clays can be found in the reed peat bed, which could either be the edge of the tidal basis shifting over time or small tidal channels that cut through the reed.

In the tidal deposits, the flooding of the Pleistocene surface is also visible in the slow disappearance of the basal peat layer and transition to distal clays. Closer to the surface the abandonment and filling in of the tidal system can be distinguished with the transition back to peats. The transition from reed peat to woody peat also indicates the lowering of relative groundwater levels, showing again the transition from a very wet and partially flooded environment to a dryer environment.

Below: Figure 5.4b: Subsection 3 overview map.



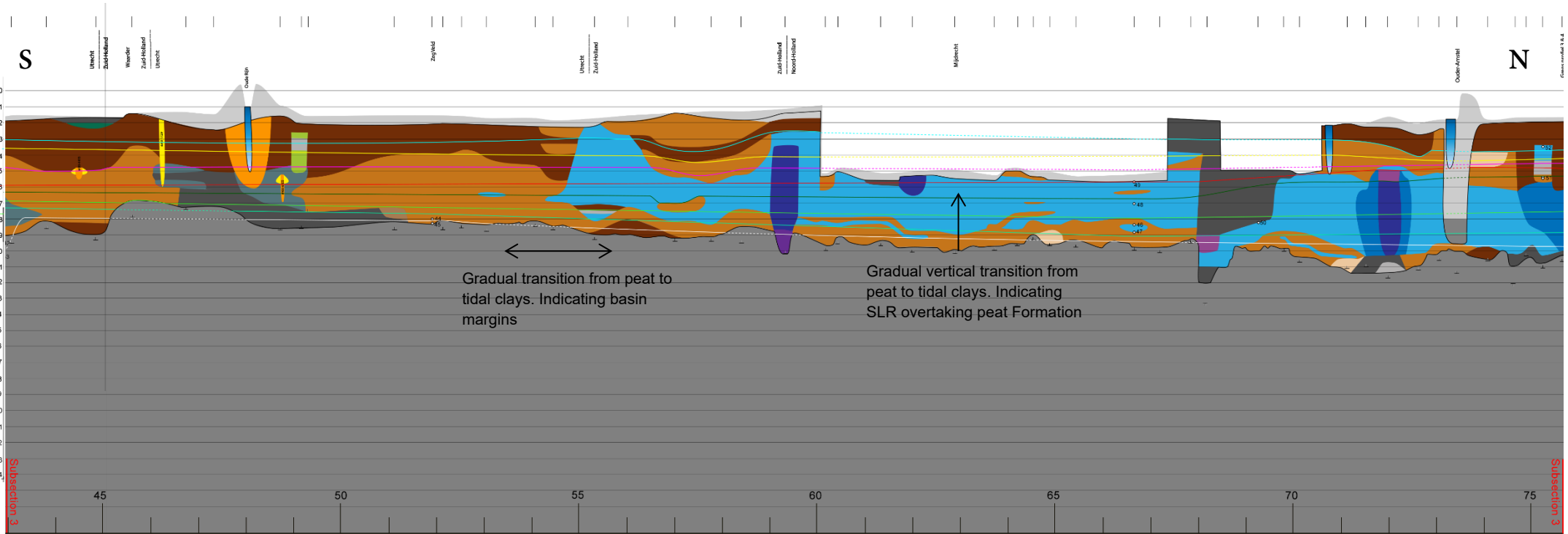


Figure 5.4a: Lithogenetic profile of subsection 3.

5.1.4 Subsection 4: Amsterdam

The fourth subsection crosses the capital city of Amsterdam. It is 20.8km long and is based on 50 cores, with an average distance between cores of 416 m. Above the basal peat layer thick layers of tidal deposits are present. In some areas tidal channels scoured deep into the Pleistocene surface.

Towards the north large sand bodies of old tidal channels dominate the cross-section. The Pleistocene surface rapidly lowers to -24m Dutch O.D. from km 92 onwards. Basal peat layers are mostly absent here.

At the southern end, clays and peat layers indicate low energy environments that are a continuation of the tidal basin edge from subsection 3. Around Amsterdam the Amstel river carved deep into the older Holocene deposits. Amsterdam is also build on top of thick layers of anthropogenic deposits as mentioned in De Gans, (2015).

After km 85, from about -4m towards the surface the sediments sequence changes from sand to clays to peat (black arrow). This succession of sediments indicates the infilling of the tidal basin when sea level rise and the corresponding creation of accommodation space slowed down and the balance shifted towards sediment infilling together with the closing of the coastline, which created favourable conditions for peat formation. Based on the isochrones, the high energy environments disappeared somewhere between 5000 and 5500BP, making way for distal tidal clays indicating a loss of energy in the system. At the final stages reed peat covered these distal clays, indicating even lower energy environments.

Between the sand bodies of the channels, some basal peat is still present, which is often covered by distal tidal clays. So, in some areas a very nice sequence is preserved showing the slow drowning of the Pleistocene surface and the formation of basal peat. The basal peat is followed by tidal clays which indicate that the drowning of the land happened faster than the formation of peat. Eventually, higher energy environments formed in the form of moving tidal channels, which slowly got abandoned during the Middle-Holocene indicated by sandy clays on top of sands.

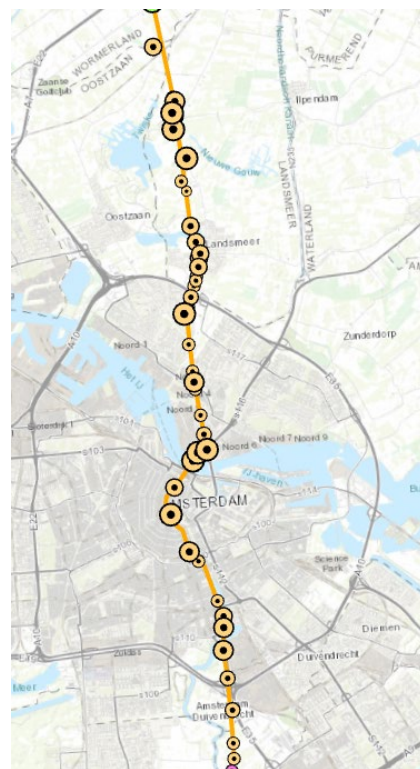


Figure 5.5b: Subsection 4 overview map.

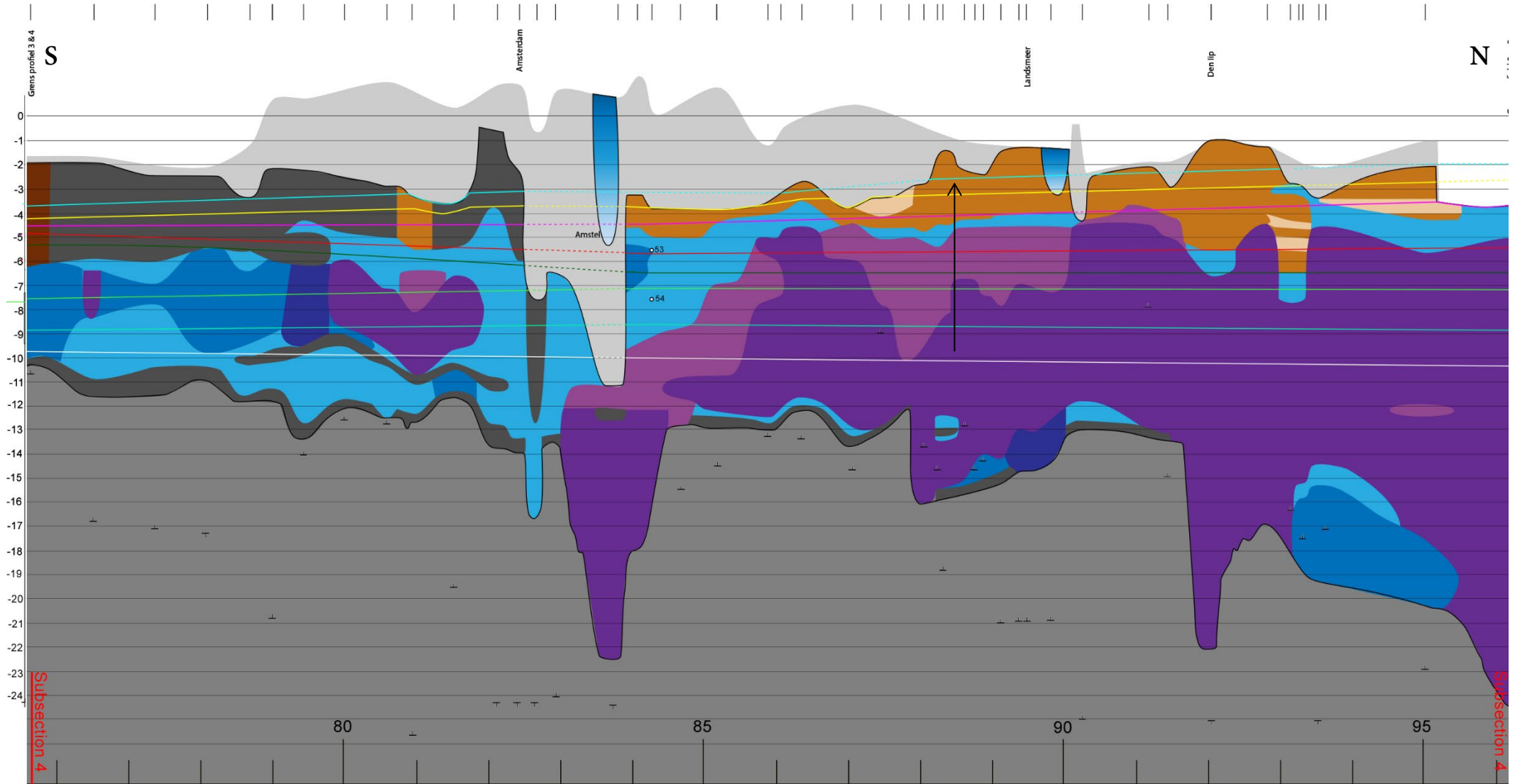


Figure 5.5a: Lithogenetic profile of subsection 4.

5.1.5 Subsection 5: Beemster polders

The second to last subsection lies north of Amsterdam and covers the deepest parts of the northern paleo valley. The cross-section is 25km long and is made using 32 cores. This subsection contains seven 14C-samples which are located further from the cross-section.

This cross-section is dominated by sand from tidal channels, which is likely the reason why most cores did not reach to the Pleistocene surface, resulting in limited detail for the deeper parts of the cross-section. Km 140 roughly marks the central and deepest part of the northern Paleo valley, which appears to be mainly filled with tidal channel sands, while no basal peat was found in this area of the cross-section.

Similar to subsection 4 the decrease in energy can be seen in the transition from sand to clay and peat, up until km 117. Note that most peat is excavated at some point, leaving large excavation pits in the cross-section's surface. From km 117 onwards the sands and sandy clays of channels and channel fills nearly reach the surface. These sandy deposits are likely from the Bergen inlet channel (fig 5.6C), which was active up until ~3000 BP. When it was a drainage channel for the surrounding peat lands

Around the same area at 117km there is a sharp border in the Pleistocene surface which is interpreted as a channel on the edge of the paleo valley. To the north of this edge basal peat is still present on top of the Pleistocene surface.

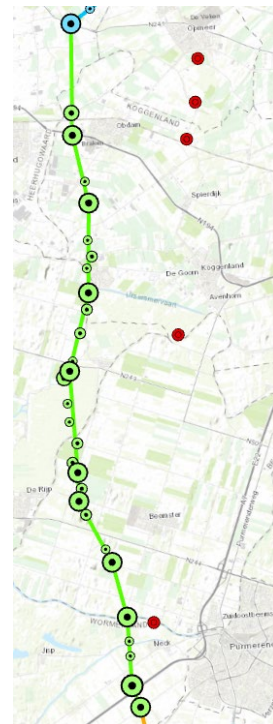


Figure 5.6b: Subsection 5 overview map.

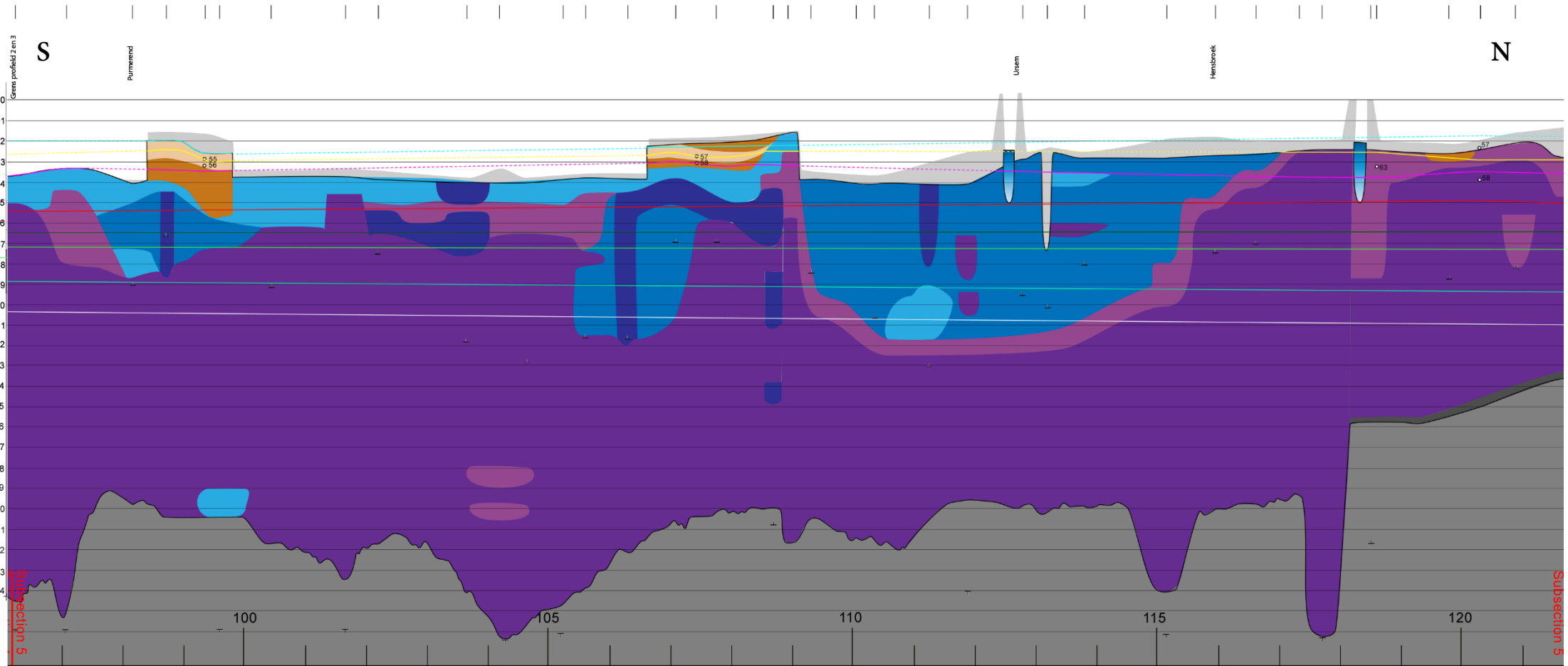


Figure 5.6a: Lithogenetic profile of subsection 6.

5.1.6 Subsection 6: Wieringen

The most northern subsection is 24.6 kilometres long and is based on 59 cores. Here, 23 14C samples are used, including 8 that were later added. The subsection shows a rising Pleistocene surface to the north, indicating the northern side of the paleo valley. It also appears to show the northern edge of the tidal basin. Large deposits of distal clays indicate lower energy environments further away from the large tidal channels from the previous cross-section. There are still many smaller tidal channels recognized in the cross-section.

One significant tidal channel at km 140 possibly scoured into the Pleistocene surface and shifted towards the south (black arrow) over a significant time period. Between km 127 and 135 a large sand body indicates other substantial tidal channels that likely shifted position over time. These channels or single channel seemed to have halted their deposition of sand between 6500 and 6000 BP. The peat layer at the top again indicates the transition away from flooded tidal areas due to the infilling of the tidal basin.

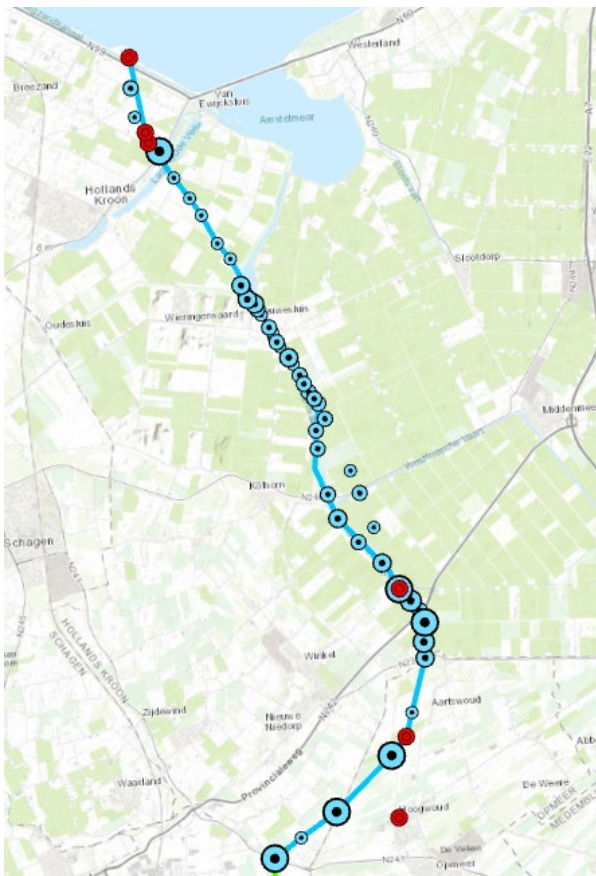


Figure 5.7b: Subsection 5 overview map.

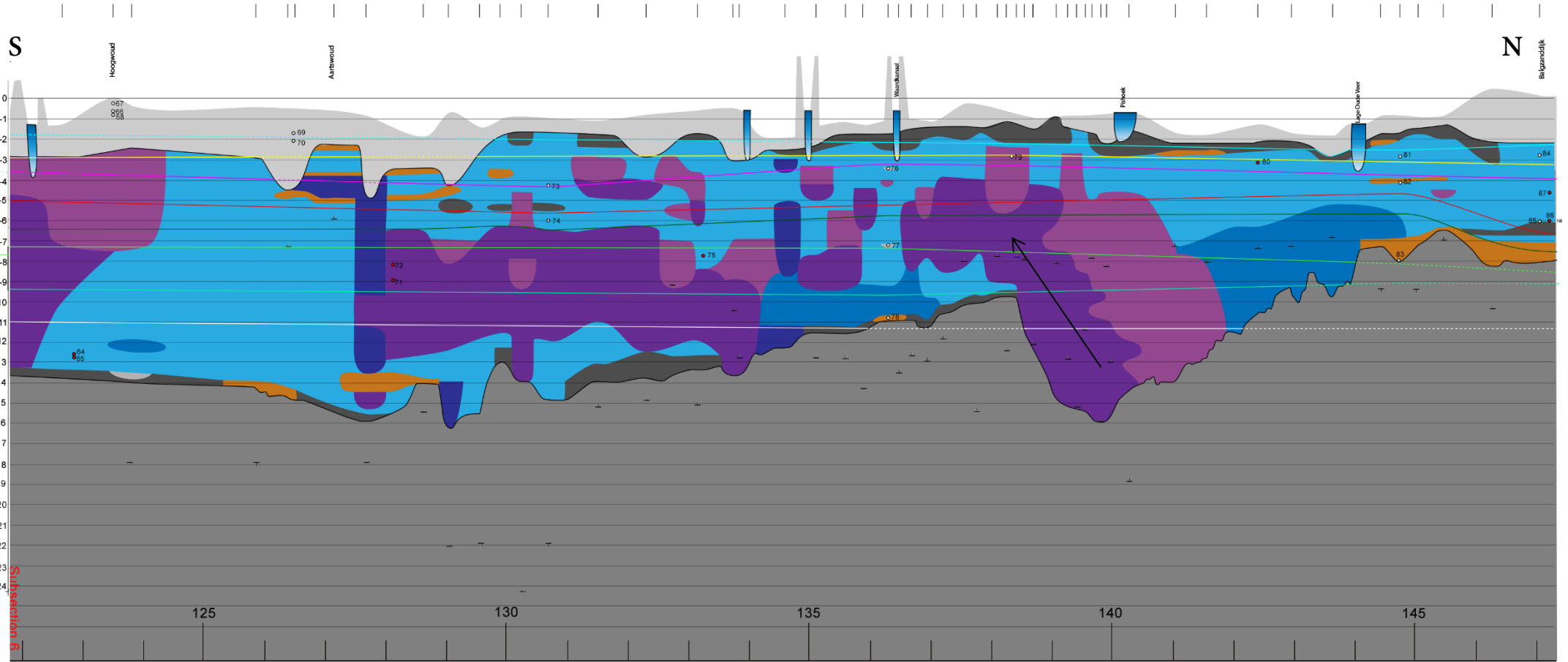


Figure 5.7a: Lithogenetic profile of subsection 6.

5.1.7 Peat layer thickness

Along the whole cross-section, the thickness of peat layers is measured at five-kilometre intervals and at three different depth regions (0 to -5m, -5 to -10m, and -10 to -15m). In order to estimate where and how much compaction could play a role in isochrone depth variations. The bar graphs of figure 5.1.7 show the results.

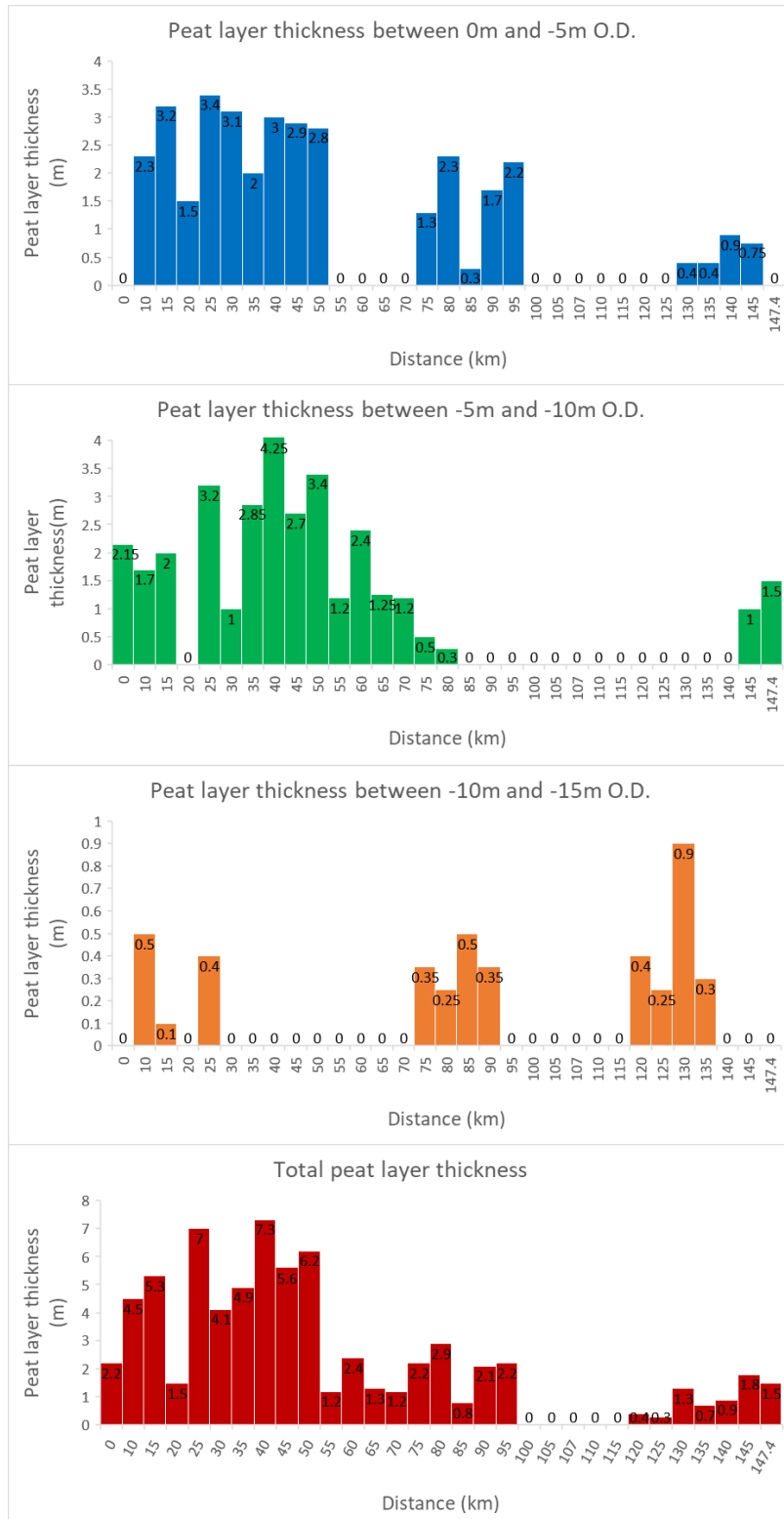


Figure 5.1.7: Bar plots that indicate peat layer thickness at 5 km intervals along the cross-section.

5.2 Isochrones from the cross-section

5.2.1 Reconstructed isochrones

The isochrones have been reconstructed from the lithographic profile with samples at every 5km and at the location of 14C samples, where the isochrones-age indication is most accurate. The graph also contains the original 14C-sample depths and ages for the original dataset (black) and the extra 14C-samples (red). The results are shown in figure 5.2.1. Note that $x=0$ is the most southern point of the cross-section and $y=0$ equals 0 meters Dutch O.D.

The original 14C-samples are plotted at their original depths and are labelled with their calibrated age in yrs cal BP. Data points for 8000BP and 8500BP are included, even though no isochrones for these ages could be constructed. The isochrones are continued to the south and are connected with the extra 14C-samples that were collected by a dashed line. I chose to connect the extra 14C-samples directly to the first 14C-samples at $X=5.9$. A larger scale image can be found in appendix C.

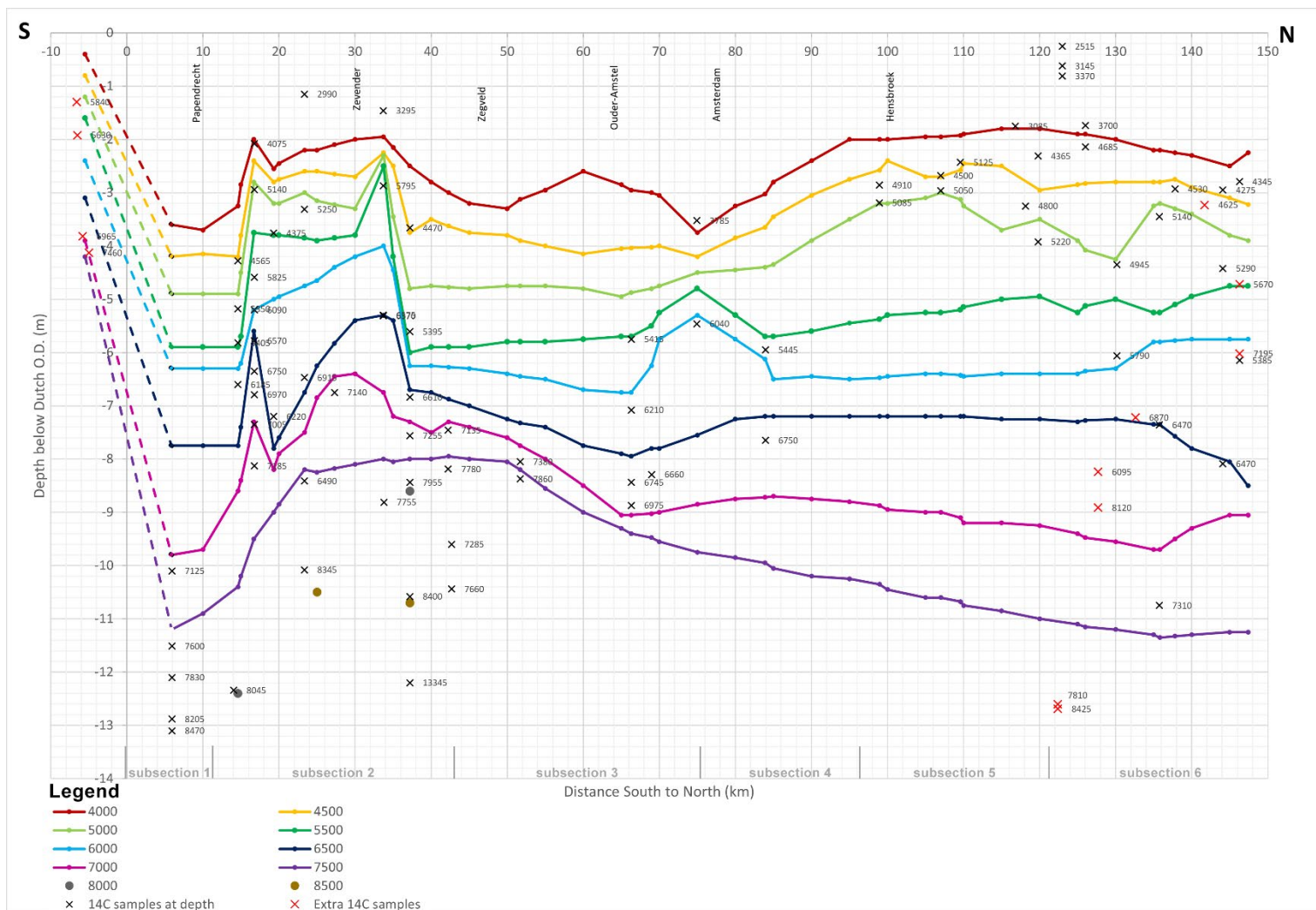


Figure 5.2.1: isochrones extracted from the vertical profile (Appendix D) at 5km intervals. Including extra 14C samples that were taken at a later stage.

5.2.2 Interpolated isochrones

The data from De Wit et al. (in prep.), described in section 3.4, is plotted in figure 5.2.2, using the same methods and style as figure 5.2.1. A series of graphs, where the measured and interpolated isochrones are plotted in one graph per age, can be found in appendix F. Because the authors exclusively used samples dated samples from Basal peats, which limits the influence of compaction since basal peats are located on relatively incompressible Pleistocene substrates.

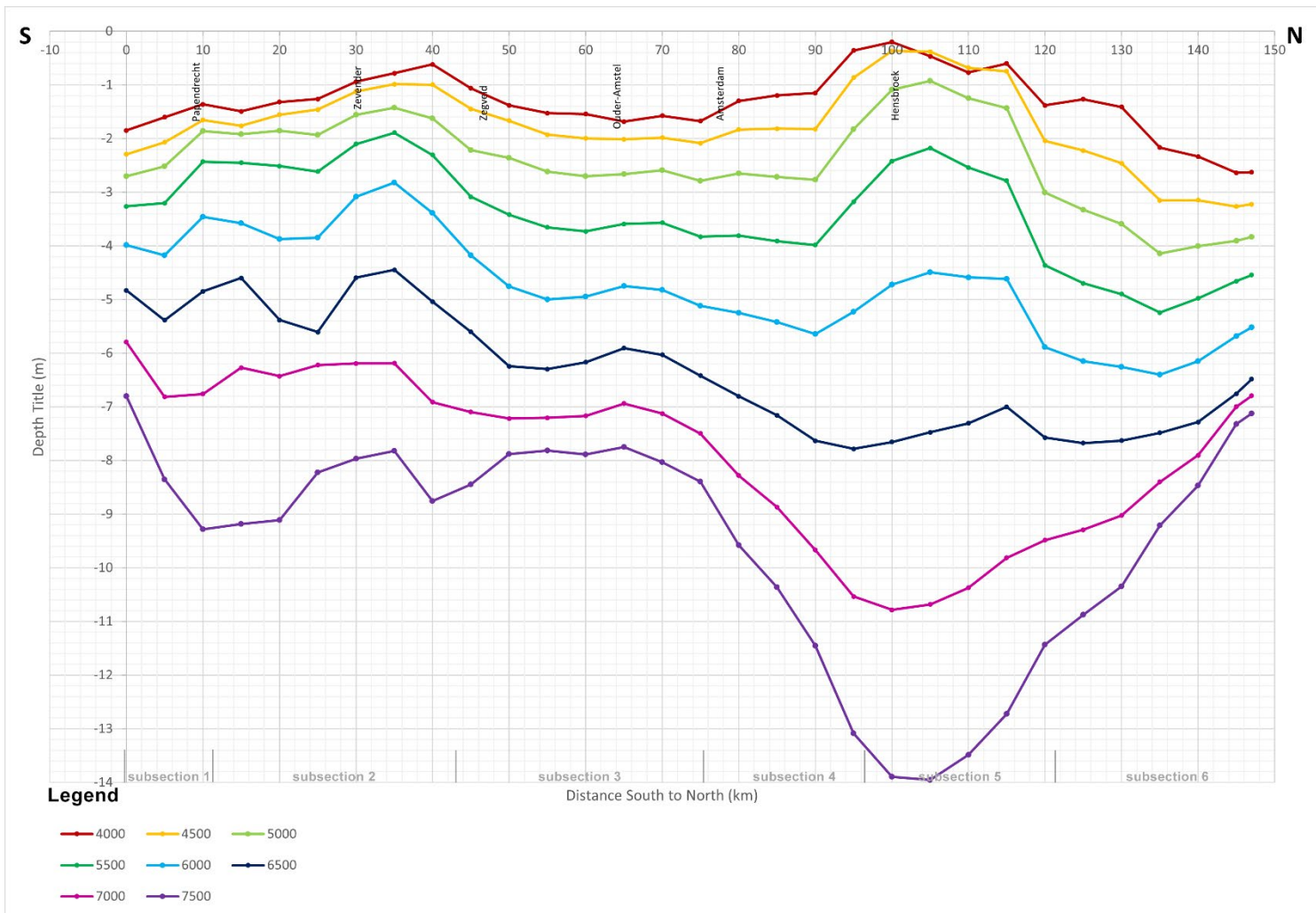


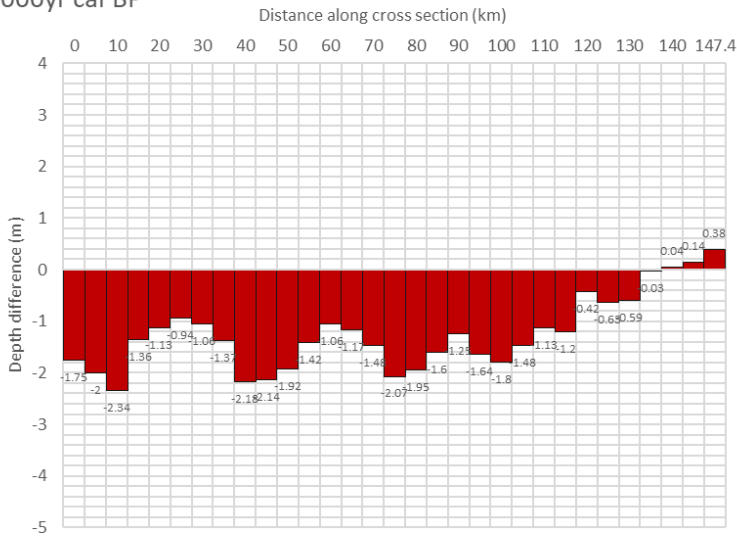
Figure 5.2.2: isochrones from 4000BP to 7500BP from the interpolated dataset of De Wit et al., 2022

5.2.3 Comparison measured and interpolated isochrones

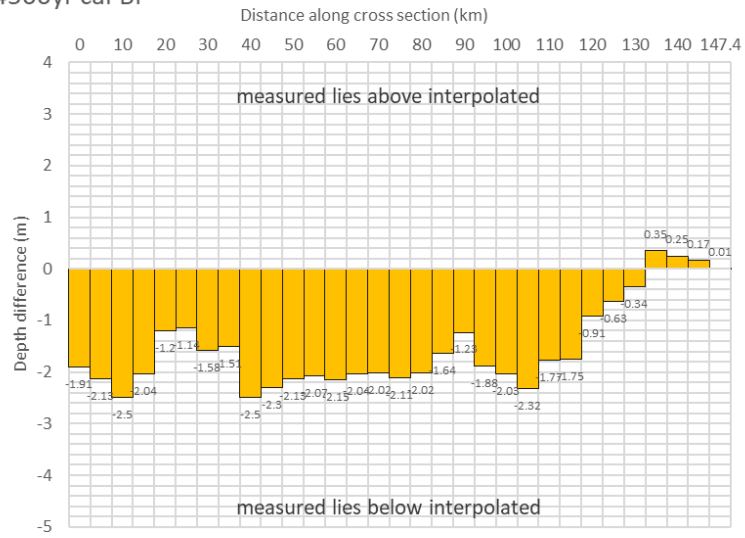
To compare my results to those of De Wit et al., (in prep.), the depth differences between the measured and interpolated isochrones is calculated at each 5km interval. The results can be found as bar plots in figure 5.2.3. If the bar is above $y=0$ this means that the reconstructed isochrones are at a shallower depth compared to the interpolated isochrone. Bars below $y=0$ mean that the reconstructed isochrones lay deeper than interpolated isochrones.

The measured isochrone is generally lower than the interpolated isochrone, with the exceptions occurring mostly at the northern end of the cross-section. The maximum distance that the measured isochrone can be found above the interpolated isochrone is 3.45 meters. While the measured isochrone lies 4.4 meters lower than the interpolated isochrones in the most extreme case. Both are found in the comparison of 7500BP isochrones.

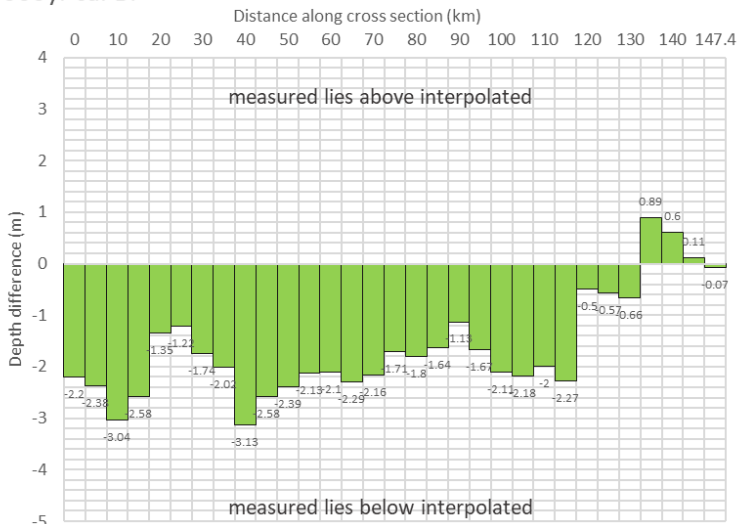
4000yr cal BP



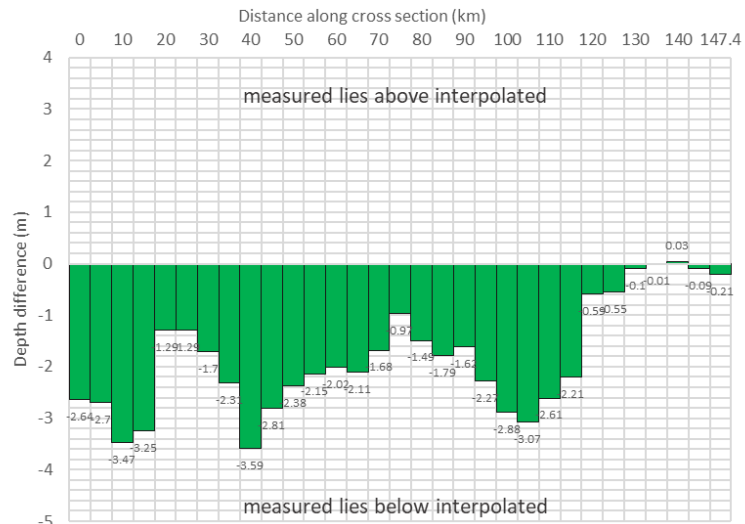
4500yr cal BP



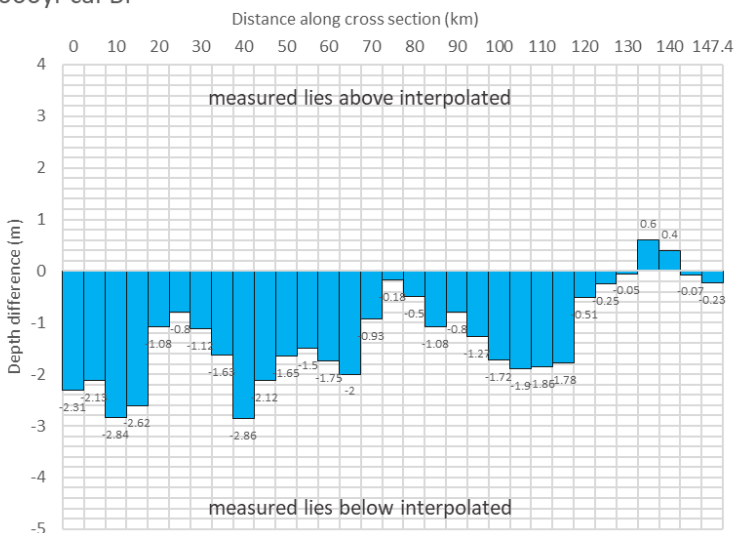
5000yr cal BP



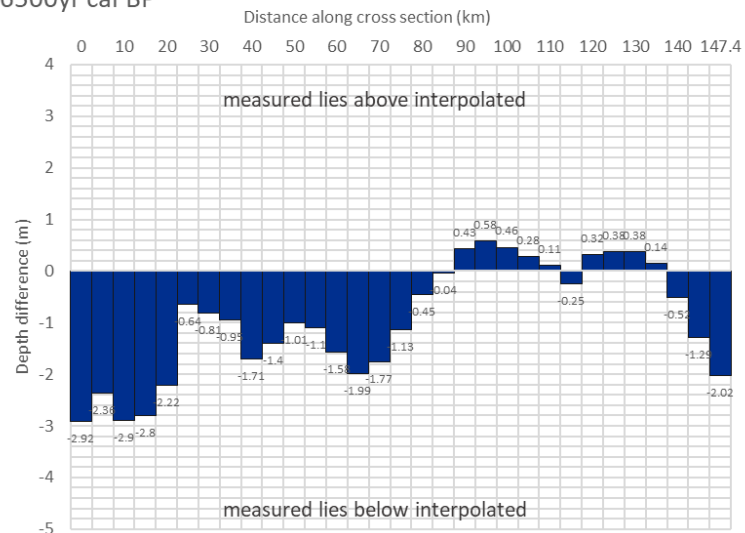
5500yr cal BP



6000yr cal BP



6500yr cal BP



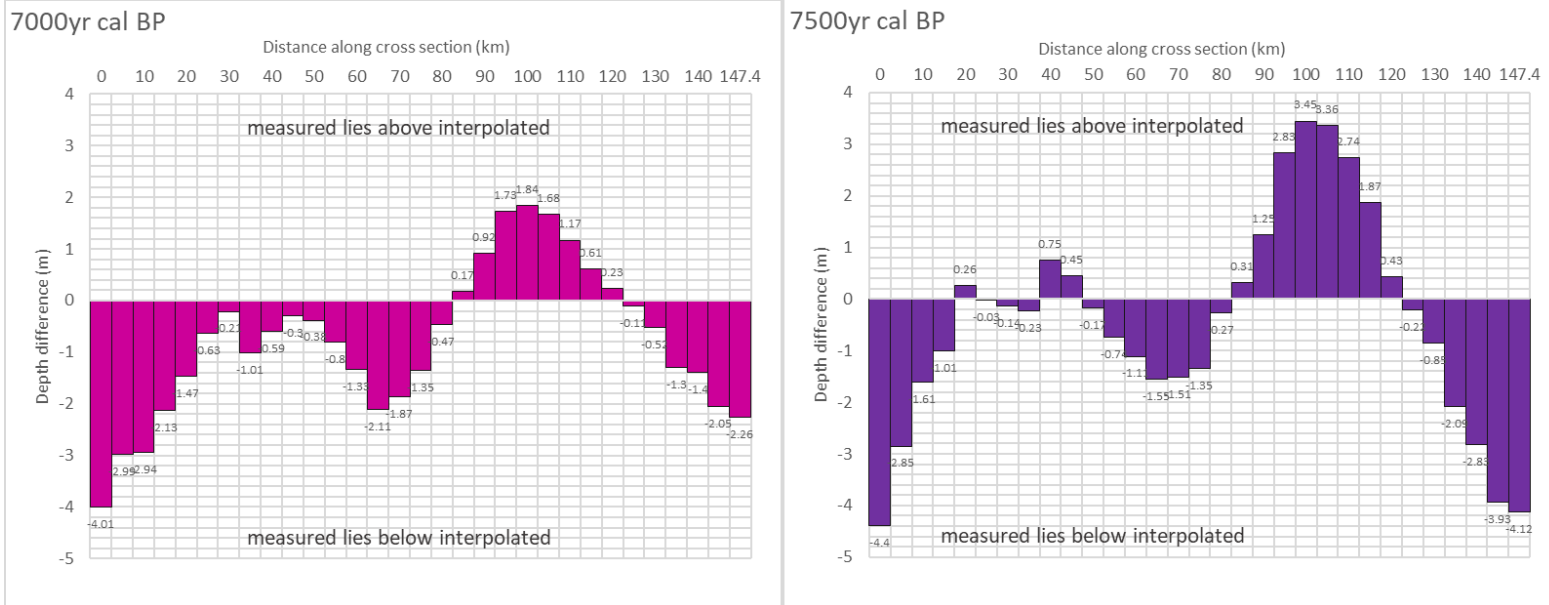


Figure 5.2.3: Bar plots showing differences in isochrone depths between reconstructed isochrones from the lithographic cross-section and interpolated isochrones from groundwater data points.

6. Discussion

The discussion of this thesis starts with the interpretation of the overall shape of the isochrones, with a focus on several specific areas. Section 6.2 focuses on the main question of this thesis, which is the difference in isochrone depth between the south and the north of the cross-section. In section 6.3 I compare the reconstructed isochrones to the interpolated isochrones from De Wit et al., (2022). In section 6.4 an attempt to differentiate between different sources of subsidence is made. Finally, in section 6.5 the quality of this research and recommendations are discussed.

6.1 Interpreting the shape of the isochrones

In graph 5.2.1 with reconstructed isochrones from the cross-section, the characteristics of the isochrones can be seen and interpreted. The first thing that stands out is the bulge at the southern end of this graph, the location where samples were taken near and on top of river dunes. Especially the sample at the Zevender river dune is important, since here subsidence due to compaction should be limited, since the samples were taken close to the incompressible, Pleistocene sands of the river dune. Thus, limiting the effect of compaction.

6.1.1 Isochrone variations in the south

To the south of the river dunes all the isochrones dip one to two meters lower, this shape is mainly based on one group of 14C samples (samples 1 to 5) near Papendrecht (5.2.1) To see if this downward trend continues, some extra samples were plotted further south. These samples show a totally different trend. The isochrones between 5500 and 7500yrs cal BP would all lie between -1 and -4.2 meters for the extra samples (figure 4.3). Comparing this to the sample near Dordrecht ~10 to the north, the difference in depth for 7500yrs cal BP is: $(11.2 - 4.2) = \sim 7$ meters. This is a significant difference in depth over a distance of ~10km. The dip in the depth of the isochrones around Papendrecht is likely caused by subsidence due to compaction and peat oxidation. Koster et al., 2017 also found significant subsidence of Middle-Holocene peat layers in the agricultural areas around Rotterdam.

6.1.2 Isochrone trend in the north

From around 36km northward the isochrones show very different characteristics. From the Zevender river dune, all lines dip down to the north in a different fashion. The oldest two lines have an overall downward trend towards the north. In the hypothesis this downward trend was suspected based on the known differences in subsidence rates between the south and the north of the Netherlands. Thus, for the older isochrones, the results fit the hypothesis of this research. However, it is important to note that these lines are based on a single sample in the north with an age of 7310 BP. Several other samples, much further away from the cross-section are also considered. These samples offered extra data points, but it must be considered their ages might differ significantly, due to the east to west increase in ages (Koster et al., 2017). Samples 64 and 65 (figure 4.2 & Appendix B) seem to be in line with the isochrone, as well as the two youngest, additional samples (80 and 87). The remaining, extra samples show very different depth age relationships. Likely because of their distance to the east and west.

6.1.3 Depth variations in the center

Looking at the whole length of the cross-section, it is clear that none of the isochrones overlap, meaning that the relative sea level changed throughout the period that the subsurface structures formed. It is known that eustatic sea level rise stopped around 5000 cal yr BP and subsidence became the main driver for relative sea level rise after this period (Gouw & Erkens, 2007). This means that the differences in depth between the isochrones of 5000-4000yr cal BP are caused by subsidence and not by rising eustatic sea level. Finally,

influences of eustatic sea level rise and possibly glacio-isostatic movement can be seen in the change in depth differences between isochrones over time. This is especially clear at the Zevender dune at km 32 in figure 5.2.3. Here, a clear decrease in distance between isochrones the younger isochrones towards the surface can be seen.

In the centre of the cross-section, roughly between km 40 and 90 (Figure 5.2.1), the isochrones differ a lot from each other. The 4000BP line shows peaks and dips with a maximum difference of one meter between the highest point and lowest point. The 5500BP and 6000BP show an interesting peak near Ouder-Amstel at km 75. The large variation in the younger isochrones might have been caused by variation and compaction in the younger peat layers of the Holland Peat Member.

Overall the lines younger than 7000BP have relatively low points in the centre compared to the north and south (excluding the most outer edges). One explanation for this dip at the centre could be compaction of peat. Looking at figure 5.1.7, the centre contains many thick peat layers (subsections 2 to 4, Figures 5.2.3 & ...), close to the Pleistocene surface. Compaction of these peat layers can be significant and could have caused the lowering of the 14C samples. Figure 5.2.3 also suggests that peat compaction caused these differences, since constructed isochrones are lower compared to the isochrones interpolated from basal peat samples (De Wit et al., (in prep.)). For samples taken directly on river dunes (with the Zevender dune as the best example) peat compaction should be relatively limited factor This explains why the isochrones around the river dunes are at lower depths compared to the areas just south and north.

This decrease in depth between isochrones is thus very likely caused by eustatic sea level rise, but it is partly caused by glacio-isostatic movement too. Since, glacio-isostasy is not linear over time, but has increased subsidence rates towards the LGM, the subsidence rates are higher around 7500BP than 4000BP. This will result in a similar temporal trend as eustatic sea level rise, however at a much smaller scale. Because glacio-isostatic subsidence rates are a power of 10 lower than eustatic sea level rise.

6.2 Differences between South and North

6.2.1 Average depth comparison

The main focus point of this research is the difference in isochrone depths between the south and the north. Just looking at the graph of figure 5.2.1 it seems that only the two oldest isochrones show a difference between north and south. To investigate this further a comparison is done between average depths along the cross-section (Figure 6.1a).

For the graph below (fig 6.1a) the data for fig 5.2.1 is summarized in three regions along the cross-section: south, center, and north (Fig. 6.1b). The southern region contains the 14C dated samples taken between km - 5.5 and 50 (includes extra 14C samples), the central region covers km 50 to 100 and the northern section contains samples from km 100 to the northern end of the cross section at km 147.7. Taking averages filters out the short scale variation some isochrones show. The graph in figure 6.1a shows the average depth per region for each time frame (7500-4000BP).

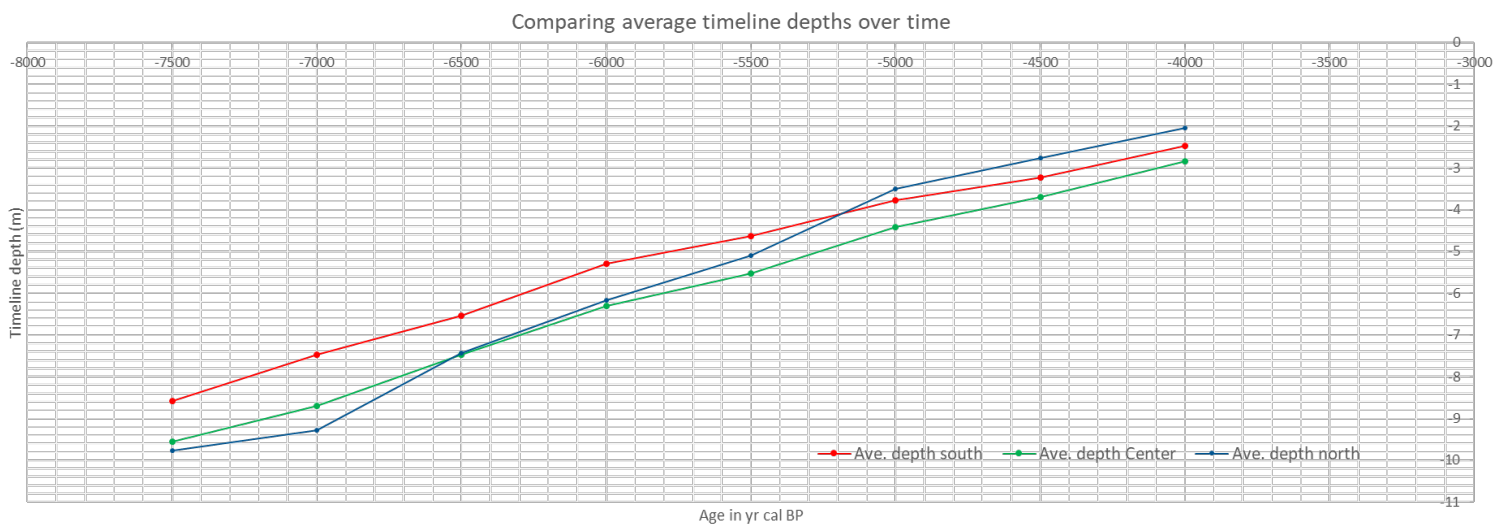


Figure 6.1a: This graph shows averaged depths of the isochrones over time for three different regions in the cross section.

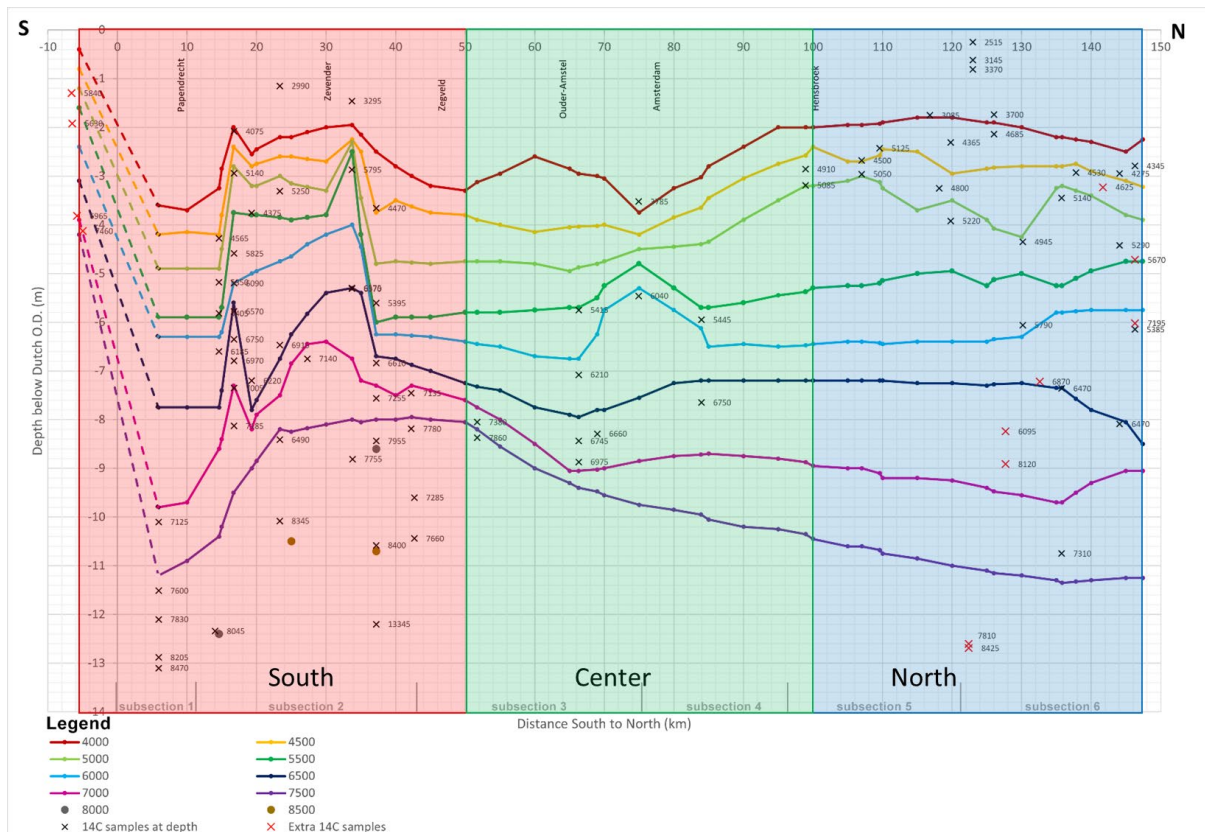


Figure 6.1b: Different regions that over which depths are averaged in figure 6.1a displayed on figure 5.2.1.

The isochrone depths are 0.46-1.8 meters (for 5500BP and 7000BP respectively) lower in the north compared to the south as was expected in the hypothesis, which is extra clear in figure 6.2 which shows the difference in average depth overtime. The trend of greater depths in the north compared to the south consists up until 5250BP after which the northern average lies roughly 0.5 meters above the southern average. Considering the amount of potential for peat compaction in the south compared to the north (figure 5.1.7), it is likely that for these younger isochrones the component of peat compaction is much clearer than the GIA or tectonic component. Which is reinforced by the fact that peat compaction rates are much higher than GIA and tectonic subsidence rates (Vink et al., 2007; Koster et al., 2017). What is clear is that the differences between the average isochrone depth between the north and the south decrease over time. Which is also indicated with the linear trend line.

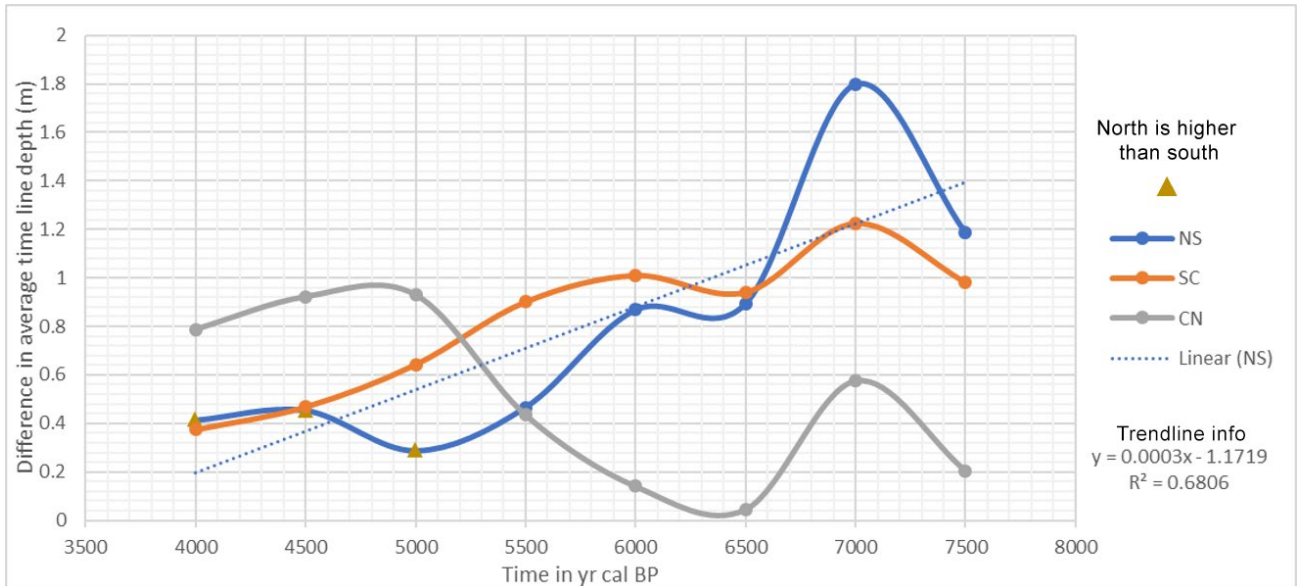


Figure 6.2: graph showing differences between lines in figure 6.1a. NS is the differences between average depths through time between the north and the south, SC between the south and central region, and CN between the central region and the northern region. Trendline shows trend of average depth over time between the south and the north. Brown triangles indicate that the northern averages lie above the southern average in figure 6.1a.

6.2.2 Selective averages comparison

To further investigate the isochrone depths over distance, figures 6.1 and 6.2 were recreated, this time only for the samples taken along the river dunes (between km 16.7 and 33,75) and several northern isochrone samples (between km 100 and 135). This is done to get a better picture of absolute differences between the south and the north, with less influence of compaction subsidence. Since, the northern data points contain few peat layers, they should also have experience minimal subsidence due to compaction of peat (section 5.1.7).

Figure 6.3a is the same as 6.1a, but using the more selective data from the south and the north. Here, the differences between average isochrone depths between the north and the south become clearer, with the south showing overall higher values and limited changes in the north. Furthermore, the average depths in the north only exceed those of the south after 4500BP, enforcing the suggestion that peat compaction influences the younger isochrones more significantly than the other subsidence components.

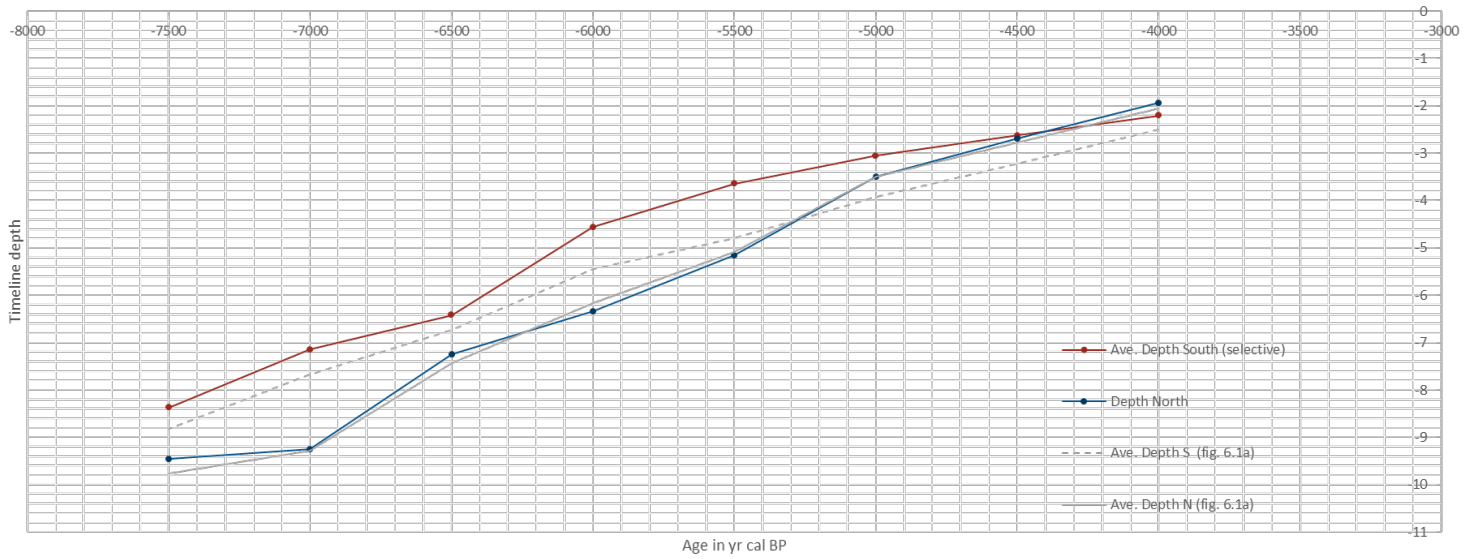


Figure 6.3a: shows the differences in average depths between the south and the north through time.

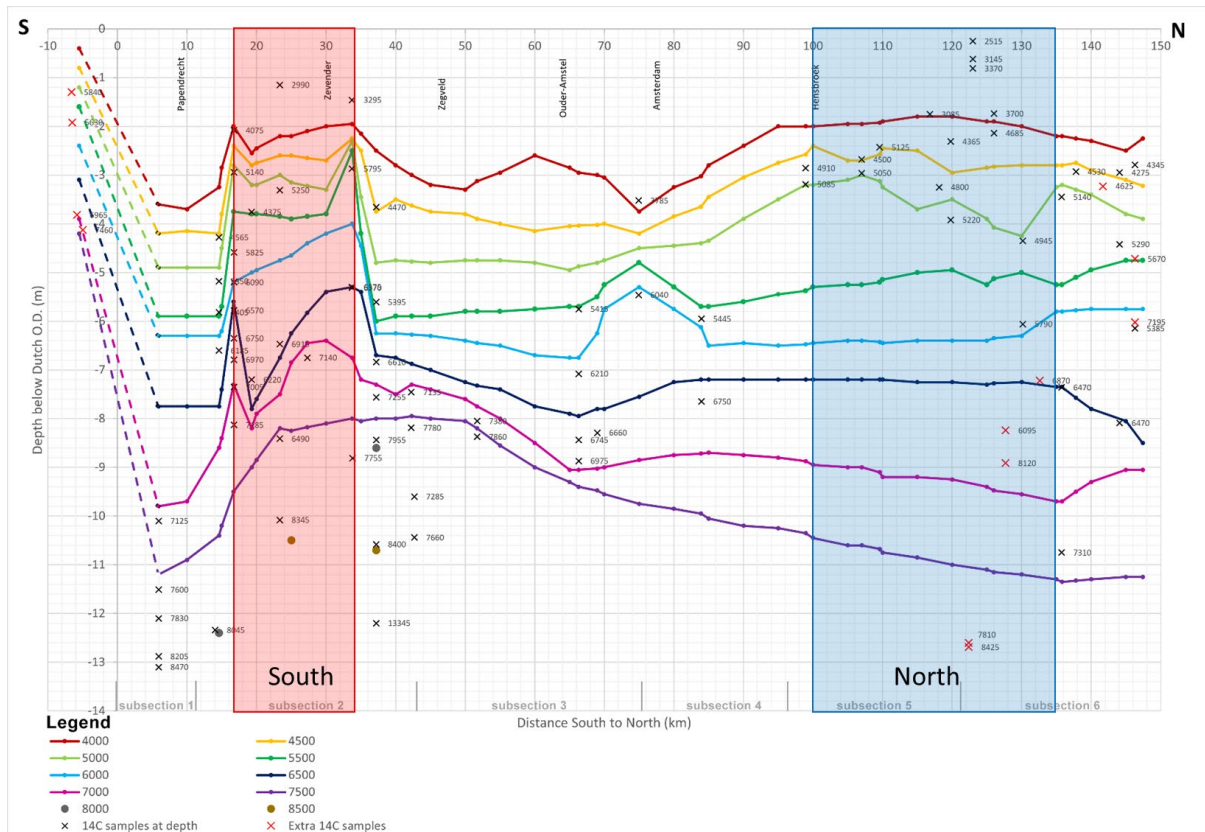


Figure 6.3b: Different regions over which depths are averaged in figure 6.5a displayed on figure 5.2.3.

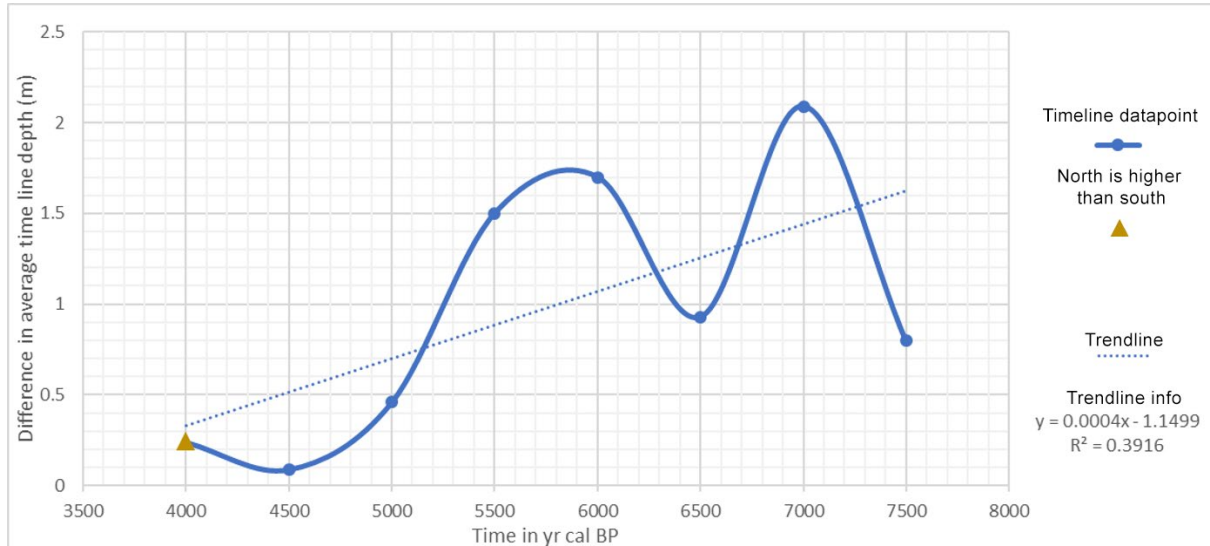


Figure 6.4: shows the difference in average depth between the north and the south. With a trendline to show the trend over time.

Figure 6.4 again shows that the average depth difference between the south and the north decreases over time, from a maximum of 2.1 meters (7000BP) to 0.09 meters (4500BP). This trend seems to be heavily influenced by the values for 5000BP to 4000BP, with a lot more variation in depth differences for older ages. The larger in depth differences for older isochrones is likely due to the fact that older isochrones have been exposed to subsidence for longer periods of time. A longer exposure to subsidence means that spatial variations in subsidence are more pronounced. Furthermore, part of the larger in depth differences for older isochrones could also be attributed to the nature of GIA, with higher subsidence rates closer to the LGM.

The differences in depth decrease over time, because less time has passed for subsidence to cause vertical displacement in younger isochrones. Plus, at the start of the Middle-Holocene GIA subsidence rates could have been significantly higher than towards the Late-Holocene (Vink et al., 2007). So, the older the sample material is, the more it has been affected by either tectonic subsidence or glacio-isostatic subsidence. Subsidence by compaction should be less prevalent in these graphs, since areas were chosen that experience little to no compaction.

6.2.3 Comparing depth differences with values from literature

The first results from De Wit et al., (2022) mention an increase of total coastal-prism accommodation space by 20 percent from the south to the north. With average subsidence rates of 0.1mm/yr in Zeeland and 0.4mm/yr in Groningen, averaged over the Holocene. Assuming that these rates were constant throughout the Middle-Holocene, the amount of estimated subsidence that occurred between both regions can be calculated and compared to the results of figure 6.2 and 6.4. The same can be done with the values from the table in figure 2.5 taken from the research of Vink et al. (2007) and Kooi et al. (1998).

So, by multiplying the subsidence rates (in mm/yr) with the ages in years should give an indication of the total amount of subsidence that has happened since this time frame. Subtracting the total subsidence value of the southern region from the northern region, results in the depth difference between the north and the south for that timeframe. Which is the same sort of data that is plotted in figure 6.2 and 6.4 above. All these values can be plotted in one graph (figure 6.5) to see if the values from figures 6.2 and 6.4 fit within values from literature. Note that data from figure 6.2 and 6.4 is filtered to only include timeframes at which the Northern line lies below the southern line.

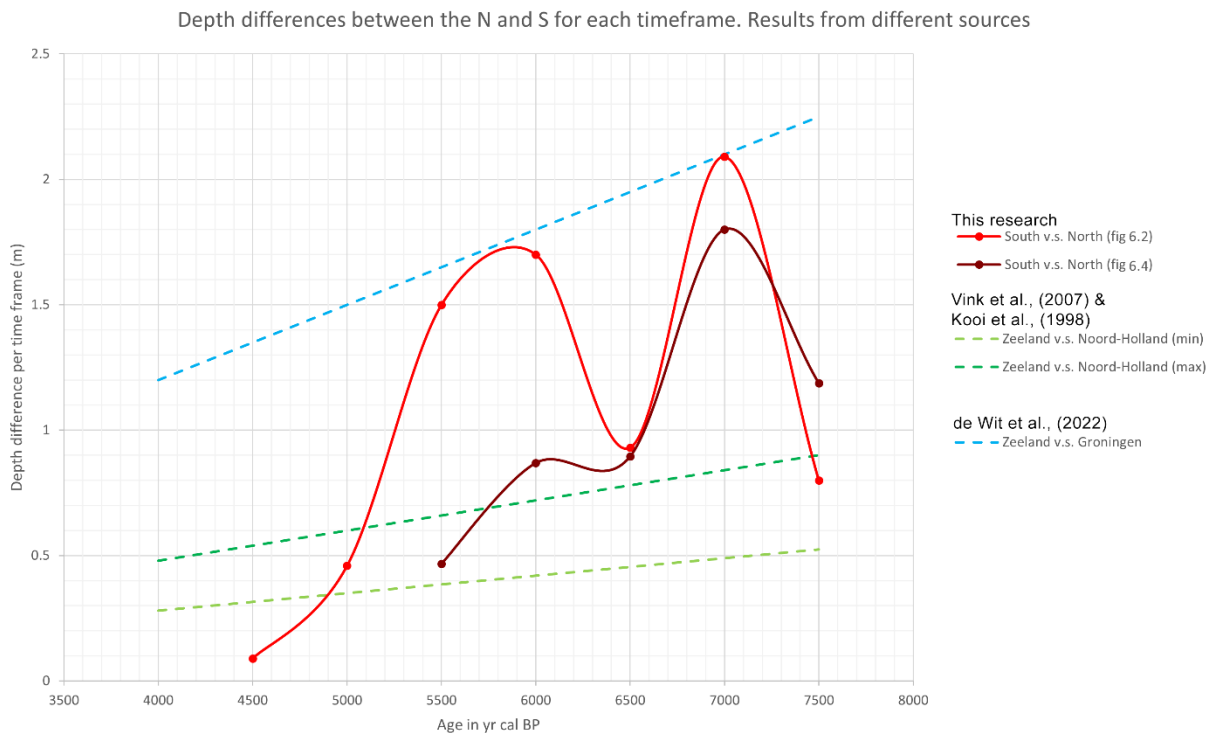


Figure 6.5: Differences in the amount of subsidence between southern, central and northern regions in the Netherlands. Looking at depth differences at each timeframe.

For the values from figure 6.2 the values for are pretty close to those of Vink et al. (2007) and Kooi et al. (1998), but are generally higher. The value for 7000BP is closer to the values from De Wit et al., (2022). For figure 6.4 the values differ more wildly, with some close to Vink et al. (2007) and Kooi et al. (1998) and some close to De Wit et al., (2022). All in all, the values from this research are pretty similar to what is expected from literature, but the values do vary a lot more between timeframes. Since the difference between isochrone depths increases with the distance between the data points, due to the increasing subsidence rates towards the north (e.g. Dordrecht-Wieringen v.s. Zeeland-Groningen) it is expected that my data lies between that of Vink et al. (2007) and Kooi et al. (1998) (Zeeland-Noord-Holland) and De Wit et al., (2022) (Zeeland-Groningen). This expectation seems to have been met.

6.3 Interpreting differences between measured and interpolated

From figure 5.2.4 it is clear that there are significant differences in depth between measured and interpolated isochrones. In this section, I discuss possible causes for these differences between measured and interpolated isochrones.

Starting with the difference in techniques used between this research and the research by De Wit et al. (2022). In their research, the authors use a combination of trend-fitting between paleo-groundwater indicators and interpolation techniques, such as kriging. Their goal is to create a large-scale, 3D-map that predicts paleo-water level through time. Their choice of using dated samples from exclusively basal peat layers, means that subsidence is excluded from their data. For this research the influence of compaction is still present, since this research also includes dated peat samples from interlaced peat beds.

To see how much compaction could have played a role, the peat thicknesses from figure 5.1.7 are compared with the differences in isochrone depths in figure 5.2.3. Especially in between km -5 to 95km of the cross-

section, peat compaction could be a major reason for the differences in isochrones. Here, the distances between the measured and interpolated isochrones are larger in areas that contain the thickest peat layers.

The river dune area (km 16-32), where the cross-section based results are less impacted by peat compaction, can also be recognized in the graphs of figure 5.2.3 as an area where differences between reconstructed and interpolated isochrones are smaller than the surrounding area. Indicating that around river dunes the reconstructed isochrones data points are closer to the groundwater data points that were used for the interpolated isochrones. The differences between constructed and interpolated isochrones for the above mentioned area show the long term peat compaction component of the total subsidence.

Subsidence due to peat compaction, however, cannot explain all the differences between the measured and interpolated isochrones. One reason could be that the difference in methods between this research and the research by De Wit et al. (2022) resulted in different isochrone depths near field data points. It is probable that this difference is not much great than a couple of decimetres.

In the northern part of the cross-section (km 100 to 135) severe subsidence due to peat compaction is also unlikely, due to the lack of (thick) peat layers. The large differences between measured and interpolated isochrones, especially for 7000 and 7500BP is in a large part caused by the limited accuracy of the reconstructed isochrones for the older ages. Due to the limited amount of 14c data points the reconstructed isochrones show a relatively linear line in the northern section, which connects only a couple of 14C data points. In the Interpolated isochrone, you can clearly see that the isochrones follow the shape of the paleo valley. Which causes them to dip far below the measured isochrone. It is plausible that the reconstructed isochrones should also follow the shape of the paleo valley. But that detail was not obtained from the limited data.

Lastly, the graphs of 4000-6000BP in figure 5.2.3 show that the reconstructed isochrones raise above interpolated isochrones in the last ~15km. This could be due to inaccuracies in the reconstructed isochrones. It could also be the effect of the edge of the paleo valley, at which groundwater levels usually rise. Possibly this effect is stronger in the reconstructed isochrones, compared to the interpolated isochrones.

6.4 Differentiating between different sources of land subsidence

One of the challenges in this research is trying to differentiate between different origins (glacio-isostasy, background tectonics, and compaction) of subsidence along the cross-section. Unfortunately, no exact ratios could be obtained from this research. However, something can be said about the influence of different subsidence components on the isochrones.

Based on the differences between the interpolated and measured isochrone, plus the overall shape of the isochrones, it is clear that subsidence due to compaction is prevalent in the Southern half of the cross-section. While figure 6.4, 6.6 and 6.7 indicate that the depth differences between the north and the south are probably caused by tectonics and GIA.

6.5 How suitable is this cross-section for researching differences in subsidence

This research tested the concept of using a coastal plain wide cross-section for subsidence research. Even though the results of this research are limited, the use of large cross-sections in studying subsidence appears promising. Results of the deepest isochrones show a trend that fits the hypotheses of this research with isochrones dipping towards the north. Indicating higher subsidence rates at the northern end of the cross-section, compared to the south.

Several improvements can be made both in the data availability and quality of this research. The accuracy of the isochrones between km 90 and 147,7 is fairly poor for isochrones older than 5500BP, due to the lack of older 14C samples. Extra 14C samples within the range of these older isochrones would greatly improve the quality of the results. However, finding suitable material for 14C dating could pose a challenge, since large sandy bodies dominate the subsurface and peat layers are limited. The tidal sands do have areas with high amounts of organic debris which might offer dating possibilities or more, deeper coring could find more peat locations at lower depths.

To continue with the 14C samples. During the proposal phase, the plan was to look at the time range of 9000-5000BP. Due to the lack of samples older than 7500yr cal BP in the Holocene dated peat samples, the decision was made to have 7500BP as the oldest isochrone, while at the same time moving the younger limit to 4000BP to still have a decent time range. Increasing the lower limit to at least 8500BP should be feasible, since this time range did occur occasionally in 14C samples near the cross-section. There is however some uncertainty in the amount of suitable substrate in the Holocene deposits for ages above 7500BP. A consideration can also be made to use dated samples from interlaced peat beds that can be Pleistocene river deposits (Waalre and Kreftenheye Formation), since these have also been affected by GIA and tectonic subsidence (Westerhoff et al., 2008; Increasing this time range, also increases the temporal resolution, giving better insight into subsidence during the Early-Atlantic and earlier (figure 2.5).

Another way to improve the quality of the research is to test the east-west position of the cross-section. The age-depth relations do not only differ in the north-south direction, but also in the east-west direction. Samples of the same age will lay deeper towards the west and shallower towards the east. Thus the orientation of the cross-section is important in how big the depth differences in the north and south direction appear. Finding the right orientation which limits this east-west effect will help in the proper quantification in the depth differences in the north-south direction.

Finally, improvements could be made on the density of cores used in this research. In this research, the average distance between cores is: ~610 meters, with many areas where the distance between cores is around 1km. The average distance between cores in Hijma (2009) and Gouw & Erkens (2007) is ~203m and ~90m respectively. This means that the cross-section core density of this research is 6 to 3 times less dense, compared to similar research. Due to the size of this cross-section and some limitations in core availability, reaching an average distance between cores of 100 to 200m might be challenging for a plain wide cross-section. However, with the LLG-data from the UU and by gathering extra cores in important locations, improvements can be made.

Having a higher core density could solve an issue I experienced in using lithostratigraphy for age control. Due to the large distances in cores, the detail of stratigraphic structures was fairly low. This prompted me to be (overly) careful in using stratigraphy for isochrone construction, possibly resulting in a decreased quality of the isochrones.

7. Conclusions

This thesis is a trial in using coastal plain-wide cross-sections to research spatial differences in subsidence over long distances. A 148 km. The methods used in this research show potential in quantifying subsidence through a significant part of the Dutch coastal plain, but further improvements are recommended to achieve higher data quality. Improvements such more detailed lithological descriptions by increasing the amount of used cores, improving isochrone quality with extra 14C samples in the north and by increasing temporal resolution to 9000 BP.

With the methods of this research a difference in average isochrone depth up to 2 meters was found. Where the isochrones were lower in the north compared to the south. This trend of lower isochrone depths in the north was most noticeable in isochrones for the ages 7000 BP and 7500 BP.

The differences between the south and the north are most likely caused by glacio-isostatic adjustment and background subsidence, while compaction of peat has a bigger influence on smaller spatial scales and in the shapes younger isochrones.

The influence of peat compaction is also clear when comparing the measured isochrone depths of this research to the interpolated isochrone depths from De Wit et al., 2022. Significant differences up to 4 meters exists between the two datasets. In the southern region of the cross-section this difference can largely be explained by the presence of peat layers and their compaction. In the north, where peat is scarce the differences are more likely explained by lower accuracies in reconstructed isochrones due to the lack of older 14C samples.

Acknowledgements

I want to thank Dr. Kim M. Cohen for his supervision and support during this thesis research and for the data he provided throughout the project. I would also like to thank PhD Candidate Kim De Wit for supplying me with the interpolated dataset that played an important role in this research and for the valuable discussions that I had with her throughout my research. Lastly, I would like to thank TNO for providing the full core descriptions from their DINO database.

References

- AHN3 available through ArcGIS Living Atlas: Actueel Hoogtebestand Nederland, (Jan. 2022), https://services.arcgis.com/nSZVuSZjHpEZZbRo/arcgis/rest/services/Kaartbladen_AHN3/FeatureServer
- Arfai, J., Franke, D., Lutz, R., Reinhardt, L., Kley, J., & Gaedicke, C. (2018). Rapid quaternary subsidence in the northwestern German North Sea. *Scientific reports*, 8(1), 1-12.
- Van Asch N. (2007). Palaeo Seepage In The Holocene Subsurface Near Woerden, Central Netherlands, Faculty of Geosciences, Department of Physical Geography, Utrecht University
- Van Asselen, S., Stouthamer, E., & Van Asch, T. W. (2009). Effects of peat compaction on delta evolution: a review on processes, responses, measuring and modeling. *Earth-Science Reviews*, 92(1-2), 35-51.
- van Asselen, S., Erkens, G., Stouthamer, E., Woolderink, H. A., Geeraert, R. E., & Hefting, M. M. (2018). The relative contribution of peat compaction and oxidation to subsidence in built-up areas in the Rhine-Meuse delta, The Netherlands. *Science of the Total Environment*, 636, 177-191.
- Van Asch, N. (2007). Palaeo Seepage in The Holocene Subsurface Near Woerden, Central Netherlands, MSc. Thesis. Utrecht University
- Changxing, S., Dian, Z., Lianyuan, Y., Bingyuan, L., Zulu, Z., & Ouyang, Z. (2007). Land subsidence as a result of sediment consolidation in the Yellow River Delta. *Journal of Coastal Research*, 23(1), 173-181.
- de Gans, W. (2015). The geology of the Amstel river in Amsterdam (Netherlands): Man versus nature. *Netherlands Journal of Geosciences*, 94(4), 361-373.
- Gouw, M. J. P., & Erkens, G. (2007). Architecture of the Holocene Rhine-Meuse delta (the Netherlands)-a result of changing external controls. *Netherlands Journal of Geosciences*, 86(1), 23-54.
- de Haas, T., Pierik, H. J., Van der Spek, A. J. F., Cohen, K. M., Van Maanen, B., & Kleinhans, M. G. (2018). Holocene evolution of tidal systems in The Netherlands: Effects of rivers, coastal boundary conditions, eco-engineering species, inherited relief and human interference. *Earth-Science Reviews*, 177, 139-163.
- Hijma, M. P., Cohen, K. M., Hoffmann, G., Van der Spek, A. J., & Stouthamer, E. (2009). From river valley to estuary: the evolution of the Rhine mouth in the early to middle Holocene (western Netherlands, Rhine-Meuse delta). *Netherlands Journal of Geosciences*, 88(1), 13-53.
- Hijma, M. P., & Cohen, K. M. (2010). Timing and magnitude of the sea-level jump preludeing the 8200 yr event. *Geology*, 38(3), 275-278.
- Kiden, P., Denys, L., & Johnston, P. (2002). Late Quaternary sea-level change and isostatic and tectonic land movements along the Belgian–Dutch North Sea coast: geological data and model results. *Journal of Quaternary Science: Published for the Quaternary Research Association*, 17(5-6), 535-546.
- Kooi, H., & De Vries, J. J. (1998). Land subsidence and hydrodynamic compaction of sedimentary basins. *Hydrology and Earth System Sciences*, 2(2/3), 159-171.

- Kooi, H., & Erkens, G. (2020). Modelling subsidence due to Holocene soft-sediment deformation in the Netherlands under dynamic water table conditions. *Proceedings of the International Association of Hydrological Sciences*, 382, 493-498.
- Koster, K., Stafleu, J., & Cohen, K. M. (2017). Generic 3D interpolation of Holocene base-level rise and provision of accommodation space, developed for the Netherlands coastal plain and infilled palaeovalleys. *Basin Research*, 29(6), 775-797.
- Koster, K., De Lange, G., Harting, R., De Heer, E., & Middelkoop, H. (2018). Characterizing void ratio and compressibility of Holocene peat with CPT for assessing coastal-deltaic subsidence. *Quarterly Journal of Engineering Geology and Hydrogeology*, 51(2), 210-218.
- Liu, C. W., Lin, W. S., Shang, C., & Liu, S. H. (2001). The effect of clay dehydration on land subsidence in the Yun-Lin coastal area, Taiwan. *Environmental Geology*, 40(4), 518-527.
- Meijles, E. W., Kiden, P., Streurman, H. J., Van der Plicht, J., Vos, P. C., Gehrels, W. R., & Kopp, R. E. (2018). Holocene relative mean sea-level changes in the Wadden Sea area, northern Netherlands. *Journal of Quaternary Science*, 33(8), 905-923.
- Pierik, H. J., Cohen, K. M., Vos, P. C., Van der Spek, A. J. F., & Stouthamer, E. (2017). Late Holocene coastal-plain evolution of the Netherlands: the role of natural preconditions in human-induced sea ingressions. *Proceedings of the Geologists' Association*, 128(2), 180-197.
- Törnqvist, T.E., Hijma, M.P., 2012. Links between Early Holocene ice-sheet decay, sealevel rise and abrupt climate change. *Nat. Geosci.* 5 (9), 601–606.
- TNO, (2020), Detaillering Van De bovenste lagen met GeoTOP, Site: <https://www.dinoloket.nl/detaillering-Van-de-bovenste-lagen-met-geotop>
- Vermeersen, B. L., Slangen, A. B., Gerkema, T., Baart, F., Cohen, K. M., Dangendorf, S., ... & Van Der Wegen, M. (2018). Sea-level change in the Dutch Wadden Sea. *Netherlands Journal of Geosciences*, 97(3), 79-127.
- Vink, A., Steffen, H., Reinhardt, L., & Kaufmann, G. (2007). Holocene relative sea-level change, isostatic subsidence and the radial viscosity structure of the mantle of northwest Europe (Belgium, the Netherlands, Germany, southern North Sea). *Quaternary Science Reviews*, 26(25-28), 3249-3275.
- Vonhögen, L. M., Doornenbal, P. J., Lange, G. D., Fokker, P. A., & Gunnink, J. L. (2010). Subsidence in the Holocene delta of the Netherlands.
- Vos, P. (2015). *Origin of the Dutch coastal landscape: long-term landscape evolution of the Netherlands during the Holocene, described and visualized in national, regional and local palaeogeographical map series*. Barkhuis. ISBN: 9492444429, 9789492444424
- Vos, P., De Koning, J., & Van Eerden, R. (2015). Landscape history of the Oer-IJ tidal system, Noord-Holland (the Netherlands). *Netherlands Journal of Geosciences*, 94(4), 295-332.
- Weerts, H.J.T. 2003. Beschrijving lithostratigrafische eenheid. Nederlands Instituut voor Toegepaste Geowetenschappen TNO. Utrecht.

Weerts, H.J.T., Busschers, F.S. 2003. Beschrijving lithostratigrafische eenheid. Nederlands Instituut voor Toegepaste Geowetenschappen TNO. Utrecht.

Westerhoff W.E., De Mulder E.F.J., De Gans W. (1987). Geologische Kaart Van Nederland: Alkmaar West (19 W) & Alkmaar Oost (19 O). Rijks Geologische Dienst

Westerhoff, W. E., Kemna, H. A., & Boenigk, W. (2008). The confluence area of Rhine, Meuse, and Belgian rivers: Late Pliocene and Early Pleistocene fluvial history of the northern Lower Rhine Embayment. *Netherlands Journal of Geosciences-Geologie en Mijnbouw*, 87(1), 107.

de Wit, K., Van De Wal, R. S. W., and Cohen, K. M.: Reconstructing large scale differential subsidence in the Netherlands using a spatio-temporal 3D paleo-groundwater level interpolation, EGU General Assembly 2022, Vienna, Austria, 23–27 May 2022, EGU22-8350, <https://doi.org/10.5194/egusphere-egu22-8350>, 2022.

APPENDIX A

Core number	x-coordinate (RD-NEW)	y-coordinate (RD-NEW)	Height to Dutch O.D. (m)	Core depth (m)	Subsection
B14B0123	118800	544840	0.35	-10.4	6
B14B0140	119430	543170	-1	-34	6
B14B0398	119750	542460	-1.9	-6.9	6
B14B0439	119450	543140	-0.9	-6.15	6
B14B0442	119100	543680	-1		6
B14B0480	118850	544090	-1	-7	6
B14E0005	121490	539160	3.13	-11.4	6
B14E0006	121560	539090	1.48	-10.5	6
B14E0007	121380	539340	3.34	-13.02	6
B14E0008	121400	539250	-0.65	-12.1	6
B14E0217	122170	537940	-0.6	-7.8	6
B14E0219	122380	537640	-0.5	-15.4	6
B14E0245	121660	538940	-1.15	-12.85	6
B14E0246	121750	538780	-1	-8.15	6
B14E0248	121930	538450	-1	-12.1	6
B14E0249	122010	538320	-0.95	-7.95	6
B14E0251	122030	538200	-0.85	-7.85	6
B14E0252	122100	538060	-0.7	-12.4	6
B14E0290	121400	539280	-2.3	-8.3	6
B14E0300	121280	539580	-0.8	-18.8	6
B14E0303	121450	539450	-1.17	-3.57	6
B14E0305	121420	539210	-1.8	-15.9	6
B14E0306	121580	539200	-1.15	-7.85	6
B14E0307	121600	539080	-0.9	-15.2	6
B14E0336	120750	540700	-1.9	-8.1	6
B14E0339	121055	540280	-1.8	-7.3	6
B14E0377	120390	541450	-1.4	-7.4	6
B14E0379	120120	541910	-1.8	-7.3	6
B14G0033	125400	530600	-1.5	-46.5	6
B14G0058	125345	529685	-1.9	-15.4	6
B14G0069	124800	531500	-1.48	-52.48	6
B14G0086	123055	536410	-1.25	-10.95	6
B14G0086	123055	536410	-1.25	-10.95	6
B14G0088	125290	530920	-1.05	-13.9	6
B14G0089	125340	530100	-0.75	-22	6
B14G0090	125080	531180	-1	-24.2	6
B14G0165	121840	525290	-1.3	-7.3	6
B14G0176	122795	525890	-0.4	-32.4	6
B14G0398	124310	527240	-0.5	-32.5	6
B14G0452	124910	528310	-0.7	-5.95	6
B14G0691	123840	532780	-0.85	-14.85	6
B14G0700	124410	532200	-1.15	-15.15	6

B14G0742	123350	533420	-0.65	-15.05	6
B14G0749	124260	533130	-3	-9.2	6
B14G0793	123140	534060	-0.65	-12.75	6
B14G0794	123960	534040	-4.45	-10.45	6
B14G0796	123760	534630	-2.9	-8.9	6
B14G0847	122960	535250	-1.05	-12.75	6
B14G0850	122950	535720	-1.3	-12.8	6
B14G0906	122960	536540	-1.5	-13.5	6
B14G0908	122720	536940	-1.2	-12.9	6
B14G0909	122830	536720	-1.15	-12.65	6
B14G0916	123200	536005	-1.45	-14.25	6
B14G0951	122630	537170	-0.85	-11.85	6
B14G0952	122480	537460	-0.35	-8.05	6
B19E0091	121125	524805	0.18	-69.82	6
B14G0787	122850	534750	-2.3	-8.8	6
B14G0106	125490	528790	-1	-32	6
B14G0393	124460	527630	-1.1	-7.3	6
B19E0158	120920	521620	-2.1	-21.6	5
B19E0094	120900	520820	-1.93	-121.93	5
B19E0624	121230	519140	-1.8	-7.4	5
B19E0093	121310	518365	-1.88	-69.88	5
B19E0537	121180	517040	-2.5	-8	5
B19E0491	121290	516450	-2.3	-10.1	5
B19E0489	121080	516040	-2.5	-9.5	5
B19E0092	121078	515161	-2.49	-57.49	5
B19E0383	120980	514570	-3	-13	5
B19E0336	120680	513740	-3.6	-10.6	5
B19E0298	120350	512760	-3.4	-8.4	5
B19G0225	120215	512410	-1.53	-51.53	5
B19G0348	120000	512180	-3.1	-20.7	5
B19G0897	120060	511260	-1.9	-6.9	5
B19G0852	120080	510600	-1.9	-6.9	5
B19G0808	120310	509820	-3.6	-11.6	5
B19G0810	120090	509140	-3.6	-11.6	5
B19G0224	120250	508775	-3.65	-123.65	5
B19G0732	120350	508190	-3.8	-12.8	5
B19G0019	120220	507748	-3.4	-73.4	5
B19G0732	120440	507250	-3.8	-11.8	5
B19G0663	121050	505970	-3.5	-7.5	5
B19G0235	121250	505490	-3.4	-62.4	5
B19G0169	121650	503500	-1.95	-57.95	5
B19G0549	121660	502630	-1.6	-6.6	5
B19G0550	121660	502100	-4	-9	5
B19G0223	121650	501040	-3.28	-150.38	5
B19G0170	121900	500250	-3.65	-64.65	5

B19E0925	120920	523950	-1.6	-8.2	5
B19G0627	121330	504320	-3.4	-9.1	5
B19E0616	120900	519780	-2	-7	5
B19E0823	121330	522880	-2.3	-8.7	5
B25E0892	122500	488560	0	-101.75	4
B25E0892	122500	488560	0	-101.75	4
B25E0868	121840	499070	-1.1	-22.85	4
B25E0871	122270	497700	-1.4	-17.1	4
B25E0273	122300	497620	-2.1	-27.15	4
B25E0879	122140	497390	-2	-17.5	4
B25E0891	122210	497330	-1	-85	4
B25E0825	122300	497230	-1.3	-16.3	4
B25E0275	122210	496900	-1.28	-45.38	4
B25E0349	122500	496130	-1.03	-52.03	4
B25E0834	122320	495540	-1.9	-14.9	4
B25E1471	122440	495280	-1.9	-7.9	4
B25E0271	122480	494370	-2.35	-24.95	4
B25E1981	122587	493949	-1.38	-20.88	4
B25E0368	122680	493640	1.38	-20.88	4
B25E0369	122640	493530	-1.37	-20.87	4
B25E0370	122610	493300	-1.46	-20.96	4
B25E0047	122361	492531	-0.8	-18.8	4
B25E0371	122540	493060	-1.05	-14.25	4
B25E0391	122520	492950	-2.04	-14.64	4
B25E0385	122462	492815	-1.09	-12.8	4
B25E0389	122333	492465	-1.46	-14.66	4
B25E0387	122276	492278	-0.5	-13.7	4
B25E0899	122160	492110	-3.5	-33.75	4
B25E0446	122220	491310	0.37	-14.63	4
B25E0426	122270	490610	-2.55	-13.35	4
B25E0535	122290	490330	-0.54	-25.14	4
B25E0430	122310	490140	-1.25	-13.25	4
B25E0547	122400	489460	1.11	-14.49	4
B25E0078	122450	488960	0.52	-15.48	4
B25E0541	122260	488500	1.65	-58.95	4
B25E0735	122120	488300	0.7	-40	4
B25E0110	121592	487640	1	-24	4
B25G0208	121450	486945	1.2	-89.6	4
B25G0095	121860	485950	0.9	-25.6	4
B25G0557	122080	485690	1.34	-12.76	4
B25G2330	122499	484630	0.65	-14.05	4
B25G0016	122628	484223	0.71	-20.79	4
B25G0678	122610	483930	-1.15	-26.15	4
B25G0172	122560	483340	-2.11	-27.11	4
B25G0173	122620	482610	-2.08	-17.08	4

B25G0176	122690	481780	-1.78	-16.78	4
B25G1634	122650	480920	-1.8	-10.7	4
B25G1632	122640	480520	-1.8	-11.1	4
B25G1632	122640	480520	-1.8	-11.1	4
B25E1194	122320	491690	-3	-9	4
B25G0565	121730	486510	0.28	-19.52	4
B25G0549	122430	485170	-2.7	-12.6	4
B25G0211	121430	487420	-0.7	-30.7	4
B25G0269	121240	487220	1.2	-123.1	4
B25G1631	122560	480200	-1.8	-10.3	3
B25G0187	122400	479980	-1.8	-26.8	3
B25G1535	122130	479480	-1.8	-10.6	3
B25G2736	121926	478862	-0.18	-11.38	3
B25G1401	121750	478525	-1.8	-10.6	3
B25G1397	121520	478160	-2.1	-11.2	3
B25G1284	121075	477705	-1.8	-11.7	3
B25G1267	120760	477345	-2.1	-11	3
B25G1272	120550	477020	-2.1	-11.1	3
B25G1174	120020	476190	-5.2	-10.7	3
B25D0695	119820	475940	-5	-10	3
B31B0956	119650	474120	-1.8	-9.5	3
B31B0862	119870	472950	-5.25	-9.95	3
B31B0863	119870	472950	-5.25	-9.95	3
B31B0805	119600	471760	-5.4	-9.8	3
B31B0812	119520	471220	-5.1	-9.7	3
B31B0719	119400	470885	-5.1	-9.3	3
B31B0725	119325	470560	-4.9	-9.7	3
B31B0730	119190	470090	-5.4	-10	3
B31B0639	119020	469280	-5	-10.2	3
B31B0576	118820	468400	-5.1	-10.1	3
B31B0521	118840	467745	-5.2	-9.7	3
B31B0468	118620	466875	-4.9	-9.61	3
B31B0467	118400	466640	-5.2	-10	3
B31B0415	118220	465805	-1.2	-10.2	3
B31B0979	117960	464910	-1.4	-9.5	3
B31B0358	117860	464300	-1.3	-9.4	3
B31B0285	117580	463590	-1.4	-9.4	3
B31B0235	117310	462640	-1.6	-8.8	3
B31D1334	117015	461975	-1.8	-9.3	3
B31D1326	116860	461130	-1.9	-8.7	3
B31D1265	116840	460770	-1.8	-8.5	3
B31D1206	116720	459750	-1.8	-8.8	3
B31D1204	116720	459220	-1.6	-8.6	3
B31D1052	116470	457840	-1.6	-8.7	3
B31D0984	116400	456020	-1.6	-7.6	3

B31D0895	116420	455880	-1.6	-8.6	3
B31D0892	116480	455440	-1	-8.7	3
B31D0018	116478	454048	-1.62	-12.12	3
B31D0662	116430	453460	-1.4	-7.41	3
B31D0531	116360	452330	-1.5	-7.9	3
B31D0330	116460	450530	-1.6	-8.6	3
B38B2027	116419	449795	-1.5	-9.5	3
B38B2026	116548	449402	-1.7	-10.1	3
B31B0030	119583	474455	-2	-31	3
B31B0905	119950	473475	-5.1	-10.1	3
B31D1145	116180	458810	-1.7	-8.7	3
B31D0426	116415	451570	-1.7	-9.3	3
B38B2026	116548	449402	-1.7	-10.1	2
B38B2019	116516	449053	-1.3	-9.8	2
B38B1912	116673	448830	-1.2	-10	2
B38B1781	117136	447339	-1.6	-12.2	2
B38B1668	117245	446881	-1.5	-13.5	2
B38B1220	118493	443984	-1.5	-10.7	2
B38B1215	118806	443750	-1.3	-10.7	2
B38B0940	119268	441511	-1	-9	2
B38B0817	118730	440437	-0.8	-10.8	2
B38B0682	117551	439928	-1.1	-11.6	2
B38B0011	116997	439703	-0.8	-16.3	2
B38B0660	115719	439208	-1.6	-12	2
B38B0516	115188	438979	-1.1	-12.1	2
B38B0008	114550	438650	-0.75	-15.75	2
B38B0494	114400	438321	-1.2	-12	2
B38B0495	114391	438038	-1.1	-11.6	2
B38D3315	114460	436545	-0.9	-11.9	2
B38D3324	114438	436433	-1.1	-12.9	2
B38D3299	114365	436194	-1.3	-12.7	2
B38D3139	114017	435162	-1.4	-12.4	2
B38D2524	112810	433465	-1.2	-12.2	2
B38D2122	112245	432820	-1.6	-12.6	2
B38D2109	111376	432603	-1.6	-9.6	2
B38D2029	110360	432125	-1.67	-12.67	2
B38C1955	109666	431651	-1.8	-12.8	2
B38C1682	107302	430640	-1.3	-11.2	2
B38C1700	107145	430690	-0.7	-7.2	2
B38C1308	106528	428780	-1.4	-12.4	2
B38C0529	106055	428020	-0.3	-14.3	2
B38C0808	106090	426820	-1.5	-19.5	2
B38B1425	118484	444457	-1.3	-12.1	2
B38B1058	118834	442891	-1.4	-11.4	2
B38B0681	116467	439763	-1.1	-10.1	2

B38D0038	113966	434788	-1.02	-13.02	2
B38D2926	113953	434128	-1.5	-12.7	2
B38C1709	108776	430116	-1.25	-9.25	2
B38C1489	106370	429493	-1.3	-12	2
B38C0605	105870	425490	0.7	-21.3	1
B44A0021	105690	424930	0.6	-20.9	1
B44A1154	105624	424583	-1.15	-11.15	1
B44A0086	105010	423595	-0.1	-20.1	1
B44A0236	105190	421810	-0.6	-11.2	1
B44A0237	105040	421420	-0.6	-14.1	1
B44A0910	104750	420670	-0.6	-9.3	1
B44A0846	104120	419700	-0.3	-7.8	1
B44A0842	103830	419215	-0.3	-7.2	1
B44A0809	103740	418740	-0.3	-6.3	1
B44A1335	103379	417674	-0.32	-17.42	1
B44A0139	103070	416240	-1.4	-26.4	1
B44A0220	105680	422760	-0.82	-23.8	1
B44A0923	105025	420980	-0.3	-7.2	1
B44A1193	102805	417120	-4.77	-7.16	1

Appendix B 14C sample list

Lab ID nr	14C age	14C error	14C Calibrated yr cal BP	x-coordinate	y coordinate	Surface elevation (m O.D.)	Depth below surface (m OD)	Sample Name	Dated material and source material	Reference in cross-section
GrA-11303	5110	50	5840	105465	410062	-1.3		RAAP-report 304:53	Charcoal	E1
GrA-11306	4890	50	5630	105458	410145	-1.92		RAAP-report 304-53	Charcoal	E2
GrA-11301	6090	50	6965	105160	410807	-3.82		RAAP-report 304:45	Charcoal	E3
GrA-11302	6550	50	7460	104894	411525	-4.13		RAAP-report 304:43	Charcoal	E4
UtC-13820	7000	50	7830	99861	421423	-1	-12.1	HSL-Zuid-K19-M6	Salix Cenera leaf fragments (brackish silty gyttja)	1
UtC-13816	7670	60	8470	99861	421423	-1	-13.1	HSL-Zuid-K19	Wood / roots (peat)	2
UtC-13817	7390	60	8205	99861	421423	-1	-12.88	HSL-Zuid-K19	TM (brackish silty gyttja)	3
UtC-13818	6229	47	7125	99861	421423	-1	-10.1	HSL-Zuid-K19	TM (brackish silty gyttja)	4
UtC-13819	6740	50	7600	99861	421423	-1	-11.51	HSL-Zuid-K19-M5	Salix Cenera leaf fragments (brackish silty gyttja)	5
UtC-10290	7221	49	8045	106520	429300	-1.27	-12.34	Alblas99-01	TBM (clayey peat)	6

GrN-10089	5410	70	6185	106725	429775	-1.5	-6.6	Oud-Alblas West 1	Clayey Phragmites (-Carex) peat	7
GrN-10090	4670	70	5405	106725	429775	-1.5	-5.82	Oud-Alblas West 2	Slightly earthed peat with pieces of wood	8
GrN-10091	4630	70	5350	106725	429775	-1.5	-5.18	Oud-Alblas West 3	Very clayey peat with some twigs	9
GrN-10092	4050	60	4565	106725	429775	-1.5	-4.28	Oud-Alblas West 4	Clayey wood peat	10
GrA-07124	3720	70	7185	108204	430555	-0.87	-2.08	Oud Alblas 9	TBM (sand)	11
GrA-07125	4500	80	7005	108206	430559	-0.98	-2.94	Oud Alblas 10	TBM (sand)	12
GrA-07123	5090	90	6970	108212	430561	-1.14	-4.59	Oud Alblas 2	TBM (wood peat)	13
GrA-06511	5300	60	6750	108214	430565	-1.16	-5.2	Oud Alblas 3	TBM (wood peat)	14
GrA-07113	5770	70	6570	108218	430569	-1.21	-5.78	Oud Alblas 4	TBM (wood peat)	15
GrA-06512	5920	60	6090	108222	430573	-1.38	-6.35	Oud Alblas 5	TBMs (wood peat)	16
GrA-06514	6090	60	5825	108227	430578	-1.3	-6.79	Oud Alblas 6	TBM (wood peat)	17
GrA-07128	6120	80	5140	108237	430588	-1.18	-7.35	Oud Alblas 7	TBM (wood peat)	18
GrA-06513	6280	60	4075	108264	430605	-1.56	-8.13	Oud Alblas 8	TBM (wood peat)	19
GrN-10888	3940	60	4375	110370	432187	-1.7	-3.76	Oud-Alblas Oost 1	Slightly clayey wood peat	20
GrN-10889	5420	40	6220	110370	432187	-1.7	-7.2	Oud-Alblas Oost 2	Clayey peat with some wood and reed	21
GrN-00191	4590	150	5250	113865	434050	-0.38	-3.31	Brandwijk 4	Fen-wood peat	22

GrN-00192	2830	135	2990	113865	434050	-0.15	-1.15	Brandwijk 2	Fen-wood peat	23
GrN-00189	5665	200	6490	113865	434050	-0.86	-8.41	Brandwijk 6.1		24
GrN-00201	7540	170	8345	113865	434050	-0.86	-10.08	Brandwijk 6.2	Fen-wood peat	25
GrN-00203	6050	200	6915	113865	434050	-0.57	-6.47	Brandwijk 5	Fen-wood peat	26
GrN-18971	6240	50	7140	114500	437800	-1.12	-6.75	Bergstoep I	Charcoal	27
UtC-11756	5775	48	3295	119496	441227	-0.9	-5.3	Zevender-1A	Wood (bark fragments)	28
UtC-11757	5586	50	5795	119496	441227	-0.9	-5.31	Zevender-1B	Wood (root fragments)	29
UtC-13813	5050	50	6575	119494	441231	-0.89	-2.87	Zevender-5	TM (peat)	30
UtC-13812	3100	70	6370	119485	441248	-0.83	-1.46	Zevender-3	TM (wood peat)	31
UtC-13814	6910	90	7755	119462	441306	-0.9	-8.81	Zevender-7	TM (wood peat)	32
GrN-09403	3995	40	4470	118500	444475	-1.56	-3.66	PB Polsbroek I	Wood peat	33
GrN-09404	4650	40	5395	118500	444475	-1.56	-5.61	PB Polsbroek II	Wood peat with gyttja	34
GrN-09405	5810	40	6610	118500	444475	-1.56	-6.84	PB Polsbroek III	Phragmites peat	35
GrN-09406	6335	45	7255	118500	444475	-1.56	-7.56	Polsbroek IV	Slightly clayey Phragmites peat	36
GrN-09407	7135	45	7955	118500	444475	-1.56	-8.44	Polsbroek V	Strongly clayey Phragmites peat	37
GrN-09408	7600	45	8400	118500	444475	-1.56	-10.58	Polsbroek VI	Slightly clayey Phragmites peat	38

GrN-09409	11470	60	13345	118500	444475	-1.56	-12.2	Polsbroek IX	Peat	39
UtC-12336	6238	49	7135	117317	449201	-1.4	-7.46	Ruigeweide I	Peat	40
UtC-12337	6950	50	7780	117317	449201	-1.4	-8.19	Ruigeweide II	Peat	41
UtC-14572	6360	60	7285	117142	449759	-1.67	-9.6	Dekzand W DZW-21	Scirpus macrofossils (peat)	42
UtC-14571	6810	80	7660	117142	449759	-1.67	-10.44	Dekzand W DZW-37	Alnus macrofossils (basal peat)	43
GrN-08760	6480	45	7860	116715	458575	-1.56	-8.05	Zegveld (Z2)	Phragmites peat with piece of bark	44
GrN-08761	7030	45	7380	116675	458600	-1.61	-8.37	Zegveld (Z1)	Phragmites peat with pieces of wood	45
GrN-13487	5920	45	6745	119870	472950	-5.25	-8.44	Waverveen II-1	Phragmites peat	46
GrN-13488	6095	45	6975	119870	472950	-5.25	-8.87	Waverveen II-2	Phragmites peat	47
GrN-13484	5410	40	6210	119750	472950	-3.82	-7.08	Waverveen I-2	Clayey Phragmites peat	48
GrN-13483	4690	40	5415	119750	472950	-3.82	-5.75	Waverveen I-1	Phragmites peat	49
GrN-10834	5850	60	6660	119466	475532	0	-8.29	Nes a/d Amstel Ia		50
GrN-18712	5250	50	6040	122640	480520	-1.8	-5.46	Klein Duivendrechtse Polder I (GrN-18712)	Base of Phragmites peat intercalation in gyttja	51
GrN-06717	3515	35	3785	122640	480520	-1.8	-3.52	Klein Duivendrechtse Polder III	Phragmites peat, end open water	52
GrN-21601	4720	40	5445	122500	488560	0	-5.95	Willemsluizen I Amsterdam	Peat	53
GrN-21602	5920	70	6750	122500	488560	0	-7.65	Willemsluizen II Amsterdam	Peaty clay with woodfragments, imbedden in Calais (Wormer)	54

GrN-08664	4335	35	4910	122580	503240	-1.7	-2.86	Neck I	Phragmites peat with Eriophorum	55
GrN-08665	4440	60	5085	122580	503240	-1.7	-3.19	Neck II	Base of slightly clayish Phragmites peat	56
GrN-08669	3930	80	4365	117920	510980		-2.31	Spanbroek I	Phragmites peat - Hollandveen	57
GrN-08671	4565	40	5220	117920	510980	-0.78	-3.92	Spanbroek III		58
GrN-08667	4010	60	5125	117920	510980	-1.93	-2.68	Menningweerdijk I		59
GrN-08668	4425	40	3085	117920	510980	-1.93	-2.96	Menningweerdijk II		60
GrN-04619	4485	85	5435	124165	513445	0	-2.43	Oostmijzen	Base of gyttja overlying clay and underlying peat	61
GrN-03546	2930	80	4365	124950	520400	0	-1.75	Wogmeer		62
GrN-08673	4250	35	4800	125350	521700	-0.99	-3.25	Zandwerven A	Peat	63
GrN-08098	6980	40	7810	137980	524265	-12.6		Zwaagdijk II	Phragmites peat - Basisveen	64
GrN-10245	7620	60	8415	137980	524265	-12.69		Zwaadijk III	Top of "sterk zandige mor" directly under the Basisveen; Ah horizon top Pleistocene?	65
GrN-06602	2975	30	3145	124390	525630	0	-0.62	Hoogwoud		66
GrN-06601	2440	30	2515	124390	525630	0	-0.25	Hoogwoud		67
GrN-06603	3150	35	3370	124390	525630	0	-0.81	Hoogwoud		68
GrN-05554	3440	90	3700	124720	527700	0	-1.74	Aardswoud 1	Peaty clay	69
GrN-05555	4160	65	4685	124720	527700	0	-2.14	Aardswoud 2	Peaty clay	70

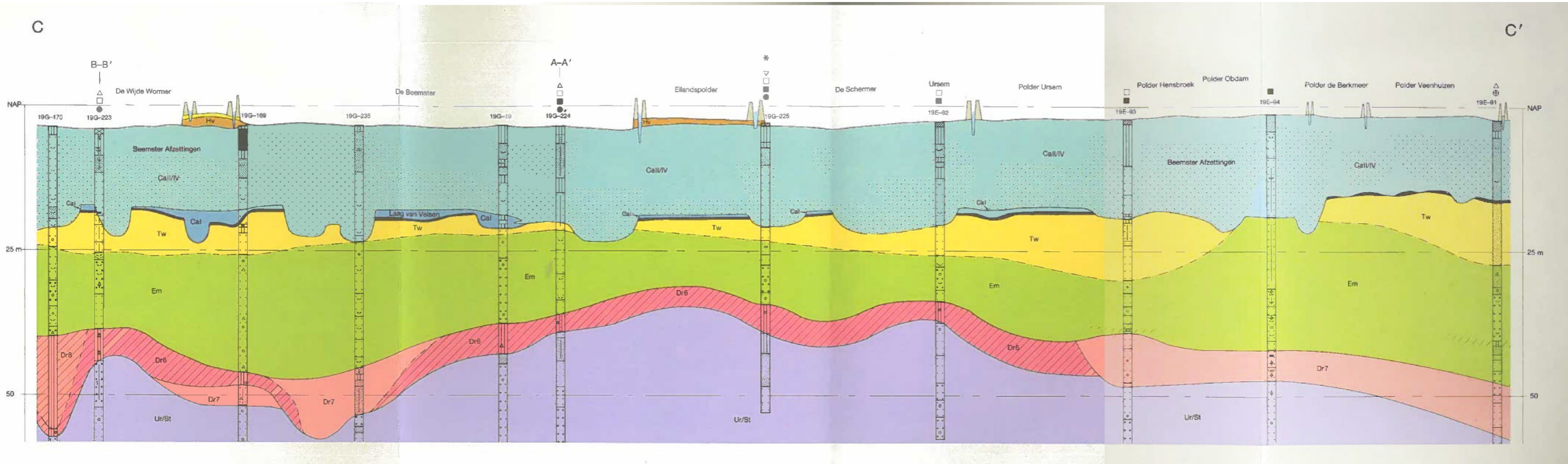
GrN-01123	7310	65	8120	107525	530450	-8.91		Burgervlotbrug 2	Base of Basisveen	71
GrN-01131	5310	65	6095	107525	530450	-8.24		Burgervlotbrug 1	Top of Basisveen	72
GrN-05946	4360	45	4945	124810	531510	0	-4.35	Wieringermeer C11 b		73
GrN-06315	5045	60	5790	124810	531510	0	-6.06	Wieringermeer C11 c		74
GrN-01624	6020	70	6870	109300	534050	-7.22		St. Maartensvlotbrug 4	Base of Basisveen. Location of Jelgersma estimated appr as the same as De Mulder & Bosch, but in reality it deviates	75
GrN-05904	4480	45	5140	123055	536410	-1.25	-3.45	Wieringermeer Waardweg I	Clayish gyttja	76
GrN-05905	5685	40	6470	123055	536410	-1.25	-7.36	Wieringermeer Waardweg II	Gyttja with Phragmites	77
GrN-14270	6390	70	7310	123055	536410	-1.25	-10.75	Wieringermeer: Waardweg III	Peat	78
GrN-05945	4040	45	4530	122170	538180	0	-2.93	Wieringermeer B1		79
GrN-01116	4090	55	4625	113500	541900	-3.23		Schermer Omval	Peat bed	80
GrN-00819	3865	85	4275	119160	543400	0	-2.95	Anna Paulowna Ia		81
GrN-00820	4605	85	5290	119160	543400	0	-4.42	Anna Paulowna Ib		82
GrN-00824	5665	105	6470	119160	543400	0	-8.09	Anna Paulowna II		83
GrN-06313	3920	55	4345	118820	545630	0	-2.79	Balgzanddijk km. 6.3 a		84
GrN-06314	4630	40	5385	118820	545630	0	-6.15	Balgzanddijk km. 6.3 b		85

GrN-00455	6320	185	5670	112050	548300	-6.02		Koegras I 5	Basisveen in excavation pit. Pit Koegras I	86
GrN-00476	4925	190	7195	112050	548300	-4.72		Koegras II 2	Basisveen in excavation pit. Pit Koegras I = Koegras II. Samples from different sections within pit	87

Appendix C – Cross-sections from literature

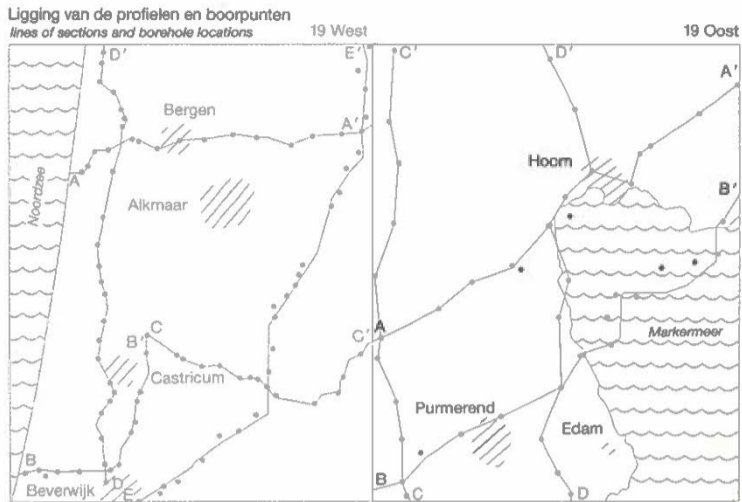
Cross-sections from literature that were used in constructing the cross-section of Andeweg, 2022. Ordered as mentioned in section 3.2 in the main text.

Westerhoff et al., 1987 – Alkmaar Oost, Cross-section C-C'



The legend can be found on the next page.

Legend: Westerhoff et al., 1987 – Alkmaar Oost, Cross-section C-C'



LEGENDA STRATIGRAFIE LEGEND STRATIGRAPHY

KWARTAIR QUATERNARY

HOLOCENE HOLOCENE

Westland Formatie Westland Formation

	Afzettingen van Duinkerke III Dunkirk III Deposits	—	IJse Afzettingen Ice Deposits
	Afzettingen van Duinkerke II en III Dunkirk II and III Deposits	—	Almere- en Zuiderzee Afzettingen Almere- and Zuiderzee Deposits
	Hollandveen Holland Peat		
	Afz. v. Duinkerke 0 en Afz. v. Calais IV Dunkirk 0 Deposits and Calais IV Deposits	—	Hauwert Complex Hauwert Complex
	Afzettingen van Calais II, III en IV Calais II, III and IV Deposits	—	Beemster Afzettingen Beemster Deposits
	Afzettingen van Calais I Calais I Deposits	—	Laag van Velsen Velsen Bed
	Basisveen Lower Peat		

PLEISTOCENE PLEISTOCENE

	Formatie van Twente, hoofdzakelijk dekzand Twente Formation, mainly coversands
	Eem Formatie (Em) en Formatie van Kreftenheye (Kr) Eem Formation (Em) and Kreftenheye Formation (Kr)
	Formatie van Drente, lacustroglaciale afzettingen Drente Formation, lacustroglacial deposits
	Formatie van Drente, fluvioglaciale afzettingen Drente Formation, fluvioglacial deposits
	Formatie van Drente, grondmorene (keileem) Drente Formation, till (boulder clay)
	Formatie van Eindhoven Eindhoven Formation
	Formaties van Urk en Sterksel Urk and Sterksel Formations

TOEVOEGINGEN ADDITIONS

	Vermoedelijk gestuwde afzettingen (Form. v. Eindhoven en Form. v. Urk en Sterksel) Probably ice-pushed deposits (Eindhoven Form., and Urk and Sterksel Form.)
	Klei (Eem Form. en Form. v. Urk en Sterksel) of keileem (Form. v. Drente) Clay (Eem Form., Urk and Sterksel Form.) or boulder clay (Drente Form.)
	Zand, soms kleilig (Westland Formatie) Sand, clayey (Westland Formation)
	Vegetatieniveau (venige klei tot kleilig veen, soms veen) Vegetation horizon (peaty clay - clayey peat, occasionally peat)

DIVERSEN MISCELLANEOUS

	Water
	Opgebracht Raised
	Grens onzeker Boundary uncertain
19F-71	RGD-archiefnummer RGD file number

* Geprojecteerde boring
Projected borehole

LABORATORIUM ONDERZOEK LABORATORY INVESTIGATIONS

	Sedimentologie (granulometrie) Sedimentology (granulometry)
	Sedimentpetrologie (zware mineralen) Sedimentpetrology (heavy minerals)
	Paleobotanie (pollen) Palaeobotany (pollen)
	Paleobotanie (diatomeeën) Palaeobotany (diatoms)
	Macropaleontologie (mollusken) Macropalaeontology (molluscs)
	Micropaleontologie (forams) Micropalaeontology (forams)
	Micropaleontologie (ostracoden) Micropalaeontology (ostracods)

LEGENDA LITHOLOGIE LEGEND LITHOLOGY

	Opgebrachte- en/of geroerde grond Raised, reworked		Kleibrokjes Pieces of clay
	Onbepaald Unknown		Leem Silt (loam)
	Stenen Cobbles		Veen Peat
	Grind Gravel		Veen, kleilig Peat, clayey
	Grindhoudend Gravel bearing		Klei, venig Clay, peaty
	Zand, zeer- en uiterst grof (300-2000 µm) Sand, very coarse		Veenbrokjes Pieces of peat
	Zand, matig fijn en matig grof (150-300 µm) Sand, fine- to coarse		Houtresten Wood
	Zand, uiterst fijn en zeer fijn (63-150 µm) Sand, fine- to very fine		Plantenresten Plant remains
	Zandig Sandy		Humeus Humic
	Sterk zandig Strongly sandy		Schelpfragmenten Shell fragments
	Zandlaagjes of lensjes Sandlayers or -lenses		Schelpen, marien Shells, marine
	Klei Clay		Schelpfragmenten, marien Shell fragments, marine
	Kleilig Clayey		Schelpfragmenten, niet marien Shell fragments, non marine
	Sterk kleilig Strongly clayey		Veel Abundant
	Verkittingen Cemented		Weinig Sparing

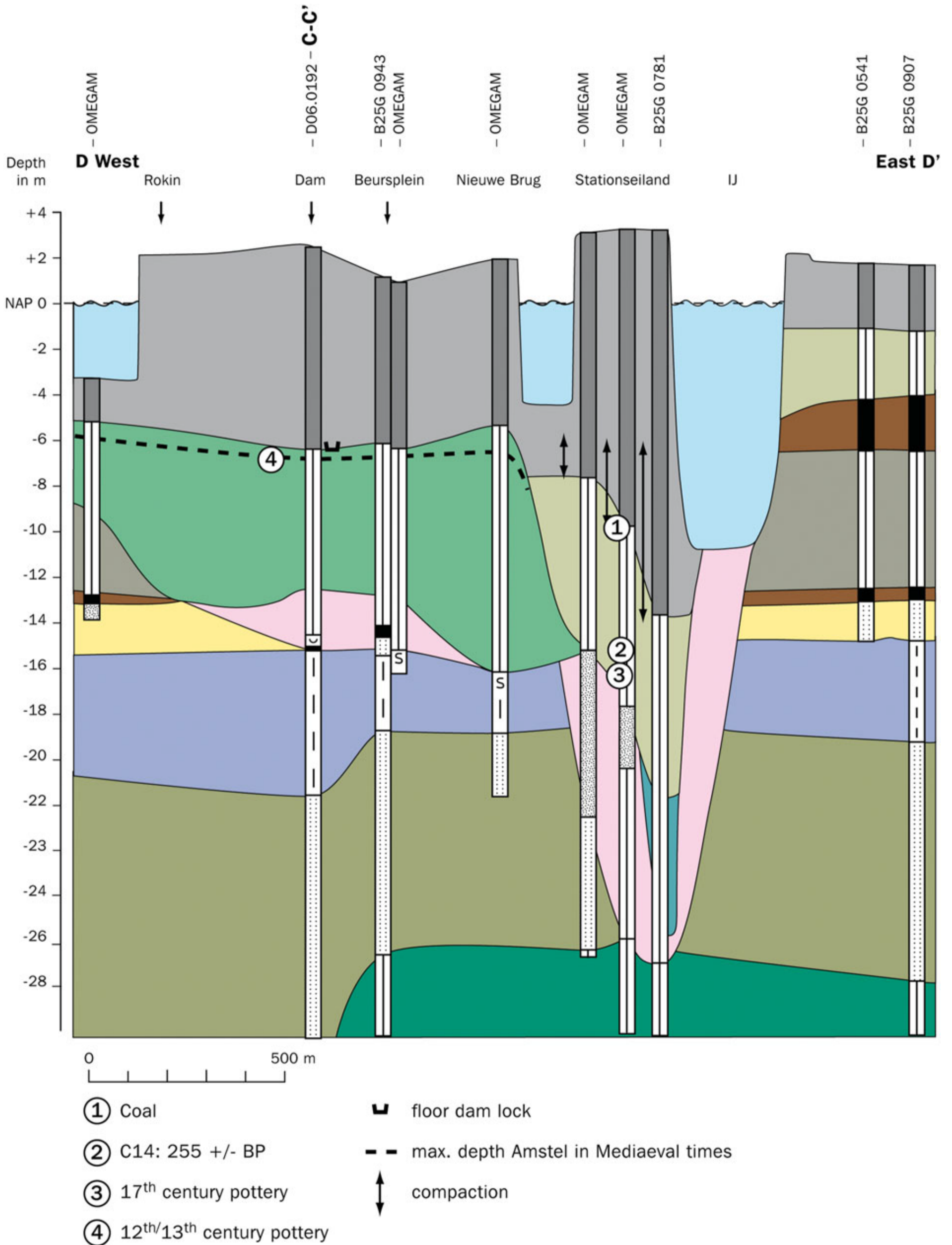
RIJKS GEOLOGISCHE DIENST
GEOLOGICAL SURVEY OF THE NETHERLANDS

Direkteur: Chr. Staudt
Director: Chr. Staudt

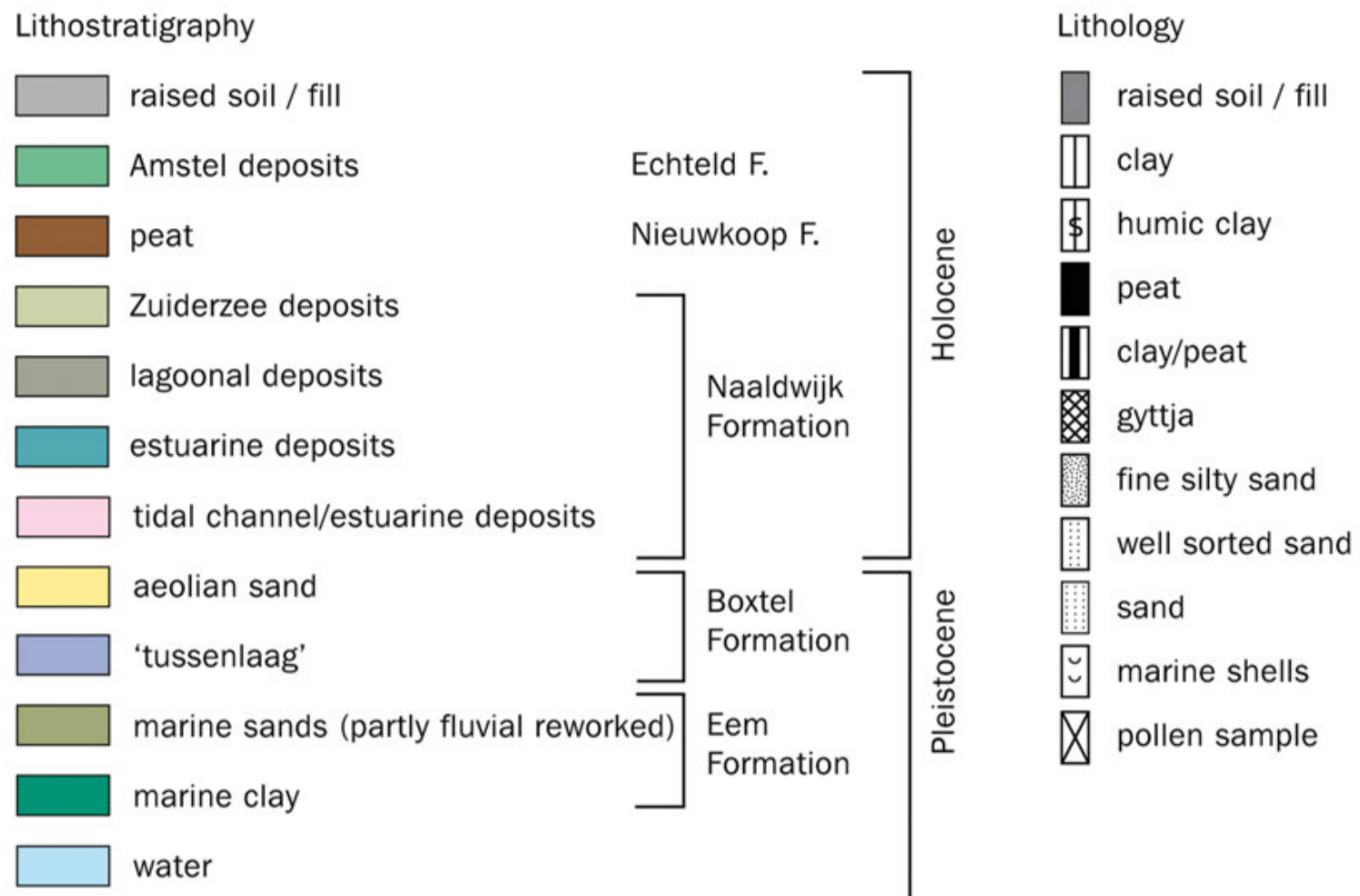
Samengesteld door E. F. J. de Mulder en J. Blokzijl; onderzoek beëindigd in 1980
Composed by E. F. J. de Mulder and J. Blokzijl; survey completed in 1980

Reference

Westerhoff W.E., De Mulder E.F.J., De Gans W. (1987).
Geologische Kaart Van Nederland: Alkmaar West (19 W) &
Alkmaar Oost (19 O). Rijks Geologische Dienst



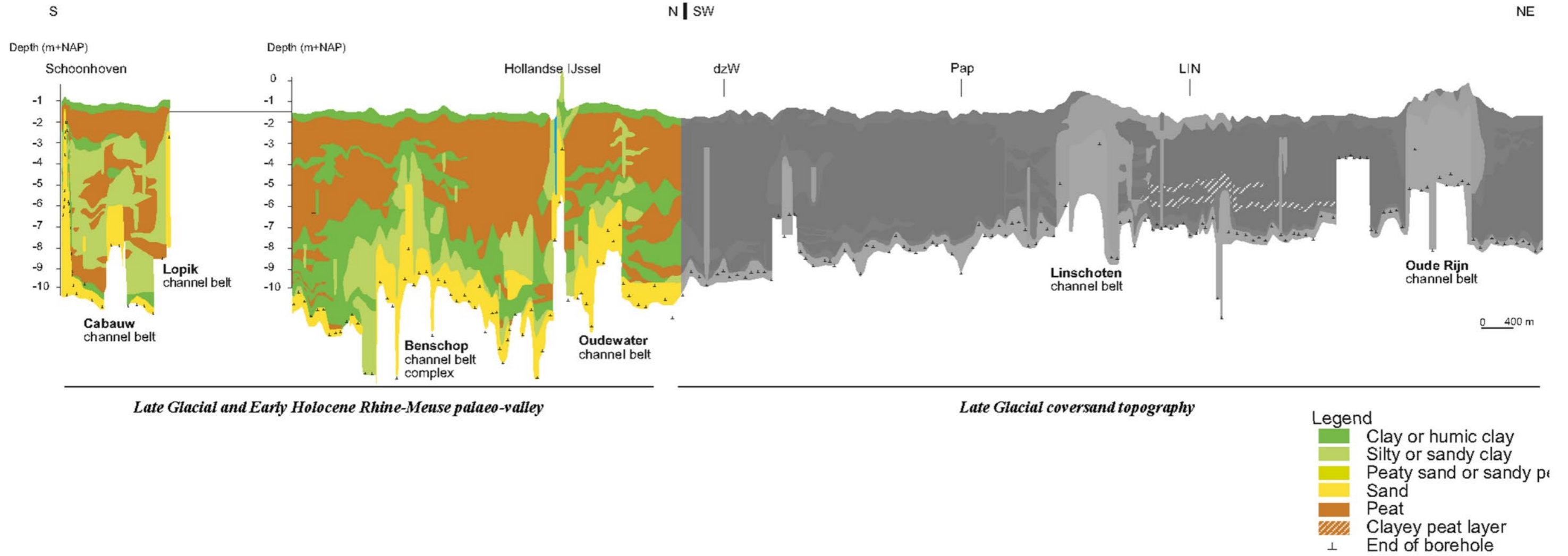
Legend: De Gans, 2015 – Amsterdam Damrak-Rokin, Cross-section D-D'



Reference

de Gans, W. (2015). The geology of the Amstel river in Amsterdam (Netherlands): Man versus nature. *Netherlands Journal of Geosciences*, 94(4), 361-373.

Van Asch, 2007 – Figure 9.



*Greyed out area is not part of the cross-section in Andeweg, 2022






Reference

Van Asch N. (2007). Palaeo Seepage In The Holocene Subsurface Near Woerden, Central Netherlands, Faculty of Geosciences, Department of Physical Geography, Utrecht University






Cross-section legend

Middle-Holocene

Naaldwijk Formation -Wormer member

-  Sand dominated channel
(Sand with shells and possible lamination)
-  Tidal channel fill
(Sandy clays)
-  Mud dominated tidal channel
(Sandy clays laminated with sandy layers)
-  Mud and sand flats
(Sandy clays with possible lamination)
-  Distal tidal clays
(Clays with possible shells and organic fragments)

Echteld Formation

-  Fluvial channel belt deposits
(Sand and gravel)
-  Levee and crevasse splay
(Sandy clays with possible lamination)
-  Fluvial channel fill
(upward fining of sediments above channel belt)
-  Proximal flood basin
(Silty clays)
-  Distal flood basin
(Humic clays)

Nieuwkoop Formation

-  Mossy peat
-  Sedge peat
-  Reed peat
-  Woody peat
-  Gyttja - lacustrine deposits
-  Undifferentiated peat





Pleistocene undifferentiated



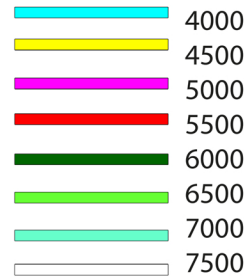
Late-Holocene undifferentiated



Symboles

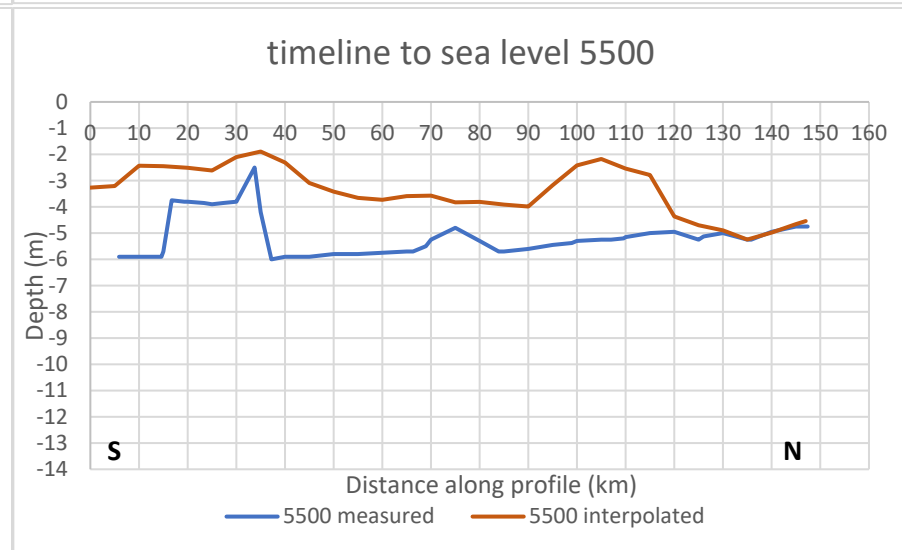
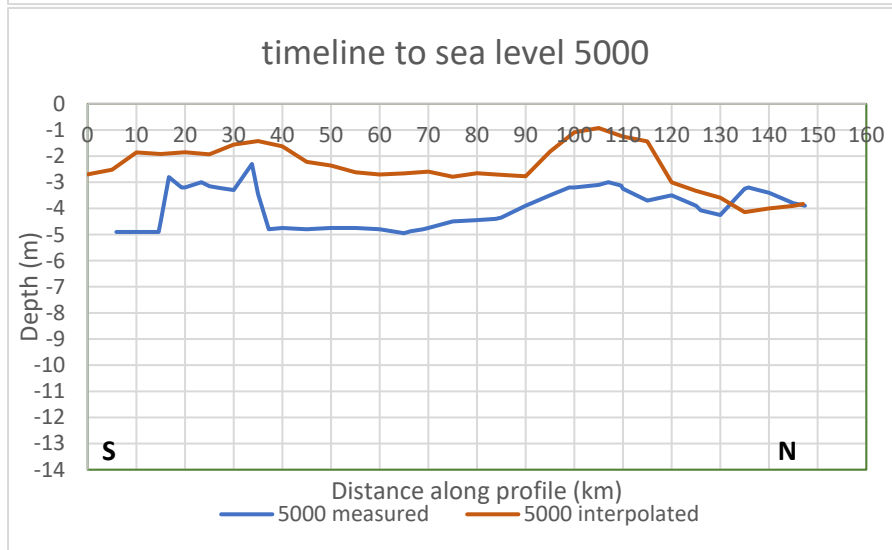
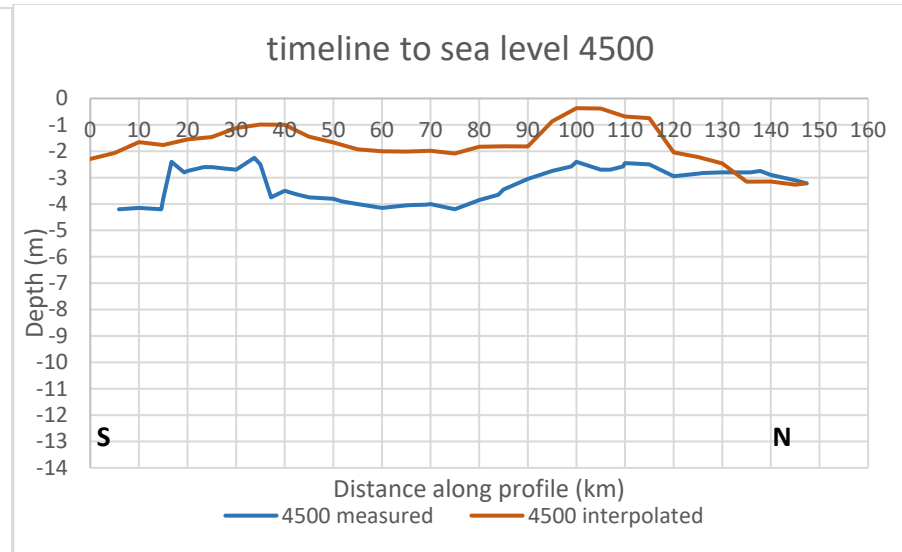
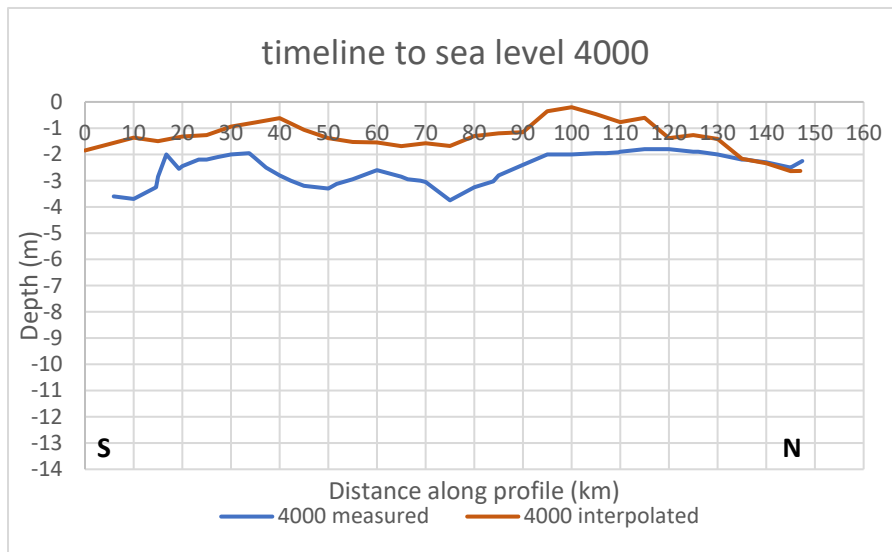
-  Core location
-  Core end
-  Core continues deeper
-  14C sample

Timelines yr cal BP

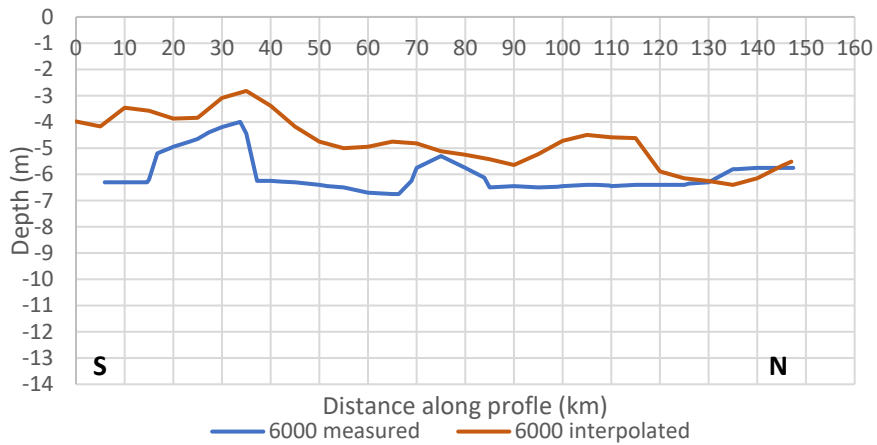


Channel ages in 14C yr
6745-6000

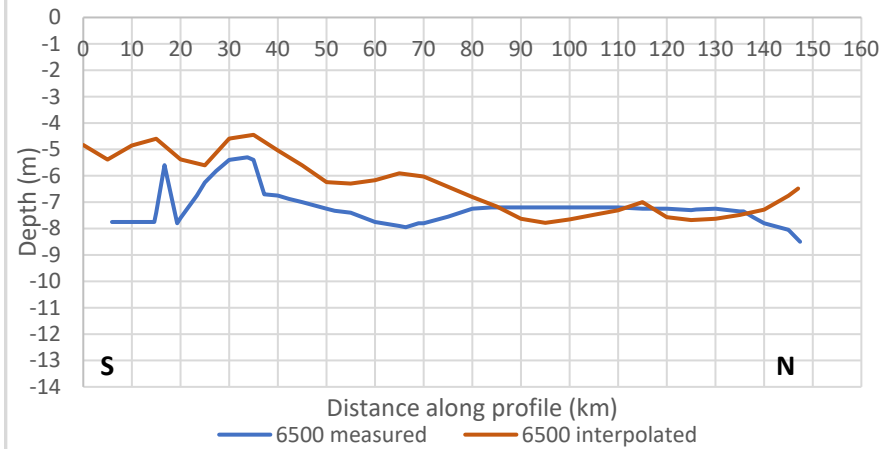
Appendix E: Individual comparisons between measured and interpolated timelines



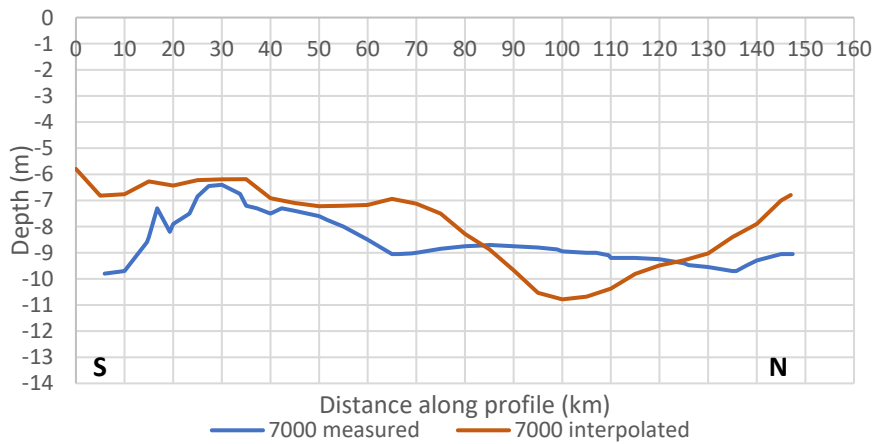
timeline to sea level 6000



timeline to sea level 6500



timeline to sea level 7000



timeline to sea level 7500

